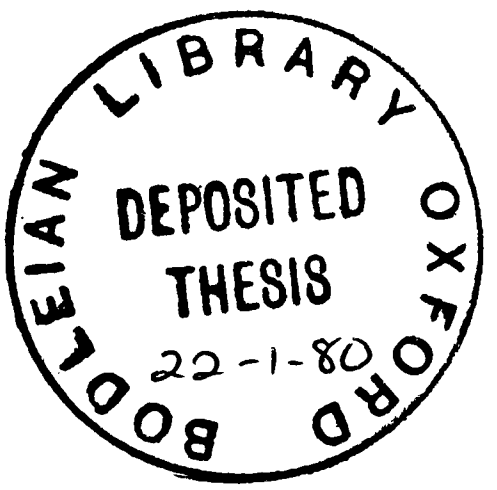
Theoretical Nuclear Physics

A. C. Merchant

Department of Theoretical Physics,
University of Oxford



A thesis submitted for the degree of Doctor of Philosophy
at the University of Oxford.

Wolfson College

August 1979

To Rejane

Theoretical Nuclear Physics

A. C. Merchant
Wolfson College, Oxford

A thesis submitted for the degree of Doctor of Philosophy

Trinity 1979

Abstract

The states in the mass 18 and 19 nuclei which are strongly excited in three- and four-nucleon transfer reactions are considered. A cluster model employing a local effective interaction with the core and approximating the requirements of the Pauli principle with an orthogonality condition is used. We present a microscopic derivation of the effective cluster-core potentials for alpha cluster states in ^{18}F and ^{19}F based on the shell model approximations to the ground states of ^{14}N and ^{15}N respectively and an alpha-nucleon scattering potential. In ^{19}F phenomenological and microscopic calculations yield essentially identical results. The predicted splitting of doublets is very small and mixing with non-cluster states is apparent in the experimental spectrum. In ^{18}F a tensor force between cluster and core is predominantly responsible for the splitting of the observed triplets. Close agreement between phenomenological and microscopic treatments occurs again. However, the latter shows that mixing of states with differing orbital angular momenta by the tensor force is important. This leads to a re-examination of the experimental candidates for cluster states, which indicates that mixing with two-particle shell model states may be important. A similar microscopic treatment is developed for trinucleon cluster states in ^{18}F and ^{18}O but is hindered by the lack of information concerning the spin-dependent terms in the nucleon-trinucleon potential. Some of the forces between cluster and core are closely related, and the results are linked with phenomenology to see what sort of nucleon-trinucleon forces are needed to reproduce the observed spectrum. Finally, the effect of core polarization on the alpha spectrum in ^{18}F is considered by mixing bands based on the ground state and excited 1^+ states of ^{14}N via the tensor force.

Acknowledgements

During the three years I spent working in the Department of Theoretical Physics I have received a great deal of help and encouragement from many sources, and would like to take this opportunity, while I am still able to hold a pen, to thank some of them. I am very grateful to Professor R. J. Elliott for awarding me a place in this Department and to the Science Research Council for a grant which supported me during my stay here.

I have enjoyed the guidance and useful criticisms of two supervisors, and am particularly indebted to both of them. Dr. B. Buck introduced me to the cluster model used so extensively in this thesis and suggested many of the problems tackled in the following pages. He also provided the bound-state programme which has been used to solve the Schrödinger equation when I could avoid the clutches of the computer no longer. When Dr. Buck left for his sabbatical year, Dr. N. Rowley took over and devoted a great deal of time to discussing and suggesting improvements to my earlier work, as well as aiding and abetting much that followed. I also sincerely apologise to him for the fortuitous nature of one of my rare victories on the snooker table. I gratefully acknowledge permission from my supervisors to include here work published jointly with both of them.

I found some notes left by Dr. H. Friedrich extremely useful at the outset and enjoyed many enlightening conversations with Drs. D.M. Brink, A.A. Pilt and B.J.B. Crowley as I progressed through the treacherous minefield of phase factors and 4π's during the later stages.

I would also like to thank my fellow students for their assistance, which was very occasionally useful, although always entertaining, but

more especially for the creation of a friendly working atmosphere in the rarified heights of the Department; so, many thanks to Angela Bonaccorso, Robbie Lindsay, Jorge Lomnitz Adler, Joaquim Lopes Neto, Geoff Maddison, Steve Marsh and Chris Wheatley.

Although I did everything possible to keep all my expressions analytic, I was eventually driven to the terminals of the dreaded PDP 10 confuser, and I gratefully acknowledge the assistance of the O.E.G. staff for securing my survival, and eventual emergence from the depths of the Nuclear Physics Department in possession of some intelligible outpourings from the beastie.

Of course, I am overwhelmingly indebted to my family for their support and encouragement throughout my academic endeavours, and gratefully acknowledge the help they have given me for many years before as well as during the time I have spent in this Department.

Finally, I would like to thank Miss M.H. Corson for the skill and speed with which she typed this thesis, despite the deterioration of my handwriting in the later stages.

Notation and Conventions

Most of the notation is, I hope, self-explanatory. The phase conventions for angular momentum couplings are the same as those employed by D.M. Brink and G.R. Satchler in Angular Momentum 2nd Edition (Clarendon Press, Oxford) 1968. In particular, when using the Wigner-Eckart theorem to evaluate matrix elements of a rank-k tensor operator with respect to the dynamical states of a system we write,

$$\langle \alpha\, JM | T_k^q | \alpha'\, JM' \rangle = (-1)^{2k} \langle \alpha J \| T_k \| \alpha' J' \rangle \langle JM' kq | JM \rangle$$

and 3-j symbols are related to Clebsh-Gordan coefficients by

$$\langle a\alpha b\beta | c-\gamma \rangle = (-1)^{a-b-\gamma} \sqrt{2c+1} \begin{pmatrix} a & b & c \\ \alpha & \beta & \gamma \end{pmatrix}$$

Table of Contents

Page No.

Abstract
Acknowledgements
Notation and Conventions
Contents

CHAPTER 1: INTRODUCTION 1

1.1) Introduction to Cluster States 1
1.2) Some Theoretical Treatments of Cluster States 4
1.3) The Buck, Dover, Vary Cluster Model. 10
1.4) The Orthogonality Condition Model. 16
1.5) Phenomenological Applications of the BDV Model 20

CHAPTER 2: ALPHA CLUSTER STATES IN ^{19}F; $^{19}F = {}^{15}N+\alpha$. 26

2.1) Experimental Evidence for Alpha Cluster States in ^{19}F. 26
2.2) Phenomenological Model of $^{19}F = {}^{15}N+\alpha$ 27
2.3) Semimicroscopic Treatment of $^{19}F = {}^{15}N+\alpha$ 29

2.3.1) The Microscopic Model 30
2.3.2) The Effective Cluster-core Potential 32
2.3.3) The Reduced Matrix Elements of $T_K(\underline{n}_i)$ 35
2.3.4) The Form Factors V_0 and V_1 38
2.3.5) Development of an Analytic Expression for $V_1(R)$ 43
2.3.6) Calculation of the Spectrum 46

2.4) Summary and Conclusions 48

CHAPTER 3: ALPHA CLUSTER STATES IN ^{18}F; $^{18}F = {}^{14}N+\alpha$ 50

3.1) Experimental Evidence for Alpha Cluster States in ^{18}F 50
3.2) The Phenomenological Model of $^{18}F = {}^{14}N+\alpha$ 54
3.3) Classical Considerations of the ^{14}N-α Interaction 59
3.4) Semimicroscopic Treatment of $^{18}F = {}^{14}N+\alpha$ 62

3.4.1) The Microscopic Model. 62
3.4.2) The Effective Cluster-core Potential 64
3.4.3) The Reduced Matrix Elements of $T_K(\underline{n}_i)$ 65
3.4.4) The Form Factors V_0, V_1 and V_2 70
3.4.5) Choice of p-shell Wavefunctions and α-nucleon Potential 75
3.4.6) The Central Potential 76
3.4.7) Calculation of the Spectrum 80

3.5) Summary and Conclusions 83

Page No.

CHAPTER 4: TRINUCLEON CLUSTER STATES IN A=18 NUCLEI 88

4.1) Experimental Evidence for Trinucleon Cluster states in A=18 Nuclei 88
4.1.1) Candidates in ^{18}F 89
4.1.2) Candidates in ^{18}O 90

4.2) Phenomenological Treatment of Trinucleon cluster states in ^{18}F and ^{18}O 92
4.3) Semimicroscopic Treatment of Trinucleon Cluster States in ^{18}F and ^{18}O 97

4.3.1) The Microscopic Model 97
4.3.2) The Effective Cluster-core Potential 100
4.3.3) The Reduced Matrix Elements of $B_K(\underline{n}_i)D_{K'}(\underline{n}_i)$ 103
4.3.4) The Form Factors V_o, $V_{\tau\tau}$, V_{SS}, V_{ST}, V_{LS_C}, V_{LS_C}, V_{TENS} and $V_{\tau TENS}$ 105

4.4) 4.4.1) Combination of Microscopic and Phenomenological Calculations 111
4.4.2) Details of Fit of Trinucleon Cluster States in ^{18}O and ^{18}F 113

4.5) Summary and Conclusions 117

CHAPTER 5: CORE POLARIZATION IN THE $^{14}N+\alpha$ SYSTEM 120

5.1) Introduction 120
5.2) Core Polarization 123
5.3) Electric Quadrupole Transitions Between Cluster States 129

APPENDICES

I Tensor Decomposition of $u(|\underline{r}-\underline{R}|)$
II The Relative Orbital Angular Momentum of Hole and Cluster
III Treatment of $C_2(\hat{\underline{R}}).C_2(\hat{\underline{r}})\underline{L}.\underline{s}$
IV Treatment of $-3C_1(\hat{\underline{R}}).C_1(\hat{\underline{r}})\underline{R}_\Lambda\underline{p}.\underline{s}$
V Treatment of $-3C_1(\hat{\underline{R}}).C_1(\hat{\underline{r}})\underline{r}_\Lambda\underline{P}.\underline{s}$
VI Treatment of $5C_2(\hat{\underline{R}}).C_2(\hat{\underline{r}})\underline{\ell}.\underline{s}$
VII Tensor Term Arising from $-3C_1(\hat{\underline{R}}).C_1(\hat{\underline{r}})\underline{R}_\Lambda\underline{p}.\underline{s}$
VIII Electric Quadrupole Transitions Between Cluster States

References
Tables
Figures

CHAPTER 1

INTRODUCTION

1.1 Introduction to Cluster States.

In the last ten years an enormous amount of experimental effort has been directed towards the identification and measurement of the many excited states of the nuclei in the mass range A = 16-20. These studies have been particularly rewarding for ^{18}F, in which some 100 or more states have been resolved below 10 MeV [1]. Amongst this plethora of new information there is a very striking subset of states, which appear to have extremely simple structures, especially noticeable in the nuclei with masses A = 18-20.

The tool which has done most to show up these special states so clearly is the multinucleon transfer reaction.[2] Such reactions, when induced by incident beams of light nuclei with energies of typically 10 MeV/nucleon, yield little information from their angular distributions which are generally rather featureless and peaked at forward angles. In fact, they are steep functions of momentum transfer, still rising at the smallest angles measured. However, their great usefulness lies in their extreme selectivity; since only a few states of the residual nucleus are at all strongly populated over a large range of excitation energies. Those states which do appear are very heavily populated and the forward peaking of the detected residual ion suggests that transfers occur during grazing collision of the nuclear cores. It has been shown that simple considerations of energy and momentum

conservation then lead to the conclusion that for high-energy projectiles the greatest transfer probabilities should occur for reactions with large, negative Q-values.[3]) Then the transferred nucleons are less tightly bound in the final state than in the incident ion. Also the z-component of angular momentum should be as large as possible (so that the transferred nucleons are in the reaction plane) resulting in final states of high spin.[3]) To make complete sense of the data, some postulates must also be made about the structure of the final states since this "trivial" L and Q-value dependence is insufficient on its own to provide a full explanation. In the case where three or four nucleons are all transferred together in a real or virtual bound state of internal relative motion the process can be regarded effectively as the transfer of a single "particle" e.g. triton, helion or alpha. This possibility suggests further that the selectively populated final states may actually look like a real triton, helion or alpha orbiting the target nucleus and therefore we shall henceforth loosely refer to such states as "cluster states". At any rate, the spectroscopic usefulness of these reactions is due to the close matching to final states of high spin, and is likely to produce states of the final nucleus with a many-particle many-hole structure.

A nucleus which can be used as a particularly simple testing ground for these ideas is ^{20}Ne, since it possesses at least two rotational bands of states which appear to be describable as an alpha particle coupled to an ^{16}O core. In this case, both constituents are very tightly bound when free (being doubly magic nuclei), and so lead us to expect that the cluster-core treatment may be well founded.

Also, since neither component possesses an intrinsic angular momentum, the cluster-core potential can only be central, so if the suggested decomposition is valid, a simple spectrum, with no spin-dependent complications should be seen. Many reactions involving alpha transfer to ^{16}O have been performed, among them (^{11}B,^{7}Li), (^{13}C,^{9}Be) [4] and (^{7}Li,t),[1,5]) and it is found that the same few states are excited in all of them, although the precise strength of excitation of a given state varies from one reaction to another for kinematic reasons. In addition, information from the (α,γ) [1,5]) reaction in combination with the transfer data enables a thorough and reliable analysis of the cluster spectrum to be made.

In addition to their rotational spacing, the states in ^{20}Ne selected by alpha transfer onto ^{16}O, have other properties which support a cluster-core picture. Those states above the threshold for alpha decay are found to have exceedingly large alpha widths, in some cases, close to the Wigner single particle limit. Since the ground state of ^{20}Ne is a candidate for membership of the cluster-core spectrum, its r.m.s. radius can be measured and compared with model predictions. Finally, electric quadrupole transition rates between proposed cluster states have been measured, and can be calculated to good accuracy by treating them as single particle transitions involving an alpha particle.

Since such a treatment was so successful for those states in ^{20}Ne which are strongly excited in alpha transfer onto ^{16}O or have large alpha decay widths, it was logical to ask if the other states in the mass 18 and 19 nuclei, which are similarly excited in multinucleon transfer reactions are amenable to this cluster-core treatment. With

the experimental data now available, the nuclei and decompositions which most forcibly suggested themselves were: $^{19}F = {}^{15}N+\alpha$, $^{19}F = {}^{16}O+t$, $^{19}Ne = {}^{16}O+{}^{3}He$, $^{19}Ne = {}^{15}O+\alpha$, $^{18}F = {}^{14}N+\alpha$, $^{18}F = {}^{15}N+{}^{3}He$, $^{18}O = {}^{15}N+t$. In this thesis we shall be primarily concerned with understanding the states selectively excited in ^{18}F and ^{18}O by three and four nucleon transfer reactions.

1.2 Some Theoretical Treatments of Cluster States.

A fair number of models have previously been employed to describe the rotational bands of cluster states in light nuclei. Amongst them are i) the full shell model,[7]) ii) the SU_3 model,[8]) iii) the Bloch-Brink cluster model,[9]) iv) the deformed oscillator model,[10]) v) the generator co-ordinate method[11]) and vi) the resonating group method.[12]) We shall briefly outline the physical reasonings upon which some of these various approaches are based before introducing the treatment we propose to use ourselves. This treatment is similar to that of the resonating group method, except that a different effective potential is used and the Pauli Principle is approximately taken into account by the choice of the quantum numbers of relative motion between cluster and core, which results in enormous simplifications.

With all the models listed above, one wishes to produce wave functions (without explicitly solving the Schrödinger equation for an A-particle system) to calculate such quantities as the energy levels, r.m.s. radii, electromagnetic transition rates and static moments and alpha decay widths for comparison with the corresponding experimentally

measured values. If we assume that the potential energy of such an A-particle system can be adequately described in terms of two-body interactions, the Hamiltonian in question may be written as

$$H = \sum_{i=1}^{A} \frac{\underline{P}_i^2}{2m_n} + \sum_{i<j} V_{ij} \qquad (1.1)$$

where $\underline{P}_i$ is the momentum of the ith particle, m_n is the mass of a nucleon and V_{ij} is the interaction between nucleons i and j. Since the eigenfunctions of this Hamiltonian can not be found exactly, the various models employ differing physically motivated simplifications, to produce approximate solutions of the many-body Schrödinger equation.

First of all we consider the application of the full shell model to the problem. In this approach to nuclei in the mass range A = 18-20 [7]) an inert ^{16}O core is assumed and the active particles distributed among the $d_{5/2}$, $d_{3/2}$ and $s_{1/2}$ single-particle orbits. All possible configurations made from particles in these j-shells are included in the basis space, in which a residual nucleon-nucleon interaction is then diagonalized. Of course, higher lying single-particle orbits have a finite probability of being occupied by the active particles, but are excluded because, for the states of lowest energy in the final nucleus, this probability is generally small. Also, the matrix to be diagonalized would become impossibly large with the inclusion of higher major shells than the (sd). Although many low-lying states can be very well described in this manner, it seems that the cluster states we wish to consider do contain significant contributions from higher shells, and

it is these contributions which are essential to build up the necessary degree of spatial correlation of the nucleons forming the cluster for a really good description. Hence, the truncation of the shell model basis at the (sd) shell results in wavefunctions for the cluster states which are only a fair approximation for the energies of the physically observed states. When these wave functions are used to calculate electromagnetic properties and alpha decay widths they are found to be highly unsatisfactory. For example, the electromagnetic transition rates between cluster states are generally in the same ratios as experimental determinations, but require the use of an effective charge of about 0.5 to obtain the same absolute magnitudes. Also the alpha decay widths predicted in the shell model are typically factors of 5-10 smaller than experiment.

Exactly the same problems persist in the SU_3 model. This is essentially just a sub-model of the full shell model, restricting attention to sd-shell orbitals, and using the irreducible representations of the group SU_3 to classify states of several particles placed in the sd-shell. The states of maximum orbital symmetry are identified with the cluster states. The advantage of the SU_3 model over the full shell model is that it gives a greater physical insight into the nature of the various states, although a great similarity with the overall results of the full shell model can be expected.

In fact, SU_3 wave functions have been found to have overlaps in excess of 80% with those of the full shell model. (However, caution should be exercised in interpreting this figure since it is possible for small changes in the wavefunction to drastically alter the prediction of a measurable quantity). The crux of the problem seems to be that

the wavefunctions of both SU_3 and full shell models describe the cluster as only loosely correlated and overlapping the core to a very large extent, whereas the observed properties and subsequent models indicate that the cluster should be more tightly correlated, resembling a real alpha particle, and that cluster and core are really distinct entities.

The shell model just considered indicates a need to obtain a much greater degree of spatial correlation between the cluster nucleons if all the properties of the cluster states are to be reproduced. Therefore, it is expected that those models which build in clustering explicitly will be more successful. One calculation of this sort for alpha cluster states in ^{20}Ne is provided by the Bloch-Brink cluster model.[9] This model is applicable to nuclei containing 4N nucleons and treats them as being constructed from N "alpha particles". Each "alpha particle" is placed at a fixed centre $\underline{R}_i$, which is treated as a parameter, and the system is described by N single particle wave functions centred on the various $\underline{R}_i$. It is then possible to construct a 4N nucleon state by requiring each orbital state to be occupied by two protons and two neutrons, so that a 4N-particle normalized Slater determinant wavefunction results. This resultant wavefunction will have maximum orbital symmetry, spin S = 0 and isospin T = 0. Generally oscillator functions are used for the N single particle wavefunctions, and the cluster size will then depend on the oscillator parameter, b.

To deal with the various states of a 4N nucleus, different configurations of the constituent alphas are assumed. For example, some states of ^{12}C may be treated in terms of three alphas situated at

the vertices of an equilateral triangle, and others as three equally spaced alphas in a straight line. Once a configuration has been chosen, the energy of the system is minimized by varying the separation parameter. Finally, it is usually necessary to project out the states of definite angular momentum and parity to obtain satisfactory wave functions. In the case of ^{20}Ne, the alpha cluster states of interest to us are treated as an arrangement of four alphas at the vertices of a regular tetrahedron and a fifth alpha situated "below" the centre of the tetrahedron. When the separation parameters are varied to minimize the energy a wavefunction is produced which describes one alpha particle outside a "core" of four alpha particles which look like ^{16}O. This separation of the fifth alpha from the others allows a much improved series of predictions to be made for the properties of alpha cluster states in ^{20}Ne, and illustrates the value of building in the clustering explicitly. Unfortunately, it is only applicable to 4N nuclei, so a different technique is needed for the mass 18,19 nuclei .

A model which considers a decomposition of the nucleus into cluster and core which might be applicable to the mass 18,19 nuclei is the Resonating Group Method.[12]) In its simplest single channel form this model allows one to write a wavefunction for a nucleus which separates into two clusters containing A_1 and A_2 particles as:

$$\Psi(\underline{r}_1, \ldots \underline{r}_A) = \mathcal{Z}(\underline{R}_c)\mathcal{A}\left\{\phi_1(\underline{A}_1)\phi_2(\underline{A}_2)\tilde{g}(\underline{R})\right\} \qquad (1.3)$$

where $Z(\underline{R}_c)$ describes the motion of the centre of mass of the nucleus, ϕ_1 and ϕ_2 represent antisymmetrized internal states of the two clusters (whose internal co-ordinates are labelled $\underline{A}_1$ and $\underline{A}_2$), $\tilde{g}(\underline{R})$ is a function

of relative motion and the antisymmetrizer $\mathcal{A} = \Sigma(-1)^P P$ (with P an operator producing even and odd permutations of nucleons) exchanges nucleon between the clusters. The variational principle can then be applied to Ψ as follows;

$$\delta \langle \Psi | \mathcal{H} - \mathcal{E} | \Psi \rangle = 0 \qquad (1.4a)$$

with $\mathcal{H}$ the Hamiltonian and ε the total energy of the system. Hence

$$\langle \delta\Psi | \mathcal{H} - \mathcal{E} | \Psi \rangle + \langle \Psi | \mathcal{H} - \mathcal{E} | \delta\Psi \rangle = 0 \qquad (1.4b)$$

The ket $|\delta\Psi\rangle$ is the variation of $|\Psi\rangle$, the bra $\langle\Psi|$ the variation of the bra conjugate to $|\Psi\rangle$. Since eq. 1.4b is satisfied by any infinitesimal ket $|\delta\Psi\rangle$, we may replace $|\delta\Psi\rangle$ by $i|\delta\Psi\rangle$ (and consequently $\langle\delta\Psi|$ by $-i\langle\delta\Psi|$) to obtain a second equation

$$-i \langle \delta\Psi | \mathcal{H} - \mathcal{E} | \Psi \rangle + i \langle \Psi | \mathcal{H} - \mathcal{E} | \delta\Psi \rangle = 0 \qquad (1.4c)$$

We can now take linear combinations of eqs. 1.4b and 1.4c to obtain the two equivalent equations

$$\langle \delta\Psi | \mathcal{H} - \mathcal{E} | \Psi \rangle = 0 \quad , \quad \langle \Psi | \mathcal{H} - \mathcal{E} | \delta\Psi \rangle = 0 \qquad (1.5)$$

Using this in conjunction with eq. 1.3 (from which we drop the centre of mass term for convenience) we may rewrite Ψ in the form

$$\Psi = \int d^3x \; \tilde{g}(\underline{x}) \mathcal{A} \{ \phi_1(\underline{A}_1) \phi_2(\underline{A}_2) \delta(\underline{x} - \underline{R}) \} \qquad (1.6)$$

so that the integral form of the R.G.M. equation follows

$$\int K(\underline{x}, \underline{x}') \tilde{g}(\underline{x}') \, d^3x = 0 \qquad (1.7)$$

where

$$K(\underline{x}, \underline{x}') = \langle \phi_1(\underline{A}_1) \phi_2(\underline{A}_2) \delta(\underline{x} - \underline{R}) | (\mathcal{H} - \mathcal{E}) \mathcal{A} | \phi_1(\underline{A}_1) \phi_2(\underline{A}_2) \delta(\underline{x}' - \underline{R}) \rangle \qquad (1.8)$$

is the full R.G.M. kernel. Unfortunately, severe mathematical difficulties are encountered in applying this model to cluster states

in nuclei with mass numbers A = 18,19 because the kernels of eq. 1.8 are non-local. In fact, they can only be evaluated if some simplifying assumptions are made about the internal structure of the nucleus under consideration. For example, the nucleus ^{8}Be might be approximately dealt with by treating it as two alpha particles and writing the wave function in terms of single particle oscillator determinants. However, this model does provide a basis from which to construct another cluster model to treat cluster states in the mass 18,19 nuclei as consisting of an A_1-particle core and an A_2-particle cluster, which is our desired goal. This model, which we intend to use ourselves, will be discussed in the next section.

1.3 The Buck, Dover, Vary Cluster Model.[13])

The whole philosophy of any cluster model approach to nuclear structure is to select a much smaller set of basic states than is used in the huge shell model calculations. The members of this smaller basis are chosen on the grounds that they are expected to be particularly suitable for describing a certain restricted set of states in the final nucleus which have very simple structures. Thus, those states in the full basis which are excluded from the smaller basis would not be important for the final states under consideration. In addition, the smaller basis may include some states which are important to describe the final states fully, but had to be omitted from the full shell model calculation on grounds of mathematical manageability. The aim of a cluster model is not to replace the more detailed shell model (which can, in principle, be applied to describe all the states

of a nucleus) but simply to perform calculations of observable quantities for a restricted class of states with simple structures in a straightforward manner. At the same time, it can provide an intuitively appealing and physically transparent model of such states.

This is precisely the kind of approach which might be expected to succeed in treating that small class of states so dramatically selected in the multinucleon transfer reactions discussed in section 1.1. The full shell model requires an extremely large basis to describe these states in a satisfactory manner, and the inclusion of states from many high lying shells appears to be necessary to build up the required spatial correlations of the cluster nucleons. We therefore propose to use the cluster model introduced by Buck, Dover and Vary [13] to deal with these cluster states.

The BDV model treats a system of states which exhibit the properties of a "massive" core being orbited by a "light" cluster. An effective cluster-core potential is obtained from a simple folding procedure and the bound states and single particle resonances which result are identified with the highly selected states observed in experiments which involve a transfer of the cluster to the core. The folded potential [14] is taken as a convolution of the densities of the two constituents with a suitably chosen effective nucleon-nucleon interaction in the form:

$$V(R) = \int \rho_{A_1}(\underline{r})\, \rho_{A_2}(\underline{r}')\, G(\underline{R}-\underline{r}+\underline{r}')\, d^3r\, d^3r' \qquad (1.9)$$

where $\rho_{A_1}(\underline{r})$ is the ground state density of the core (containing A_1 particles). $\rho_{A_2}(\underline{r}')$ is the analogous quantity for the cluster (A_2 particles) and G is the effective NN interaction (see Fig. 2a for the

definitions of $\underline{R},\underline{r},\underline{r}'$). Alternative foldings of a nucleon-nucleus optical potential with the cluster density, which thus treat the cluster and core in an unsymmetrical fashion, have also been used, but Dover and Vary prefer this symmetrical form because it is identical to the first term in a consistent density expansion of the optical potential.[15]) For simplicity, G is taken to be local, and to have been averaged over all spin and isospin states. In fact, the very simplest treatment, which is found to be adequate for a description of the properties of the cluster states of interest to us, takes G to be parametrized by a Dirac delta function with an adjustable strength $\bar{f}$ in the form

$$G = -\frac{2\pi\hbar^2}{m_n}\bar{f}\,\delta(\underline{R}-\underline{r}+\underline{r}') \qquad (1.10)$$

where m_n is the mass of a nucleon. With this approximation the convolution integral of eq. 1.9 reduces to a single folding integral with

$$V(R) = -\frac{2\pi\hbar^2}{m_n}\bar{f}\int\rho_{A_1}(\underline{r})\,\rho_{A_2}(\underline{r}-\underline{R})\,d^3r \qquad (1.11)$$

In the BDV structure calculations $\bar{f}$ is taken to be real, with a magnitude which is chosen to reproduce a single low-lying, experimentally well-identified level in the band of cluster states under consideration. To fit different bands it is found to be necessary to vary $\bar{f}$ (even if the bands in question are in the same nucleus) but $\bar{f}$ may be held constant for the levels within a given band.

There are two remaining problems to be dealt with before any nuclei can be examined. Firstly, we have to decide which form to adopt for the densities of cluster and core, and secondly, how to

take into account the Pauli principle. There are two possibilities for choosing the densities. In the simplest one (which is the one actually used for the structure calculations) the proton density is extracted from electron scattering data, and the neutron density assumed to equal it. Alternatively, the two densities may be taken from Hartree-Fock or shell-model calculations by evaluating

$$\rho = \sum_i W_i \left| \phi_i(\underline{r}) \right|^2 \qquad (1.12)$$

with the index i ranging over all occupied proton and neutron bound states, ϕ_i is a single particle wavefunction and W_i the statistical weight. Somewhat surprisingly, it turns out that this latter method gives consistently better results in the treatment of scattering,[14] but it is passed over in favour of the simplicity of the first approach for structure calculations.

It is clear that the major requirements of the Pauli exclusion principle must somehow be satisfied, and this is done by treating the cluster as a single particle with principal quantum number N (the number of nodes in the radial part of the wavefunction) and orbital angular momentum L, which describe its motion about the core. As the cluster is assumed always to be in its ground state, all the available quanta go into the relative motion, and the minimum of these quanta which will be permitted must be sufficient to place all the cluster nucleons in shell model orbitals outside the core. Specifically, in the case of those nuclei in the mass range A = 18-20, the core will always consist of 16 or less nucleons whilst the cluster will contain 3 or 4 nucleons (which number we denote by A_2,

as before). Even in those systems where there is sufficient space remaining in the p-shell to accommodate some of the cluster nucleons, we insist that they occupy orbitals in the (sd) shell, or still higher shells, so we are dealing with multi-particle multi-hole states. Since each of the A_2 nucleons in the cluster must have at least two quanta, we can relate the quantum numbers N and L, which describe the motion of the cluster as a whole, by summing the individual quantum numbers of the constituent nucleons of the cluster as follows:

$$2N+L = \sum_{i=1}^{A_2} (2n_i + l_i) \geq 2A_2 \qquad (1.13)$$

As an example of the application of this "oscillator rule", consider the decomposition $^{20}Ne = {}^{16}O+\alpha$. The four nucleons comprising the alpha particle are placed in the (sd) shell or higher, where they possess a total of at least 8 quanta, which must go into the relative motion of cluster and core. This method of treating the exclusion principle is only really expected to be successful for the treatment of cluster states in light nuclei, where both the protons and neutrons which make up the cluster can be put into the same shell. For heavier nuclei, where the neutron number exceeds the proton number, we would be required to build a cluster with nucleons from different shells, and it would be unreasonable to expect such clusters to behave like real alpha particles or tritons, so a different procedure would be needed to deal with clustering in heavy nuclei.

This method of dealing with the effects of antisymmetrization by a suitable choice of the quantum numbers of relative motion between cluster and core is more extensively discussed, and applied

to several light nuclear systems (e.g. $^{8}Be = \alpha+\alpha$, $^{6}Li = \alpha+d$) by Wildermuth and Tang.[16]) As an illustration of the arguments used by them, we briefly sketch their consideration of ^{8}Be. Initally, a single particle oscillator Schrödinger equation is considered, which leads to single particle solutions which are products of oscillator functions (multiplied by appropriate spin and isospin functions). These single particle solutions give rise to a complete set of antisymmetrized functions, which can therefore be used to expand any antisymmetrized 8-nucleon wavefunction. Then new coordinates appropriate to an α-α cluster representation are introduced (essentially centre of mass and relative coordinates of the two components). The Hamiltonian can then be decomposed into terms dealing with the internal motions of the two alpha clusters and their relative coordinates. This, in turn, allows one to write eigenfunctions as products of two internal functions a relative function and a centre of mass term. These functions can also be used to form a complete set of antisymmetrized oscillator cluster functions. However, all that has been done is to change coordinates, which can not affect the physical meaning of the Hamiltonian, so the energy eigenvalues associated with both sets of wavefunctions must be identical. Hence, the cluster functions of a given energy can be written as a superposition of products of degenerate single particle solutions corresponding to the same energy. Now, since the lowest possible energy configuration in the single particle picture (if we are not to violate the Pauli principle) is $(0_s)^4(0_p)^4$, which has four oscillator quanta of excitation, it follows that the cluster function must also describe a state of at least four quanta; otherwise, it will vanish upon antisymmetrization. This

question of the treatment of the Pauli principle will be considered more formally in the next section.

In conclusion, we note that the following three assumptions were made when the BDV cluster model was first introduced; i) The correlation between the constituent nucleons of the cluster are assumed to be the same in the presence of the core as in free space. ii) Exchange effects between nucleons in the cluster and the core are ignored. iii) A zero-range effective NN interaction is used. In the microscopic treatment which will be presented for comparison with a phenomenological application of the BDV model, the non-central terms in a cluster-core potential will be found by summing a cluster-nucleon potential over all the core nucleons. The cluster-nucleon potential used will be the real part of the appropriate optical potential, in keeping with assumption (i). However, if this was found to be unsatisfactory, the parameters of the potential could be varied to obtain a more suitable cluster-core interaction. Also, the use of an optical potential will contain some exchange effects, so this is not entirely neglected in the microscopic treatment, and also the optical potential will have a finite range. In view of the excellent agreement between experimental measurements and BDV cluster model predictions of r.m.s. radii, energy spectra electromagnetic static moments and transition rates and alpha decay widths for the cluster states under consideration it is concluded that the assumptions listed are reasonable.

1.4 The Orthogonality Condition Model.[17,18]

In view of the importance of the treatment of the Pauli principle presented in the last section, an outline of its justification in terms

of a simplification of the Resonating Group Method (RGM) first introduced by Saito[17]) and known as the Orthogonality Condition Model (OCM) is called for. The motivation for proposing the O.C.M. was to circumvent the difficulties arising from the non-locality of the R.G.M. kernels (eq. 1.8) as follows. The Schrödinger equation is solved for a cluster-core potential of the folding type under the additional restriction that the solutions must be orthogonal to those states of relative motion which are forbidden by the Pauli principle. (The so-called redundant states, whose many body wavefunctions vanish identically). In general, non-locality still persists because a projection operator is needed to remove these states. However, in some cases the redundant states are so similar to bound states of the local Hamiltonian that the orthonormality condition may be satisfied by finding all solutions and simply rejecting those which approximate the redundant states. (In our calculations, these are the states with less than $2A_2$ quanta in the relative motion where A_2 is the number of nucleons in the cluster, which must be placed in the (sd) shell). The work of Saito shows that this approach is valid if one of the components is a light particle, and Buck et al.[18]) show that it can also be used for heavier systems (e.g. ^{16}O-^{16}O scattering). Basically, it is true provided the local potential is essentially energy independent so that the eigenstates are all orthogonal to each other.

For a more formal statement of this procedure we return to equations (1.5) and (1.6) and for convenience define

$$\left.\begin{matrix} A(\underline{x},\underline{x}') \\ H(\underline{x},\underline{x}') \end{matrix}\right\} = \langle \phi_1(\underline{A}_1)\phi_2(\underline{A}_2)\delta(\underline{x}-\underline{R}) \left| \begin{matrix} \mathcal{N} \\ \mathcal{H}\mathcal{N} \end{matrix} \right| \phi_1(\underline{A}_1)\phi_2(\underline{A}_2)\delta(\underline{x}'-\underline{R}) \rangle \qquad (1.14)$$

so that the many-body Schrödinger equation, (1.5) can be written

$$H|\tilde{g}\rangle = \mathcal{E}A|\tilde{g}\rangle \tag{1.15}$$

with $|\tilde{g}\rangle$ defined in (1.3) and we have used the relations $[\mathcal{H},\mathcal{A}] = 0$ and $\mathcal{A}^2 \propto \mathcal{A}$. We may now separate $\mathcal{A}$ into a sum of direct and exchange parts as follows,

$$\mathcal{A} = 1 - \theta \tag{1.16}$$

which permits us to rewrite A as

$$A(\underline{X},\underline{X}') = \delta(\underline{x}-\underline{x}') - \theta(\underline{X},\underline{X}') \tag{1.17}$$

where θ is a bounded Hermitian operator assumed to have a complete set of orthornormal states. Now, writing the many-body Hamiltonian $\mathcal{H}$ as a sum of cluster internal Hamiltonians, $\mathcal{H}_1$ and $\mathcal{H}_2$, a relative kinetic energy operator, $-\frac{h^2}{2\mu}\nabla^2_{\underline{x}}$ and an inter-cluster potential energy $\tilde{V}_{12}$,

$$\mathcal{H} = \mathcal{H}_1 + \mathcal{H}_2 + \mathcal{T}_c + \tilde{V}_{12} \tag{1.18}$$

and similarly the total energy as a sum of internal cluster energies, ε_1 and ε_2, and a relative energy E_c,

$$\mathcal{E} = \epsilon_1 + \epsilon_2 + E_c \tag{1.19}$$

equation (1.19) reduces to

$$H_c|\tilde{g}\rangle = E_c A|\tilde{g}\rangle \tag{1.20}$$

and the relative Hamiltonian H_c is defined by

$$H_c(\underline{X},\underline{X}') = \langle\phi_1'\phi_2'\delta(\underline{x}-\underline{R})|(\mathcal{T}_c+\tilde{V}_{12})\mathcal{A}'|\phi_1\phi_2\delta(\underline{x}'-\underline{R})\rangle \tag{1.21}$$

It is at this juncture that the O.C.M. is introduced to simplify the evaluation of $H_c(\underline{X},\underline{X}')$. Briefly, the approach of Saito proceeds as follows; The exchange part of the antisymmetrizer, $\theta(XX')$ of (1.17), is resolved in terms of its eigenvalues $\lambda_{n\ell}$ and its eigenstates $\chi_{n\ell}$, which are also eigenstates of A with eigenvalues $\mu_{n\ell} = 1 - \lambda_{n\ell}$. For light systems, the first few $\mu_{n\ell}$ are zero and the rest approach 1, and those χ_γ with $\mu_{n\ell} = 0$ are identified with the R.G.M. redundant states, since their substitution in (1.6) yields zero. Hence, it is possible to replace A approximately by an operator which removes such states, namely

$$A \to \Lambda = 1 - \sum_{\gamma}' |\chi_\gamma\rangle\langle\chi_\gamma| \qquad (1.22)$$

(where the sum runs over the redundant states). Also, H_c is replaced by its local part

$$H_c(\underline{X},\underline{X}') \approx [T_c + V_c(\underline{X})]\,\delta(\underline{X}-\underline{X}') \qquad (1.23)$$

where

$$T_c = -\left(\hbar^2/2\mu\right)\nabla_{\underline{X}}^2 \qquad (1.24)$$

and

$$V_c(\underline{X}) = \langle\phi_1\phi_2|\,V_{12}\,|\phi_1\phi_2\,\delta(\underline{x}-\underline{X})\rangle \qquad (1.25)$$

Unfortunately, this H_c is unsatisfactory since it ought to annihilate the redundant states and doesn't, consequently it is modified to become

$$H_c \approx \Lambda\,[T_c + V_c]\,\Lambda \qquad (1.26)$$

giving a wave equation

$$\Lambda\,[T_c + V_c]\,\Lambda\,|\tilde{g}\rangle = E_c\,\Lambda\,|\tilde{g}\rangle \qquad (1.27)$$

Defining $|g\rangle = \Lambda|\tilde{g}\rangle$, which has no redundant components, we obtain the Saito equation

$$\mathcal{A}\left[T_c+V_c\right]|g\rangle = E_c\,|g\rangle \qquad (1.28)$$

This defines the O.C.M. Only the local parts of the R.G.M. equation are retained and solved subject to the constraint that the solutions be orthogonal to the totally forbidden states.

Buck, Friedrich and Wheatley have derived this equation under less restrictive conditions [18] and shown that the O.C.M. is still valid in the presence of partially redundant states. However, in this case it provides an equation for $A^{\frac{1}{2}}|\tilde{g}\rangle$ and not $|g\rangle$. Since these only differ for small separations of the two components (core containing A_1 particles and cluster containing A_2), and have the same asymptotic forms, the O.C.M. is still applicable. We note that the folded cluster-core potentials have several bound states in the lower partial waves, and it should be true that their wavefunctions are similar to those of the forbidden states. Clearly, the higher bound states and single particle resonances of the Hamiltonian (which is energy-independent for a given band, since $\bar{f}$ is held constant within such a band) will be orthogonal to the lower states, and we thus fulfil the requirements of the O.C.M. by rejecting the lower states generated

1.5 Phenomenological Applications of the BDV Model.[19,20,21])

Many models and calculations have already been applied to the problem of describing the properties of those cluster states which consist of two components which are both spinless. Although it is clearly necessary for the BDV model to be able to deal with these

spinless sytems, and gratifying that its predictions for them agree so well with experiment, it must be able to treat other more complicated cluster-core systems which do carry spins to really justify its introduction. Experimentally, the cluster states in those nuclei for which either the cluster or core, or both, carry an intrinsic angular momentum are known to be split from the centroids of a rotational band. This observation indicates that spin-dependent forces in the interaction between cluster and core are important, and responsible for at least part of the splitting. These cluster states, with their more complicated interactions, are not readily amenable to a satisfactory treatment by any of the methods outlined in section 1.2, and it is in describing the properties of these systems that the BDV model proves its worth. Until now the spin-dependent forces in the cluster-core potential have been treated in a phenomenological manner, by arguing for their presence or absence on symmetry grounds (essentially invariance of the interaction under space inversion and time reversal), and then making simplifying assumptions about the magnitudes and variations of the matrix elements of the interaction. It is the aim of this thesis to put these assumptions on a more microscopic footing, and to evaluate the required matrix elements from first principles. This programme will then provide a test of the validity of the BDV model in those cases where it is successful but not yet so firmly based.

Before proceeding to carry out this scheme we review the phenomenological treatments already published which provide evidence that our proposed programme is possible, and indeed necessary. Firstly, we consider the four-nucleon cluster states which are

experimentally identified by strong selective excitation in alpha transfer onto the core. These states have large alpha decay widths (if above the alpha emission threshold) and r.m.s. radii and electromagnetic properties (static moments as well as M1 and E2 transition rates) consistent with an alpha-core constitution. These calculations may be subdivided into three classes, according as the core carries spin 0, $\frac{1}{2}$ or 1.

For spin-0 cores, as in $^{20}Ne = {}^{16}O+\alpha$, $^{18}F = {}^{14}C+\alpha$ (and even $^{16}O = {}^{12}C_{gs}+\alpha$) the interaction is purely central, and obtained from the folding procedure outlined in section 1.3.[13]) The wavefunctions produced on solving the Schrödinger equation make predictions which are generally very close to the experimentally measured quantities listed. An almost perfectly rotational spectrum is produced, and the only real problem arises for the topmost member of the band having $J^{\pi} = 8^{+}$. The model places this level at a much higher energy than its experimental counterpart. At the present time it is not clear whether this is due to some inadequacy on the part of the central cluster-core potential or to substantial mixing with other states having the same quantum numbers but different structures. In the case of the $K^{\pi} = 0^{+}$ band in ^{20}Ne the BDV model predicts the $J^{\pi} = 8^{+}$ member to lie between 14 and 15 MeV. However, the multinucleon transfer reactions $^{16}O(^{11}B,{}^{7}Li)^{20}Ne$ and $^{15}N(^{12}C,{}^{7}Li)^{20}Ne$ (the latter is assumed to be a sequential nucleon-alpha transfer process) select, fairly strongly, 8^{+} states at around 12,16 and 17 MeV.[3]) This strongly suggests that mixing with states of a different structure is important, and we feel that it is worth mentioning here because it will arise again later, to complicate the analysis of our microscopic results.

When the core carries a spin of $\frac{1}{2}$, a spin-orbit force is allowed by symmetry considerations, but the observed splitting into doublets of the rotational spectrum in, for example, $^{19}F = {}^{15}N+\alpha$ is extremely small. In fact, the doublet separation in ^{19}F is so small and irregular (in the sense that it exhibits none of the systematic features that would be expected from a pure spin-orbit effect) that it is ignored in the phenomenological treatment.[19]) Again excellent agreement with experiment is obtained for the propertics listed earlier, and a similar problem to that occurring with the 8^+ state in ^{20}Ne is experienced with the topmost ($\frac{15}{2}^-$ - $\frac{17}{2}^-$) doublet. (See Fig. 1).

It is also possible to find an alpha cluster system in which the core has a spin of 1; namely $^{18}F = {}^{14}N+\alpha$. Experimentally, the cluster states of this system exhibit large splittings (typically $\sim$ 1 MeV) and certainly don't follow a simple spin-orbit pattern (see Fig. 4). Symmetry considerations permit a tensor force (essentially a manifestation of the interaction of the alpha with the quadrupole shape deformation of the core), and when such a force is introduced into a phenomenological treatement good agreement between model and experiment occurs.[20]) The aim of the microscopic treatment to be presented for these last two systems is to understand and explain at a more basic level the strengths of the spin-orbit and tensor parts of the interaction which are introduced. Also, the limitations of the model may become apparent through the experimentally observed prominence of neglected effects when the splittings are small (as in ^{19}F) or with a need to consider excitation of cluster, core or both at high energies.

The model has also been applied to three-nucleon cluster states, and these can be subdivided into two classes, according as the core carries spin-0 or $\frac{1}{2}$. An example of the former is the system $^{19}F = {}^{16}O+t.{}^{19})$ A spin-orbit force is the only addition to the central part of the interaction which is permitted by symmetry considerations, and phenomenologically included by taking a derivative of the central term and choosing a strength to reproduce the splitting of the doublets,

$$V_{so}(R) = V_{so}\left(\frac{\hbar}{m_\pi c}\right)^2 \frac{1}{R}\left|\frac{dV(R)}{dR}\right| \underline{l}.\underline{\sigma} \qquad (1.29)$$

where the symbols have their usual meaning. V(R) is the folded central potential, and a strength, V_{so}, of a few MeV (2.5 MeV for the lowest $^{16}O+t$ band) is needed to fit the (this time large) spin-orbit splitting of the rotational centroids into doublets. The problem with the state of highest J is again apparent since the model predicts a $13/2^+$ state at about 7 MeV, whilst experimental candidates are seen at around 4.5 MeV and 10.5 MeV.

Finally, we have spins of $\frac{1}{2}$ on both cluster and core for the decomposition $^{18}F = {}^{15}N+{}^{3}He$, $^{18}F = {}^{15}O+t$ (which must be mixed), and $^{18}O = {}^{15}N+t.{}^{21})$ This is the most complicated system of all, with spin-orbit, spin-spin and tensor forces allowed and the possibility of isospin dependence strongly suggested in the phenomenology. This case, in particular, raises many points that a microscopic treatment might be able to elucidate, and is dealt with in Chapter 4.

The use of the BDV model in the mass 18-20 nuclei, suggests that it is capable of filling the role hoped for. Namely, the provision of a simple and intuitively appealing method of calculating measured

quantities. It is found, experimentally, that when the "heavy" core carries spin, the resulting spin-orbit splitting is small (see, for example, the alpha cluster state spectrum in ^{19}F, and the splittings attributed to spin-orbit forces in the alpha cluster spectrum in ^{18}F). However, when it is the lighter component which carries spin, a far larger spin-orbit splitting is produced (as in the triton cluster states in ^{19}F, and the splitting attributed to spin-orbit forces in the trinucleon cluster states in ^{18}F and ^{18}O). Also, the alpha cluster states appear to be described better in the model than the trinucleon cluster states, as would be expected on consideration of the free alpha particle and trinucleon binding energies of 28 MeV and 8 MeV respectively. These observations, together with the strengths and sometimes origins of the non-central forces acting between the two constituents of a cluster state are the sort of things we hope to understand and explain at a more basic level in a microscopic approach. In addition, certain limitations due to approximations implicit in the model may become apparent, and enable a more thorough physical understanding to be achieved of this small but important subset of states in the light nuclei.

CHAPTER 2

ALPHA CLUSTER STATES IN ^{19}F

$^{19}F = {}^{15}N+\alpha$

2.1 Experimental Evidence for Alpha Cluster States in ^{19}F.

If we make the assumption that mixing with trinucleon cluster states (having a cluster structure $^{16}O+t$) is generally unimportant, the signature of an alpha cluster state in ^{19}F should be strong, selective excitation in alpha transfer to ^{15}N, together with large alpha decay widths for those levels above the alpha emission threshold (about 4 MeV). The earliest experiment of this type was performed by Middleton et al.,[22] namely $^{15}N(^{7}Li,t)^{19}F$, and clearly selected the $\frac{1}{2}^-$ at 0.11 MeV, the $\frac{5}{2}^- - \frac{3}{2}^-$ doublet at 1.35 and 1.45 MeV, the $\frac{9}{2}^- - \frac{7}{2}^-$ doublet at 4.04 and 4.00 MeV and the $\frac{13}{2}^-$ state at 8.29 MeV (see Fig. 1). Some uncertainty surrounds the identification of this latter state's partner having $J^\pi = \frac{11}{2}^-$, but a candidate is seen in the $^{15}N(^{13}C,^{9}Be)^{19}F$ experiment of Pilt et al.,[23] which is now thought to be the cluster model $\frac{11}{2}^-$ at 8.95 MeV, although some problems still persist.[19] The higher bombarding energy of 105 MeV in this experiment, precluding any fluctuating compound contributions which might have been present in the $(^{7}Li,t)$ transfer, was considered to be the decisive improvement. The $\frac{17}{2}^- - \frac{15}{2}^-$ doublet at 12.26 and 12.67 MeV was also detected by them.

Subsequently, Bradlow et al.[4] have confirmed the locations of the members of this band, analogous to the ground state band in ^{20}Ne,

in their work on the (^{13}C,^{9}Be) and (^{11}B,^{7}Li) transfer reactions. Their evidence for a second higher-lying positive-parity band is less definitive, since the L = 1,3 members are not favoured kinematically, whilst selective excitations are evident at higher energies but no spin-parity assignments made. Consequently, we restrict our attention to the negative-parity band shown in Fig. 1 which is now established with some confidence.

2.2 Phenomenological Model of $^{19}F = {}^{15}N+\alpha$.^{19})

If the cluster and core remain in their ground states, having intrinsic angular momenta of $\frac{1}{2}$ and 0 respectively, it is clear from simply requiring the interaction between them to be invariant under space inversion and time reversal that only central and spin-orbit forces are possible. It is equally clear from the experimental data that the splitting of the doublets formed when the orbital and intrinsic angular momenta are coupled ($J = L \pm \frac{1}{2}$) is very small and highly irregular. Since the phenomenological model only makes statements about the allowed form of the potential, and sometimes seeks to parametrize its strength by taking certain matrix elements of it to be constant, it will be unable to reproduce the finer details of this spectrum. Indeed, we expect these details to be a good indicator of the importance of effects that have been neglected such as mixing with other cluster or shell model states, or threshold effects for the $\frac{7}{2}^- - \frac{9}{2}^-$ doublet which straddles the α emission threshold of 4.013 MeV. Since the spin-orbit force is obviously not the dominant perturbation on the central potential in this case, these and other discarded effects

may well be able to make their presence felt. Therefore, the phenomenological approach contents itself with the use of a central interaction to find the energies of the centroids of the doublets, and subsequently employs the wavefunctions generated in this potential to evaluate the static and dynamic electromagnetic properties of these states.

It is inconvenient to have a cluster-core potential which is only available as a tabulated series of numbers for different separation distances, so a parametrization of the folded potential is made. The shape chosen is a symmetrized form of the Woods-Saxon potential, namely

$$V(R) = V_o \left(\frac{1 + \cosh R_o/a_o}{\cosh R/a_o + \cosh R_o/a_o} \right) \qquad (2.1)$$

By suitable choice of R_o and a_o it is possible to obtain a potential bearing a very close resemblance to the folded one, exhibiting similar rotational spectra with V_o assuming the role of $\bar{f}$ in eq. 1.11 (i.e. being varied from band to band to fit a well identified level and then held constant in that given band). For large R this potential approaches the Woods-Saxon form asymptotically, and has the desirable feature of a zero-valued derivative at the origin (so a particle placed there feels no force).

The rotational band appropriate to this model is shown in Fig. 1 and was obtained by applying the "oscillator rule" to allow for the major requirements of the Pauli principle as follows:

$$2N+L = \sum_{i=1}^{4} (2n_i + l_i) = 8 \qquad (2.2)$$

for the lowest lying band. Although there is room in the p-shell for a single cluster nucleon, this configuration would correspond to a 3p-state and, since we are only concerned with alpha cluster states on

this occasion, we put the whole cluster into the (sd)-shell by applying eq. (2.2). The values to be used for the parameters in eq. (2.1) are

V_o = -172 MeV

R_o = 2.25 fm

a_o = 0.8 fm

It should be noted that the last two parameters are chiefly responsible for determining the moment of inertia of the system, and that these same values can be used (in conjunction with different depths, V_o) to produce analogous rotational bands in ^{20}Ne and ^{18}F. This similarity gives credence to the physical picture of a cluster-core system, where similar moments of inertia for ^{14}N, ^{15}N and $^{16}O+\alpha$ systems would be expected. The model places the 8^+ (highest spin) state far too high, but fits the remaining centroids well.

2.3 Semimicroscopic Treatment of $^{19}F = {}^{15}N+\alpha$.

Just as we did not expect the phenomenological model to be able to explain the finer details of the alpha cluster spectrum in ^{19}F, we suppose that the more microscopic approach we propose will also be inadequate in this respect. However, we feel that it is instructive to perform the calculation nevertheless for the following reasons. It may give some better appreciation of the reasons for the smallness of the spin-orbit splitting and also an indication of the size of correction necessary to account for the approximations made in the model (as mentioned in the last section). Also, it will allow us to develop a method of building up a cluster-core potential from a cluster-nucleon potential

in a particularly simple case which is free from the complications of the systems to be treated later. By this is meant the possibility of treating the core ground state as a single p-shell hole in ^{16}O, and using a cluster-nucleon potential containing only two terms (central and spin-orbit) knowing that the resulting cluster-core potential can also only contain two similar terms. We now present a semimicroscopic model to be used in a generalized form applicable to a core containing A_1 particles being orbited by a cluster of A_2 particles.

2.3.1 The Microscopic Model.

If we assume that two-body forces are sufficient for a description of the interaction between nucleons in the nucleus, the many-body Hamiltonian, H, for an (A_1+A_2)-nucleon system can be written

$$H = \sum_{i=1}^{A_1+A_2} \frac{p_i^2}{2m_n} + \sum_{i<j} V_{ij} \qquad (2.3)$$

where m_n is the nucleon mass, $\underline{p}_i$ the momentum of the ith nucleon and V_{ij} the interaction between nucleons i and j. For describing states consisting of an A_2-nucleon cluster coupled to an A_1-nucleon core this may be approximately decomposed as

$$H \approx H_{A_1} + H_{A_2} + H_{rel} \qquad (2.4)$$

where H_{A_1} and H_{A_2} are the internal Hamiltonians for the core and cluster and H_{rel} depends only on their relative coordinates. This approximate Hamiltonian will have eigenfunctions which may be written as a sum of product states of the form,

$$\Psi_{JM} = \phi(\underline{A}_2) \sum_{M'(M'')} \langle SM'LM'' | JM \rangle \phi_{SM'}(\underline{A}_1) \psi_{LM''}(\underline{R}) \qquad (2.5)$$

where the intrinsic angular momentum of the system, $\underline{S}$, couples with the orbital angular momentum of the cluster about the core, $\underline{L}$, to give a total angular momentum $\underline{J}$, $\phi_{SM'}(\underline{A}_1)$ is a fully antisymmetrized core ground state wavefunction, $\phi(\underline{A}_2)$ represents the ground state of the cluster and $\psi_{LM''}(\underline{R})$ describes the relative motion of the two.

The proposed scheme is to derive an effective cluster-core potential, V_{Cc} contained in H_{rel}, from a cluster-nucleon interaction, $V_{cn}^{(i)}$, by summing over all A_1 core nucleons. Since we are attempting to approximate a fully antisymmetric (A_1+A_2) particle wavefunction, the cluster-nucleon potential should ideally contain some of the effects due to exchange of nucleons between the two components. An effective interaction which might be expected to meet this requirement is the real part of the phenomenological optical potential, as used for cluster-nucleon elastic scattering up to energies of the order of the Fermi energy in the core.

The requirement of the Pauli principle, that no two identical particles occupy the same state, is discussed in section 1.3 and catered for by applying the restriction

$$\sum_{i=1}^{A_2} (2n_i + l_i) = 2N+L \geq 2A_2 \qquad (1.13)$$

which means putting the cluster into the (sd) shell and giving all $2A_2$ available quanta to the relative motion (no cluster or core excitation). The lowest lying alpha cluster band in ^{19}F will thus

have 8 quanta allowing relative orbital angular momenta of L = 0,2,4,6,8 which correspond to N = 4,3,2,1 or 0 nodes in the radial wavefunction. For this particular system the ^{15}N core ground state is approximated as a $p_{\frac{1}{2}}$ hole in the ^{16}O closed shell $|0\rangle$;

$$|^{15}N \; S(=\tfrac{1}{2})M, T(=\tfrac{1}{2})M_T\rangle = b^{\dagger}_{\frac{1}{2}M\frac{1}{2}M_T}|0\rangle \qquad (2.6)$$

where the hole creation operator is related to a particle annihilation operator by $b^{\dagger}_{\frac{1}{2}M\frac{1}{2}M_T} = (-)^{\frac{1}{2}+M+\frac{1}{2}+M_T} a_{\frac{1}{2}-M\frac{1}{2}-M_T}$, with M and M_T being angular momentum and isospin projections for "spin" and isospin of $\frac{1}{2}$. The final ingredient needed to build up an effective cluster-core potential is a phenomenological cluster-nucleon potential. In the case of an alpha cluster the most general form for the nuclear part of its interaction with a nucleon contains two isoscalar terms (viz. central and vector spin-orbit interactions). Although most fits to scattering data only employ a central potential we shall see that it is necessary to retain the spin-orbit force in order to obtain a similar term in the final cluster-core potential. Since we are trying to discover how the spin-orbit interaction contributes to the observed splitting of the already mentioned doublets in ^{19}F it is necessary to retain both possible terms in the alpha nucleon potential.

2.3.2 The Effective Cluster Core Potential.

In this subsection we proceed with our plan of deriving an effective cluster-core potential by summing the interactions between the alpha particle and each of the core nucleons. We take the α-nucleon interaction to be

$$V_{\alpha n}^{(i)} = U_c(|\underline{r}_i - \underline{R}|) + U_{LS}(|\underline{r}_i - \underline{R}|)\, \underline{l}_{rel}^{(i)} \cdot \underline{S}_i \qquad (2.7)$$

here $\underline{R}$ and $\underline{r}_i$ are the position vectors of the alpha particle and the ith nucleon with respect to the centre of the core, $\underline{s}_i$ is the spin of the ith nucleon and $\ell_{rel}^{(i)}$ is its angular momentum relative to the alpha particle. We make tensor decompositions of the radial functions U_c and U_{LS} as follows (Appendix I)

$$U(|\underline{r}_i - \underline{R}|) = \sum_{\ell} (2\ell+1)\, U_\ell(r_i, R)\, C_\ell(\hat{\underline{R}}) \cdot C_\ell(\hat{\underline{r}}_i) \qquad (2.8)$$

where C_ℓ are spherical tensors of rank ℓ defined by

$$C_\ell^m(\hat{\underline{r}}) = \sqrt{\frac{4\pi}{2\ell+1}}\, Y_\ell^m(\hat{\underline{r}}) \qquad (2.9)$$

and

$$U_\ell(r_i, R) = \frac{1}{2}\int_{-1}^{1} U(|\underline{r}_i - \underline{R}|)\, P_\ell(\cos\theta)\, d(\cos\theta) \qquad (2.10)$$

with $\cos\theta = \hat{\underline{r}}_i \cdot \hat{\underline{R}}$. The tensors C_ℓ are more convenient for our purposes then the spherical harmonics Y_ℓ because they are simply related to the spherical components of the radius vectors by

$$\underline{r}^m = r\, C_1^m(\hat{\underline{r}}) \qquad (2.11)$$

We may write $\underline{\ell}_{rel}^{(i)} \cdot \underline{S}_i$ in the form (Appendix II)

$$\underline{l}_{rel}^{(i)} \cdot \underline{S}_i = \frac{m_\alpha}{M}\underline{l}_i \cdot \underline{S}_i + \frac{m_n}{M}\underline{L} \cdot \underline{S}_i - \frac{m_\alpha}{M}\underline{R} \wedge \underline{p}_i \cdot \underline{S}_i - \frac{m_n}{M}\underline{r}_i \wedge \underline{P} \cdot \underline{S}_i \qquad (2.12)$$

with m_n and m_α the nucleon and alpha masses respectively, $M = m_n + m_\alpha$, $\underline{R}, \underline{P}, \underline{L}$ the position, momentum and orbital angular momentum

of the cluster relative to the core, and $\underline{r}_i, \underline{p}_i, \underline{\ell}_i$ similar quantities for the ith nucleon.

It is immediately apparent that those terms associated with the decomposition of the purely central parts of $V_{\alpha n}^{(i)}$ always occur as scalar products of tensors in the alpha coordinates with tensors in the nucleon coordinates. Although the terms coming from the spin-orbit term are not in such a simple form, it is possible by recoupling these tensors to produce a similar separation as follows. We are aiming to write the whole cluster-nucleon interaction as a sum of scalar products of rank-K spherical tensors in the various coordinates of alpha particle and nucleon (denoted generally by $\underline{\alpha}$ and $\underline{n}_i$) with respect to the core.

$$V_{\alpha n}^{(i)} = \sum_{\substack{\text{All tensors of} \\ \text{all ranks K}}}^{\prime} f_K(r_i, R) A_K(\underline{\alpha}) \cdot T_K(\underline{\Omega}_i) \qquad (2.13)$$

This interaction gives a contribution to the energy of the system of

$$\left\langle \phi_{S=\frac{1}{2}}(^{15}N, \underline{\Omega}_j) \psi_L(\underline{R}) (SL) J \middle| \sum_{i=1}^{15} V_{\alpha n}^{(i)} \middle| \phi_{S=\frac{1}{2}}(^{15}N, \underline{\Omega}_j) \psi_L(\underline{R}) (SL) J \right\rangle \qquad (2.14)$$

We may now define a new rank-K spherical tensor, N_K, to enable us to rewrite this expression in the form

$$\left\langle \psi_L(\underline{R}) (SL) J \middle| \sum_K A_K(\underline{\alpha}) \cdot N_K \middle| \psi_L(\underline{R}) (SL) J \right\rangle \qquad (2.15)$$

where

$$N_K^Q = \left\langle \phi_{S=\frac{1}{2}}(^{15}N, \underline{\Omega}_j) S(M+Q) \middle| \sum_{i=1}^{15} f_K(r_i, R) T_K^Q(\underline{\Omega}_i) \middle| \phi_{S=\frac{1}{2}}(^{15}N, \underline{\Omega}_j) SM \right\rangle \qquad (2.16)$$

Application of the Wigner-Eckart theorem enables us to write the tensor N_K in terms of the equal rank tensor formed from the spin of the core, $\underline{S}$, as follows;

$$N_K^Q = \frac{\langle \phi_{S=1/2}(^{15}N,\underline{\Omega}_i) \left\| \sum_{i=1}^{15} f_K(r_i,R) T_K(\underline{\Omega}_i) \right\| \phi_{S=1/2}(^{15}N,\underline{\Omega}_i) SM \rangle S^Q}{\langle S=\tfrac{1}{2} \| S_K \| S=\tfrac{1}{2} \rangle} = F_K(R) S_K^Q \quad (2.17)$$

We now have an interaction written in terms of induced operators in the space of the core-spin, so the effective cluster-core potential can be written

$$V_{Cc} = \sum_K F_K(R) A_K(\underline{\alpha}) . S_K \quad (2.18)$$

Our next goal is to rewrite the alpha-nucleon potential in the form of eq. 2.13 (which means identifying and isolating the tensors $T_K(\underline{n}_i)$) and to evaluate the reduced matrix elements in eq. 2.17 to obtain $F_K(R)$. We shall find that simple symmetry arguments allow us to pick out in advance which $T_K(\underline{n}_i)$ can appear, and so we tackle this second part of the problem first. We also note that since we are assuming the core to remain in its ground state, with intrinsic angular momentum $S=\frac{1}{2}$, the only possible values of K are 0 and 1. Furthermore, in the case K=1, the vector $A_1(\underline{\alpha})$ must be proportional to the angular momentum $\underline{L}$ of the alpha particle ($\underline{R}$ and $\underline{P}$ being ruled out by parity and time reversal considerations), whilst K=0 obviously gives a contribution to the central part of the effective cluster-core potential.

2.3.3 The Reduced Matrix Elements of $T_K(\underline{n}_i)$.

Since we are including a spin-orbit term in the alpha-nucleon potential, we must consider the spherical tensor $T_K(\underline{n}_i)$ to be formed

by coupling one spherical tensor in the nucleon space coordinates R_{k_1} (of rank k_1), with another in the nucleon spin coordinates, S_{k_2} (of rank k_2). In the notation of Brink and Satchler [24], $T_K = T_K(R_{k_1}, S_{k_2})$, and we note immediately that $k_2=0$ for terms derived from the central part of $V_{\alpha n}^{(i)}$ whilst $k_2=1$ for those derived from the spin-orbit part. We now evaluate reduced matrix elements of T_K between ^{15}N ground state wavefunctions, which we consider as a $p_{\frac{1}{2}}$ hole in an inert ^{16}O core.

$$\langle {}^{15}N;\, S=\tfrac{1}{2} \| T_K \| {}^{15}N;\, S=\tfrac{1}{2} \rangle = \langle j_1^{-1} \| T_K \| j_1^{-1} \rangle \qquad (2.19)$$

where $|j_1^{-1}>$ represents a hole with intrinsic angular momentum of $\frac{1}{2}$. We now apply particle-hole conjugation [25] to express the single-hole matrix element in eq, 2.19 in terms of a single-particle matrix element.

$$\langle j_1^{-1} \| T_K \| j_1^{-1} \rangle = \langle 0 \| T_K \| 0 \rangle \delta_{K,0} - \langle j_1 \| \tilde{T}_K \| j_1 \rangle \qquad (2.20)$$

where $\tilde{T}_K$ is the time-reversed tensor operator $(\mathcal{T}^{-1} T_K \mathcal{T})^\dagger$ and $\mathcal{T}$ is the time reversal operator. The core expection value only contributes for scalars, and represents an ^{16}O-α potential, to which a hole-α potential is being added. As noted in section 1.5 the ^{16}O-α potential is purely central, and this is expressed in eq. 2.20 by the Kronecker delta, $\delta_{K,0}$. We decompose the contribution from the hole into its space and spin components [24] to obtain:

$$\langle {}^{15}N \| T_K \| {}^{15}N \rangle_h = -\alpha(j_1 K \ell s) \begin{Bmatrix} j_1 & j_1 & K \\ \ell & \ell & k_1 \\ s & s & k_2 \end{Bmatrix} \langle \ell \| \tilde{R}_{k_1} \| \ell \rangle \langle s \| \tilde{S}_{k_2} \| s \rangle \qquad (2.21)$$

where we define $\alpha(abcd) = \sqrt{(2a+1)(2b+1)(2c+1)(2d+1)}$, the quantity in curly brackets is the Wigner 9-j symbol, and the reduced matrix elements

on the right are taken between single-particle states with $\ell=1$ (in the p-shell) and $s=\frac{1}{2}$. If we use the symmetry property of the 9-j symbol that it is multiplied by

$$(-1)^{\Sigma \text{ arguments of 9-j symbol}}$$

on interchanging any two rows or columns, to interchange the first and second columns, which are identical, we see that the term will vanish unless $(K+k_1+k_2)$ is even, since we know that $j_1=\frac{1}{2}$, $s=\frac{1}{2}$ and $\ell=1$. This phase is basically expressing the properties of $T_K(R_{k_1},S_{k_2})$ under parity and time reversal transformations. If $k_1=1$, parity only permits $R_{k_1=1}$ to be the nucleon angular momentum $\underline{\ell}_i$ which is odd under time reversal. Similarly, since an odd k_2 means that $S_{k_2}=S_1=\underline{s}$, this is also odd under time reversal. These considerations allow us to remove the time-reversed operators from eq. 2.21 and write;

$$\langle {}^{15}N\|T_k\|{}^{15}N\rangle_h = (-1)^{1+K}\alpha(j_1 K \ell s)\begin{Bmatrix} j_1 & j_1 & K \\ \ell & \ell & k_1 \\ s & s & k_2 \end{Bmatrix}\langle \ell\|R_{k_1}\|\ell\rangle\langle s\|S_{k_2}\|s\rangle \qquad (2.22)$$

The selection rule that $K+k_1+k_2$ be an even integer restricts the possible combinations of tensor ranks (K,k_1,k_2) to the following;

SCALAR	(0,0,0)	(0,1,1)	
VECTOR	(1,0,1)	(1,2,1)	(1,1,0)

We have already noted that in the case $k_1=1$, the tensor R_{k_1} can only be proportional to $\underline{\ell}_i$. Hence, since the interaction being used (eq. 2.7 together with eqs. 2.8 and 2.12) only permits $\underline{\ell}_i$ to appear combined with $\underline{s}_i$ the third vector combination of (1,1,0) can not be obtained in this model. So, the four remaining combinations can be written as signifying contributions from the following tensors;

SCALAR	1	$\underline{\ell}\cdot\underline{s}$
VECTOR	$\underline{s}$	$T_1(C_2(\hat{\underline{r}}),\underline{s})$

where the nucleon subscripts, i, have been dropped. We are now in a position to tackle the remaining part of the problem, which is to select these "allowed" terms from the tensor decompositions of $U_c(|\underline{r}-\underline{R}|)$ and $U_{LS}(|\underline{r}-\underline{R}|)\underline{\ell}_{rel}.\underline{s}$ and thus obtain a cluster-core potential of the form

$$V_{Cc} = V_0(R) + V_1(R)\,\underline{L}.\underline{S} \qquad (2.23)$$

2.3.4 The Form Factors V_o and V_1.

The reduced matrix elements of T_K contain integrals of the p-shell radial wavefunction R(r) with the components $U_{C_{(\ell)}}(r,R)$ and $U_{LS_{(\ell)}}(r,R)$ of the tensor decomposition (eq. 2.10). It is therefore convenient to define

$$F_{A_{(\ell)}}(R) = \int_0^\infty U_{A_{(\ell)}}(r,R)\,|R(r)|^2 r^2 dr \qquad (2.24)$$

where the subscript A will be used to indicate whether we are dealing with the central or spin-orbit radial term as shown above. Furthermore, when we recouple $C_1(\hat{\underline{R}}).C_1(\hat{\underline{r}})\underline{r}\wedge\underline{\rho}.\underline{s}$ (see eqs. 2.8 and 2.12) to obtain a term containing $\underline{L}$ we will introduce an additional factor r/R and on recoupling $C_1(\hat{\underline{R}}).C_1(\hat{\underline{r}})\underline{R}\wedge\underline{\rho}.\underline{s}$ to obtain a term involving $\underline{\ell}$ we introduce a factor R/r. Hence it is similarly convenient to define;

$$F^{\pm}_{LS_{(1)}}(R) = \int_0^\infty U_{LS_{(1)}}(r,R)\,|R(r)|^2 \left(\frac{R}{r}\right)^{\pm 1} r^2 dr \qquad (2.25)$$

The tensor decomposition of the central potential $U_c(|\underline{r}-\underline{R}|)$ gives only a single contribution to the effective cluster-core potential. This occurs for $\mathcal{L} = 0$ in eq. 2.8, and corresponds to the permitted combination of tensor ranks (0,0,0). Thus $A_K(\underline{\alpha}) = 1$, $R_{k_1} = U_{C_{(0)}}(r,R)$ and $S_{k_2} = 1$, so substitution in eq. 2.22 (the 9-j symbols for all the decompositions are listed in table 1) yields simply $- F_{C_{(0)}}(R)$ as a contribution to V_o in eq. 2.23.

By writing the spin-orbit force as we have done in eq. 2.12, we see that there are four terms, which must each be dealt with separately. (1) The term $\frac{m_\alpha}{M} \underline{\ell}.\underline{s}$ is very similar to the central term just dealt with since the ^{15}N states are eigenfunctions of the operator $\underline{\ell}.\underline{s}$. Once more only $\mathcal{L} = 0$ needs to be considered in eq. 2.8 and this time we have an operator with tensor rank combination (0,1,1), with $A_K(\alpha) = 1$, $R_{k_1} = U_{LS_{(0)}}(r,R)\underline{\ell}$ and $S_{k_2} = \underline{s}$. We must take care to remember that eq. 2.22 was written down for a rank-K tensor formed from a combination of rank-k_1 and rank-k_2 tensors according to the formula;

$$T_K^Q = \sum_{q_1 (q) q_2} \langle KQ | k_1 q_1 k_2 q_2 \rangle R_{k_1}^{q_1} S_{k_2}^{q_2} \qquad (2.26)$$

and that the scalar product $\underline{\ell}.\underline{s}$ when defined as a coupling of two rank-1 tensors to a rank-0 tensor in this way contains a factor of $-\sqrt{3}$. In general

$$R_{k_1} \cdot S_{k_1} = (-1)^{k_1} \sqrt{2k_1+1}\, T_0^0(k_1,k_1) \qquad (2.27)$$

Now, using eq. 2.22 with the knowledge that $\langle J||\underline{J}||J\rangle = \sqrt{J(J+1)}$ we get a contribution to V_o of

$$-(-\sqrt{3})\frac{m_\alpha}{M}\alpha\left(\tfrac{1}{2}0|\tfrac{1}{2}\right)\begin{Bmatrix}\frac{1}{2} & \frac{1}{2} & 0\\ 1 & 1 & 1\\ \frac{1}{2} & \frac{1}{2} & 1\end{Bmatrix}\langle \ell \| U_{LS_{(0)}}(r,R)\,\underline{\ell}\,\| \ell\rangle\langle s\|\underline{s}\|s\rangle$$

$$= \frac{m_\alpha}{M} F_{LS_{(0)}}(R) \qquad (2.28)$$

We note that this could have been obtained more simply by multiplying the central result (with appropriate mass factor) by the eigenvalue of $\underline{\ell}.\underline{s}$, namely $\frac{1}{2}[j_1(j_1+1)-\ell(\ell+1)-s(s+1)] = -1$, (since $j_1=\frac{1}{2}, s=\frac{1}{2}$ and $\ell=1$)

(2) So far we have only dealt with terms which contribute to V_o, but $\frac{m_n}{M}\,\underline{L}.\underline{s}$ can only contribute to the spin-orbit part of the effective cluster-core potential, V_{Cc}. There are two ways in which this can happen; one with $\mathcal{L} = 0$ and the other with $\mathcal{L} = 2$ in eq. 2.8. These will give operators $U_{LS_{(0)}}(r,R)\underline{L}.\underline{s}$ and $5U_{LS_{(2)}}C_2(\hat{\underline{R}}).C_2(\hat{\underline{r}})\underline{L}.\underline{s}$ respectively, and on taking their reduced matrix elements we will obtain contributions to V_1(in eq. 2.23). We can see immediately that this corresponds to the allowed tensor combinations (1,0,1) and (1,2,1) since K = 1 for terms involving $\underline{L}.\underline{S}$, and in the first case the nucleon operator is simply $\underline{s}$ ($k_1=0, k_2=1$) whilst in the second case it must be a rank-1 tensor formed from $C_2(\hat{\underline{r}})$ and $\underline{s}$ ($k_1=2, k_2=1$). Taking the $\mathcal{L} = 0$ term first

i) and using eq. 2.22 with the operator $\frac{m_n}{M}U_{LS_{(0)}}(r,R)\underline{s}$ yields

$$\frac{m_n}{M}\alpha\left(\tfrac{1}{2}\|\tfrac{1}{2}\right)\begin{Bmatrix}\frac{1}{2} & \frac{1}{2} & 1\\ 1 & 1 & 0\\ \frac{1}{2} & \frac{1}{2} & 1\end{Bmatrix}\langle \ell \| U_{LS_{(0)}}(r,R)\|\ell\rangle\langle s\|\underline{s}\|s\rangle$$

We must divide this by $\langle {}^{15}N;S=\frac{1}{2}||\underline{S}||{}^{15}N;S=\frac{1}{2}\rangle$ to obtain the contribution to V_1, which is therefore

$$-\frac{1}{3}\frac{m_n}{M}F_{LS_{(0)}}(R) \qquad (2.29)$$

ii) To handle the $\ell = 2$ term we need to recouple $C_2(\hat{\underline{R}})$ and $\underline{L}$ as done in appendix III to obtain an effective α-coordinate operator proportional to $\underline{L}$. As shown there the proportionality constant is $1/\sqrt{10}$, so incorporating this into eq. 2.22 gives a term

$$\frac{5}{\sqrt{10}}\frac{m_n}{M}\alpha\left(\tfrac{1}{2}\|\tfrac{1}{2}\right)\begin{Bmatrix}\frac{1}{2} & \frac{1}{2} & 1\\ 1 & 1 & 2\\ \frac{1}{2} & \frac{1}{2} & 1\end{Bmatrix}\langle \ell \| U_{LS_{(2)}}(r,R) C_2(\hat{\underline{r}}) \| \ell \rangle \langle s \| \underline{S} \| s \rangle$$

Using the relation $\langle \ell=1 \| C_2(\hat{\underline{r}}) \| \ell=1 \rangle = -\sqrt{2/5}$ and dividing out the reduced matrix element in the spin-coordinates gives a contribution to V_1 of

$$-\frac{2}{3}\frac{m_n}{M} F_{LS_{(2)}}(R) \qquad (2.30)$$

(3) The term $-\frac{m_\alpha}{M}\ \underline{R}_\Lambda \underline{p}.\underline{s}$ is more complicated to deal with, but on close examination is found to contribute only to the central term V_o. Setting $\ell=1$, and thus introducing a term $C_1(\hat{\underline{R}}).C_1(\hat{\underline{r}})$ enables us to recouple the alpha coordinates to a scalar (K=0), whilst we can recouple $C_1(\hat{\underline{r}})$ and $\underline{p}$ to $\underline{\ell}$ in the nucleon coordinates, so producing a term very similar to that in (1) belonging to the "allowed" combination of tensor ranks (0,1,1). With $\ell = 1$, the relevant operator is $-3\frac{m_\alpha}{M}\ U_{LS_{(1)}}(r,R)\ C_1(\hat{\underline{R}}).C_1(\hat{\underline{r}})\ \underline{R}_\Lambda \underline{p}.\underline{s}$, and the recoupling of appendix IV shows that the part of the nucleon operator of interest to us is $-\frac{m_\alpha}{M}\ \frac{R}{r} U_{LS_{(1)}}(r,R)\underline{\ell}.\underline{s}$. Substitution in eq. 2.22 yields a contribution to V_o of

$$-\sqrt{3}\frac{m_\alpha}{M}\alpha\left(\tfrac{1}{2}01\tfrac{1}{2}\right)\begin{Bmatrix}\frac{1}{2} & \frac{1}{2} & 0\\ 1 & 1 & 1\\ \frac{1}{2} & \frac{1}{2} & 1\end{Bmatrix}\langle \ell \| \frac{R}{r} U_{LS_{(1)}}(r,R)\underline{\ell} \| \ell \rangle \langle s \| \underline{S} \| s \rangle$$

where the factor of $-\sqrt{3}$ is again necessary to write the dot product, $\underline{\ell}.\underline{s}$ as a coupling of two rank-1 tensors to a scalar as in eq. 2.26. Finally we obtain

$$- \frac{m_\alpha}{M} F^{+}_{LS_{(1)}}(R) \qquad (2.31)$$

(4) The final term, $-\frac{m_n}{M}\underline{r}_\Lambda\underline{P}.\underline{s}$ is similarly complicated, but behaves analogously to the term $\frac{m_n}{M}\underline{L}.\underline{s}$, giving two contributions to the spin-orbit form factor, V_1. We have to set $\mathcal{L} = 1$, introducing the scalar product $C_1(\hat{\underline{R}}).C_1(\hat{\underline{r}})$, and it is then possible to recouple $C_1(\hat{\underline{R}})$ and $\underline{P}$ to obtain an alpha operator proportional to $\underline{L}$. In the nucleon coordinates we can couple $C_1(\hat{\underline{r}})$ and $\underline{r}$ to tensors of rank 0 and 2 (rank 1 does not belong to an "allowed" combination), and then couple this tensor with $\underline{s}$ to get a final tensor of rank 1. So, the terms of interest represent the rank combinations (1,0,1) and (1,2,1). The operator we start from is $-3\frac{m_n}{M}U_{LS_{(1)}}(r,R)C_1(\hat{\underline{R}}).C_1(\hat{\underline{r}})\ \underline{r}_\Lambda\underline{P}.\underline{s}$

In appendix V we show that this may be recoupled to give an effective operator of

$$-\frac{m_n}{M}\left(\frac{r}{R}U_{LS_{(1)}}(r,R)\right)\left\{\underline{s} + \frac{\sqrt{10}}{2}T_1(C_2,\underline{s})\right\} \qquad (2.31)$$

where $T_1(C_2\underline{s})$ is the rank-1 tensor operator formed by combining $C_2(\hat{\underline{r}})$ and $\underline{s}$ as in eq. 2.26. Substitution in eq. 2.22 gives;

$$-\frac{m_n}{M}\alpha\left(\tfrac{1}{2}\|\tfrac{1}{2}\right)\left[\begin{Bmatrix}\frac{1}{2} & \frac{1}{2} & 1\\ 1 & 1 & 0\\ \frac{1}{2} & \frac{1}{2} & 1\end{Bmatrix}\langle\ell\|\frac{r}{R}U_{LS_{(1)}}(r,R)\|\ell\rangle + \frac{\sqrt{10}}{2}\begin{Bmatrix}\frac{1}{2} & \frac{1}{2} & 1\\ 1 & 1 & 2\\ \frac{1}{2} & \frac{1}{2} & 1\end{Bmatrix}\langle\ell\|\frac{r}{R}U_{LS_{(1)}}(r,R)C_2(\hat{r})\|\ell\rangle\right]\langle s\|\underline{s}\|s\rangle \qquad (2.32)$$

and on dividing out the reduced matrix element $\langle s||\underline{s}||s\rangle$ by $\langle S=\frac{1}{2}||\underline{S}||S=\frac{1}{2}\rangle$ we get a contribution to V_1 of

$$-\frac{m_n}{M}\left(-\frac{1}{3}-\frac{2}{3}\right)F^{-}_{LS_{(1)}}(R)$$

or simply

$$\frac{m_n}{M}\bar{F}_{LS_{(1)}}(R) \tag{2.33}$$

When we collect all these contributions to the form factors V_o and V_1 we obtain the final expressions:

$$V_o(R) = \langle 0\|T_k\|0\rangle\delta_{k0} - F_{C_{(0)}}(R) + \frac{m_\alpha}{M}\left[F_{LS_{(0)}}(R) - \bar{F}^{+}_{LS_{(1)}}(R)\right] \tag{2.34}$$

where the first term is the ^{16}O-α central potential, so V_o will become shallower than that with the addition of the hole-alpha contribution, as we would expect for a ^{15}N-α central potential, and

$$V_1(R) = \frac{m_n}{M}\left[\bar{F}_{LS_{(1)}}(R) - \frac{2}{3}F_{LS_{(2)}}(R) - \frac{1}{3}F_{LS_{(0)}}(R)\right] \tag{2.35}$$

Even at this stage we can see that the cluster-core spin-orbit potential will not be very strong because it is built up of contributions from the alpha-nucleon spin-oribt potential (which is itself weak) and in addition it is multiplied by the mass factor $m_n/M = 1/5$.

2.3.5 Development of an Analytic Expression for $V_1(R)$.

The major goal of this chapter of illustrating the techniques employed in building up a cluster-core potential from a cluster-nucleon interaction in a particularly simple system which is free from the complications to be encountered in subsequent studies has already been achieved. It now remains to calculate the spin-orbit splitting of the

alpha cluster doublets in the model, and to see how far this goes towards reproducing the experimentally observed separations. This exercise should provide a good indication of the size and importance of neglected effects which can be borne in mind when evaluating the results of later calculations.

The phenomenological model has already provided a good effective central cluster-core potential (eq. 2.1 with subsequently listed values for the parameters) in the sense that it reproduces the centroids of the rotational band in good agreement with experiment (Fig. 1). Since we are only interested in the splittings of the doublets from these centroids we shall use the wavefunctions generated by this central potential, together with the form-factor $V_1(R)$ derived from an alpha-nculeon spin-orbit force, to calculate the perturbation on the rotational spectrum. (This question of the central potential will be dealt with more thoroughly in the next chapter where it is more important because the central part of the alpha-nucleon force also contributes to one of the non-central perturbing forces as well as the central potential).

The remaining question is the choice of a spin-orbit part of an alpha-nucleon potential and the evaluation of the integrals (2.24) and (2.25). Since we wish to keep the calculation analytic, as far as possible, we use oscillator wavefunctions to describe the $p_{\frac{1}{2}}$ hole in $^{16}0$. The oscillator length parameter, "b", is chosen to fit the charge radius of $^{16}0$. This gives the value b = 1.72 fm. The radial p-shell wavefunction is therefore approximated by the expression;

$$R(r) = \sqrt{\frac{8}{3\sqrt{\pi}}} \frac{r}{b} e^{-r^2/2b^2} \qquad (2.36)$$

The normalization of this function is such that

$$\int_0^\infty |R(r)|^2 \frac{r^2 dr}{b^3} = 1 \qquad (2.37)$$

To obtain a spin-orbit contribution to the alpha-nucleon potential we investigate the fits to alpha-nucleon scattering data, which indicate that such a term is very small. In fact, only one article was found in which a spin-orbit term was included [26]) One particular parametrization there, used a Gaussian, which is particularly desirable in the calculation of the form factor $V_1(R)$ since it is possible to find the tensor decomposition (eq. 2.10) of this function in closed form, and also when used in conjunction with oscillator wavefunctions it allows the integrals (eq. 2.24 and eq. 2.25) to be evaluated analytically. We use this potential of Sack et al. to deal with the spin-orbit form factor but note that many more recent parametrizations of the scattering data in Gaussian form, employ a substantially smaller width for the central term than the 2.3 fm of Sack et al. As an alternative procedure we take the "best" of these more recent Gaussian potentials[27,28]) (which doesn't contain a spin-orbit term) and use its width in our own case. We then fit a spin-orbit strength to this term by looking at the $p_{1/2}$-$p_{3/2}$ doublet of resonances seen in low-energy neutron-alpha scattering ($p_{3/2}$ at around 0.89 MeV with a width of about 0.6 MeV and $p_{1/2}$ around 4.9 MeV with a width of about 4.0 MeV[29])) Since these levels are quasi-bound states of ^{5}He we can obtain an approximate value for the strength of the alpha-nucleon spin-orbit term by treating the neturon as weakly bound to the alpha particle. Using p-shell oscillator wavefunctions (eq. 2.36) with length parameter b=1.31 fm appropriate to ^{4}He, this procedure yields a strength of

7.0 MeV for a Gaussian form of width 1.9 fm. We note that this method of fitting the strength differs from that of Sack et al., where $P_{1/2}$ and $P_{3/2}$ phase shifts are fitted in elastic proton-alpha scattering. So, we use two spin-orbit terms to evaluate $V_1(R)$, which have the analytic form;

$$-U_{LS}e^{-x^2/a^2} \tag{2.38}$$

where

$$U_{LS} = 5.85\ \text{MeV} \qquad a = 2.3\ \text{fm} \tag{2.39}$$

(which is the spin-orbit term from the potential of Sack et al.) and

$$U_{LS} = 7.0\ \text{MeV} \qquad a = 1.9\ \text{fm} \tag{2.40}$$

Finally, we list the analytic expressions obtained for $\bar{F}_{LS_{(1)}}(R)$, $F_{LS_{(0)}}(R)$ and $F_{LS_{(2)}}(R)$ to be used in eq. 2.35 which result from using eqs. 2.36 and 2.38

$$F_{LS_{(0)}}(R) = -\frac{U_{LS}}{3}\left(\frac{a^2}{a^2+b^2}\right)^{5/2}\left\{3+\frac{2b^2R^2}{a^2(a^2+b^2)}\right\}e^{-\frac{R^2}{a^2+b^2}} \tag{2.41}$$

$$F_{LS_{(2)}}(R) = -\frac{2U_{LS}}{3}\left(\frac{a^2}{a^2+b^2}\right)^{5/2}\frac{b^2R^2}{a^2(a^2+b^2)}\,e^{-\frac{R^2}{a^2+b^2}} \tag{2.42}$$

$$\bar{F}_{LS_{(1)}}(R) = -\frac{2U_{LS}}{3}\frac{b^2}{a^2}\left(\frac{a^2}{a^2+b^2}\right)^{7/2}\left\{\frac{5}{2}+\frac{b^2R^2}{a^2(a^2+b^2)}\right\}e^{-\frac{R^2}{a^2+b^2}} \tag{2.43}$$

2.3.6 Calculation of the Spectrum.

The single-particle Schrödinger equation is solved for a state of given L (and hence of given N, since the condition 2N+L = 8 is

applied) in the potential

$$V(R) = V_o(R) + V_{COUL}(R) \qquad (2.44)$$

with $V_o(R)$ given by

$$V_o(R) = -V_o\left[\frac{1 + \cosh R_o/a_o}{\cosh R/a_o + \cosh R_o/a_o}\right] \qquad (2.45)$$

and V_o = 172 MeV, R_o = 2.25 fm, a_o = 0.8 fm. The Coulomb potential used was that resulting from treating the core as a uniform spherical charge distribution of radius 3.1 fm and the alpha particle as a pointlike charge. Such a Coulomb potential:

> "yields excellent agreement for the Coulomb displacement energy for the ^{19}F and ^{19}Ne ground states (3.262 MeV, compared to the experimental value of 3.257 MeV)" [19])

For those high-lying states which are only quasi bound, Jackson's procedure [30]) is followed. This involves finding the position R_B and height E_B of the potential barrier and setting $V(R) = E_B$ for $R > R_B$. This allows us to treat all the states as bound, and only introduces minimal errors in our evaluation of their energies. The wavefunctions generated by this procedure were then used to calculate the spin-orbit splitting, by evaluating matrix elements of the operator $V_1(R)\underline{L}.\underline{S}$. ($\underline{L}$ is the orbital angular momentum of the alpha cluster about the core, and $\underline{S}$ the spin of the core). The energy shift from the rotational centroid due to such an operator is given by

$$\Delta E = \tfrac{1}{2}\left[J(J+1) - L(L+1) - S(S+1)\right]\delta_L \qquad (2.46)$$

where

$$\delta_L = \int_0^\infty |\chi_L(R)|^2 V_1(R)\, dR \qquad (2.47)$$

where J is the total angular momentum of the final states, and $\chi_L(R)$ are the radial wavefunctions of relative motion between cluster and core. The quantities δ_L for both the functions $V_1(R)$ are shown in table 2. (The negative sign indicating that the state with J = L+S is to be found below that with J = L-S). The resulting spectra are not plotted in Fig. 1, since the splitting of the doublets is so small that the scale of the figure would not enable them to be distinguished from the spectrum of centroids of the phenomenological model.

2.4 Summary and Conclusions.

In this chapter a technique has been illustrated which allows an effective cluster-core potential to be derived from a cluster-nucleon potential by summing the latter over all the nucleons in the core. The particular case dealt with involved a single hole of known angular momentum in an inert ^{16}O core, and the potentials only contained central and spin-orbit terms. This will provide a good basis from which to proceed in a consideration of more complicated cluster-core systems which involve two holes in a core (e.g. the system $^{18}F = {}^{14}N+\alpha$) and/or more terms in the potentials, such as tensor forces, in the following chapters.

In contrast to some of the later calculations, all the members of the lowest negative parity band in ^{19}F are thought to be experimentally identified. Although this denies the cluster model the opportunity to predict the positions and properties of "new" high-spin states, it does illustrate the kind of discrepancies between its predictions and observation which may occur, due to the approximations made. Of

particular interest is the effect of mixing between cluster states and those of a different structure, since this would be particularly difficult to calculate in the model, as we are not able to expand the cluster states in terms of shell-model states (thus enabling us to calculate matrix elements of various operators between cluster and shell model states). Also, possible excitation of cluster and/or core is ignored. Except for the highest $\frac{17}{2}^-$ - $\frac{15}{2}^-$ doublet, where mixing with other states is thought to be very important, these neglected effects do not appear to be causing big problems. Discrepancies of around 100 keV in the lower part of the spectrum (below about 5 MeV) rising to around 0.5 MeV at higher excitation energies are noted, and even though there is uncertainty about the precise size of the spin-orbit splitting of the doublets, its smallness is readily explained in terms of the strength of the alpha-nucleon spin-orbit force and the ratio of masses $m_n/M = 1/5$. We can now make a semi-microscopic calculation of the fitting parameters in various other phenomenological cluster-model calculations, in which the forces being derived are thought to be the dominant perturbations of the central potential, with some confidence that the effects being neglected are not very large.

CHAPTER 3

ALPHA CLUSTER STATES IN ^{18}F

$^{18}F = {}^{14}N+\alpha$

3.1 Experimental Evidence for Alpha Cluster States in ^{18}F.

The spectrum of ^{18}F is very rich in states and has been the subject of intensive experimental investigation in recent years.[1] As in the case of ^{19}F we are interested in states which are strongly excited in alpha transfer reactions (this time the transfer is to a ^{14}N target) and, (if above the α-emission threshold) have large alpha decay widths, despite the possibility of decaying through many other open channels.

In searching through the experimental data to identify these alpha cluster states, we have to bear in mind that they have been treated in terms of the simple rotational model [32,33] with a notation which is not appropriate to the model we are using. The rotation notation labels one set of positive parity states (with 4p-2h configurations) as belonging to a band with $K^\pi = 1^+$, (with $J^\pi = 1^+,2^+,3^+,4^+,5^+,6^+,7^+,8^+,9^+$) and another set of states (with J^π of $1^+,3^+,5^+,7^+$) as members of a second band with $K^\pi = 0^+$. In the cluster model, these states correspond to the lowest-lying set of states, having 8 quanta in the relative motion of cluster and core, and their angular momenta result from coupling the orbital angular momentum of the alpha (L=0,2,4,6,8) to the intrinsic angular momentum of the core (S=1). So, the rotational model predicts some states of the $K^\pi = 1^+$ band to have $J^\pi = 1^+,2^+,3^+$ which in the cluster model come from L=0xS=1 $\rightarrow$ J=1^+ and L=2xS=1 $\rightarrow$J=2^+3^+ whilst a state of the $K^\pi = 0^+$ band with $J^\pi = 1^+$, comes, in the cluster

model from the remaining combination of $L=2 \times S=1 \rightarrow J=1^+$. This example illustrates the inappropriateness of the K^π notation to the cluster model, in which triplets are obtained by coupling L with S, and K has no natural interpretation. However, for convenience of reference to the experimental data we continue to use the K^π notation despite this drawback.

The experimental data for ^{19}F was sufficient to provide "good" candidates for all the states in the lowest lying alpha cluster band, but this is not the case for ^{18}F, so more speculation will be involved. The earliest alpha transfer reaction populating states in ^{18}F to be performed was $^{14}N(^7Li,t)^{18}F$ by Middleton et al. [34]) which was able to provide alpha cluster state candidates up to about 7 MeV excitation in ^{18}F. Six states were particularly strongly excited, and "accounted for more than half the summed cross-section observed at 15^o for all transitions to all states below 7 MeV". Subsequently, one of these six has been idnetified as a 2^- trinucleon cluster state, but the other five are now known to be predominantly 4p-2h states with J^π of $1^+, 2^+, 3^+, 4^+, 5^+$ [35]) at 1.701, 2.524, 3,355, 5.299 and 5.565 MeV respectively (see Fig. 4) and are thus strong alpha cluster caniddates. There are some weaker possibilities resulting from this work, including a very strongly excited state of unknown spin-parity at 7.26 MeV and two 1^+ states at 3.724 MeV and 4.361 MeV(spin-parity of the latter was recently confirmed by Davis and Abegg [36])) which are in the region expected for states formed from coupling L=2 for the alpha with S=1 for ^{14}N. In addition, we note that although Middleton claims that he could not locate the third state with parentage in the 4^+ state of ^{20}Ne, he was looking for a state with the wrong J^π having mis-assigned the 4^+ level at 5.299 MeV as 3^+. Hence, the two fairly strongly excited 3^+ levels at 6.30 MeV

and 6.48 MeV are possible band members which were overlooked.

There is also a level at 6.803 MeV which has J^{π} of $1^+,2^+$ or 3^+ which Rolfs et al. [37]) conclude would have a more complicated structure than 2p-0h if finally proved to be 3^+. We hope that the ensuing calculation can throw some extra light on the claims of these speculative states for membership of the lowest alpha cluster band. We should also mention that in an extensive analysis of many states in ^{18}F, Rolfs et al. [37]) conclude that the two levels at 3.724 MeV and 4.361 MeV (both 1^+ candidates) have substantial 2p-0h components, and Sens et al. [38]) believe the two 3^+ candidates at 6.30 MeV and 6.48 MeV to have a more complicated structure probably like 4p-2h and indeed suggest that they may carry the strength of the 3^+ expected in the triplet with parentage in the 4^+ state of ^{20}Ne.

Finally, in a later paper, Sens et al. [39]) suggest that the level seen by Middleton et al. [34]) at 7.26 MeV with such a large cross-section and unknown spin-parity is acutally identical to a 3^- state they have located at 7.289 MeV. This problem of identification on the basis of selectivity in the $^{14}N(^7Li,t)^{18}F$ reaction seems to be in part due to competing non-alpha-transfer mechanisms causing other states to be significantly excited, and also perhaps to some of the states not being in pure 4p-2h configurations. The former could be eliminated by performing the reaction at higher energies either with the same beam or one of heavier ions, as was done in the case of alpha transfer to ^{15}N.

In fact the $^{14}N(^7Li,t)^{18}F$ reaction has been repeated by Cobern and Parker [40]) (with a beam energy of 36 MeV instead of the 15 MeV used by Middleton et al.) and they have found two selectively excited levels at 9.58 MeV and 11.22 MeV whose spin-parity values are deduced to be 6^+

7^+ respectively from the slopes of the angular distributions. (These levels are found in precisely the energy region predicted by Buck, Friedrich and Pilt [20]) in their phenomenological treatment of the alpha states in ^{18}F, which will be briefly reviewed in the next section). So, these two newly located states seem to be very good candidates for alpha-cluster band membership (with $K^\pi = 1^+$ in the language of the rotational model).

A further pair of alpha transfer reactions of interest have been performed; namely $^{14}N(^{11}B,^{7}Li)^{18}F$ with a beam energy of 115 MeV and $^{14}N(^{13}C,^{9}Be)^{18}F$ at 105 MeV. [4]) These experiments reveal selective excitation of the 3^+ at 3.36 MeV, 4^+ at 5.30 MeV, 5^+ at 6.57 MeV, 6^+ at 9.58 MeV and 7^+ at 11.22 MeV which we have already concluded are almost certainly alpha cluster states. In addition, they show strong, very narrow peaks in cross-section corresponding to excitation energies of 10.60, 14.18, 15.79 and 18.62 MeV in ^{18}F, which are probably high spin states. Unfortunately, no spin-parities are assigned to these states, and although the same authors have performed three-nucleon transfer reactions to populate states in ^{18}F [41]) (and the cluster model predicts some trinucleon states to lie in this energy region) this latter experiment does not reach these energies, so we can not tell, for certain, which (if any) type of cluster state is being excited. In view of this uncertainty, we wish merely to note the existence of these states, but not to include them amongst our experimental candidates for alpha cluster states.

In conclusion, we feel that we can confidently state that the 1^+ at 1.701, 2^+ at 2.524, 3^+ at 3.355, 4^+ at 5.299, 5^+ at 6.565, 6^+ at 9.58 and 7^+ at 11.22 MeV are alpha cluster states, and the 1^+ levels at 3.722 and 4.361 MeV, together with the 3^+ levels at 6.30, 6.481 MeV and the 1^+,2^+ or 3^+ at 6.803 MeV are possible contendors, whilst the level

seen by Middleton at 7.26 MeV with unknown spin-parity can not yet be completely ruled out.

3.2 The Phenomenological Model of $^{18}F = {}^{14}N+\alpha$.

The phenomenological model of the system $^{18}F = {}^{14}N+\alpha$ was introduced in an attempt to describe the states discussed in the last section in simple terms as due to the relative motion of an alpha pariticle about a ^{14}N core, with both components remaining in their ground states, so that all available quanta go into this relative motion. The aim is then to treat the alpha cluster states as being perturbed from the rotational spectrum, produced by the central folding potential, by the non-central terms which may exist in the cluster-core potential. Since the core carries one unit of intrinsic angular momentum, a set of triplets will be produced, which is what seems to be happening experimentally, and (in rotational model language) two bands with $K^{\pi} = 0^+,1^+$ produced as already explained by coupling the orbital angular momentum of the alpha, L, with the spin of the core S=1. This model thus predicts four states which have no known experimental counterparts, namely $J^{\pi}= 8^+,9^+$ members of the $K^{\pi} = 1^+$ band, and $J^{\pi}= 5^+,7^+$ members of the $K^{\pi}= 0^+$ band, at high excitation energies.

The first step in the phenomenological model is to identify the types of interaction between cluster and core permitted by invariance under space inversion and time reversal. In addition to a purely central term, we may form scalars by taking the dot products of tensors of ranks 1 and 2 (since S=1) in the cluster and core dynamic variables. However, the only core variable with which to do this is the "spin",S, so the only

possible vector-vector contraction we may have is $\underline{L}.\underline{S}$. Similarly, the only rank-2 tensor that can be formed from the core variable, S, has components S_2^μ where

$$S_2^\mu = \sum_m \langle 2\mu | 1m | \mu - m \rangle S_1^m S_1^{\mu-m} \qquad (3.1)$$

and S_1^m are components of the core spin $\underline{S}$. A scalar can now be formed by taking the dot product with similar tensors formed from the alpha coordinates $\underline{R}$,$\underline{P}$ and $\underline{L}$ according to the usual definition

$$A_\lambda \cdot B_\lambda = \sum_\mu (-1)^\mu A_\lambda^\mu B_\lambda^{-\mu} \qquad (3.2)$$

Note that considerations fo P,T-invariance do not permit any combinations of $\underline{R}$,$\underline{P}$,$\underline{L}$ in forming the second rank cluster tensor other than

$$T_2^\mu = \sum_m \langle 2\mu | 1m | \mu - m \rangle X_i^m X_i^{\mu-m} \qquad (3.3)$$

where $\underline{X}_i$ stands for $\underline{R}$, the position vecotr, $\underline{P}$ the momentum or $\underline{L}$ the angular momentum of the alpha particle. (no mixing of $\underline{R}$,$\underline{P}$ and $\underline{L}$ is possible). The possible second rank tensor contractions involved in the interaction with a spin-1 [42,43]) core are therefore of the form

$$T_o^{(i)} = T_2(\underline{S},\underline{S}) \cdot T_2(\underline{X}_i,\underline{X}_i) \qquad (3.4)$$

(using the definitions of eqs. 3.1, 3.2 and 3.3) with $T_o^{(i)}$ multiplied by some function of the cluster-core separation, R. These tensor contractions are more commonly found in the forms,

$$T_o^{(1)} = \frac{(\underline{S}.\underline{R})^2}{R^2} - \frac{\underline{S}^2}{3} \qquad (3.5a)$$

$$T_o^{(2)} = (\underline{S}.\underline{P})^2 - \frac{\underline{S}^2 \underline{P}^2}{3} \qquad (3.5b)$$

$$T_o^{(3)} = (\underline{S}.\underline{L})^2 + \tfrac{1}{2}(\underline{S}.\underline{L}) - \frac{\underline{S}^2\underline{L}^2}{3} \qquad (3.5c)$$

where the last term has a different form from the first two because of the non-commutativity of the components of $\underline{L}$ amongst themselves. Since we have S=1, we may replace S^2 in these formulae by the number, 2, when we take matrix elements between coupled basis states $|(L,S)JM\rangle$.

With these three second rank tensor contractions, and a vector spin-orbit force, we have four terms which can split the triplets formed by the coupling LxS → J from their rotational centroids, and the next step in the phenomenological treatment is to try and parametrize their strengths in some simple way. Those levels identified experimentally show that the vector spin-orbit interaction $\underline{L}.\underline{S}$ can not be the dominant term of these four since it would cause the J = L±1 members of a given triplet to be shifted to opposite sides of the J=L member. Indeed, the experimental and theoretical investigations of analogous alpha cluster states in ^{19}F presented in the last chapter strongly suggest that this term is unimportant, being responsible for shifts of about 100 keV at most, and hence may be neglected in a first approximation since experimentally we have splittings of around 1 MeV to account for. As the vector spin-orbit force is so small, it seems reasonable to expect that the term $T_o^{(3)}$, which is quadratic in $\underline{L}.\underline{S}$, will be even smaller, so this too is neglected. As a further check on the reasonableness of this last assumption we note that it predicts large splittings of the high-L triplets which are not seen experimentally. It is also hoped that the "momentum tensor" $T_o^{(2)}$ will be small, but since it has similar matrix elements to $T_o^{(1)}$ we can neglect it, and any effects it does have will be

absorbed into $T_o^{(1)}$ through its matrix elements. Hence, the phenomenological model of Buck, Friedrich and Pilt attempts to describe the alpha cluster states in ^{18}F by means of the simple potential

$$V = V_o(R) + V_2(R) T_o^{(1)} \qquad (3.6)$$

The diagonal matrix elements of $V_2(R)T_o^{(1)}$ between coupled basis states $|(L,S)JM\rangle$ are given by;

$$\langle (LS)JM | V_2(R) T_o^{(1)} | (LS)JM \rangle = \Delta(J,L)\gamma(L,L) \qquad (3.7)$$

with

$$\Delta(L+1,L) = -\frac{1}{3}\frac{L}{2L+3} \; ; \; \Delta(L,L) = \frac{1}{3} \; ; \; \Delta(L-1,L) = -\frac{1}{3}\frac{L+1}{2L-1} \qquad (3.8)$$

and

$$\gamma(L,L) = \int_o^\infty V_2(R) |\chi_L(R)|^2 dR \qquad (3.9)$$

where $\chi_L(R)$ is the radial wavefunction for the relative motion. For a given band, the number of nodes in $\chi_L(R)$ is uniquely determined by L (eq. 1.13). In addition to these diagonal matrix elements, the tensor force can also connect states of a given J, for which L differs by 2 units, for example the two $J^\pi = 1^+$ states formed from the coupling L=0 x S=1 → 1 and L=2 x S=1 → 1. These off-diagonal matrix elements are given by

$$\langle (LS)JM | V_2(R) T_o^{(1)} | (L+2,S)JM \rangle = \frac{\sqrt{(L+1)(L+2)}}{2L+3}\gamma(L,L+2) \qquad (3.10)$$

with

$$\gamma(L,L+2) = \int_o^\infty \chi_L^*(R) V_2(R) \chi_{L+2}(R) dR \qquad (3.11)$$

To simplify the application of these considerations to finding the energies of the alpha cluster states in ^{18}F the following assumptions are made

i) Experimentally the centroids of the triplets of the band are seen to vary closely as L(L+1), so perfect rotational spacing of these

centroids is assumed (This assumption is entirely consistent with the model since the moment of inertia obtained from the folded potential is very nearly independent of L).

ii) A further simplification is introduced by assuming that the quantity $\gamma(L,L)$ is a constant, independent of L. Provided the form factor $V_2(R)$ is a smoothly varying function which encloses a large proportion of the strength of $|\chi_L(R)|^2$ this is expected to be a reasonable approximation.

iii) When a fit was made to the experimental data it was found that a very good spectrum could be obtained by ignoring the mixing introduced by the off-diagonal matrix elements of the tensor (eq. 3.10). Although it was recognized that some improvement could be made to this spectrum by assigning a small constant value to the quantity $\gamma(L,L+2)$(eq. 3.11) it was felt that this was insufficient to justify the inclusion of an extra free parameter. Hence, the no-mixing assumption, which sets $\gamma(L,L+2) = 0$, was adopted and justified by arguing that since $\gamma(L,L+2)$ is the integral of a smooth function, $V_2(R)$, multiplied by two wave functions which contain different numbers of nodes, it might be expected that the integrand would be as often positive as negative.

With these assumptions, the phenomenological model yields a simple three-parameter formula for the energy of a given J and L in the band:

$$E(J,L) = C + \alpha L(L+1) + \Delta(J,L)\gamma(L,L) \qquad (3.12)$$

The moment of inertia parameter α is fixed by experiment (and well reproduced by the folded potential) and C is the energy of the band head, leaving only $\gamma(L,L)$ free to fit the energy differences between the levels. The spectrum produced by this simple formula with $\alpha = 0.198$ MeV (which is close to the value for this same parameter in the $^{15}N+\alpha$ system, as

expected intuitively), C = 1.98 MeV and (in the notation of ref. [20]) $\beta = -\frac{1}{3}\gamma(L,L) = 0.652$ MeV is shown in Fig. 4(a) and is seen to give good agreement with the experimental data. In view of the success of this simple prescription, it is highly desirable to test the validity of the assumptions inherent in it from a more microscopic standpoint, and this is done in the section 3.4.

3.3 Classical Considerations of the ^{14}N-α Interaction.

The effective potential between the ^{14}N core and the alpha cluster (eq. 3.6) can be thought of in terms of the interaction of the alpha with the quadrupole deformation of the core. Depending on the orientation of the orbit of the alpha particle with respect to the symmetry axis of the core the alpha will interact with more or less of the core material. Classically, we can imagine the alpha orbiting a core which has prolate spheroidal shape. Then an orbit around the axis of symmetry (Fig. 5a) will bring it into contact with less core material than an orbit aligned perpendicular to the symmetry axis (Fig. 5b). Hence, if the interaction of the cluster with the core is attractive, the former orbit should be at a higher energy than the latter. We can put this idea on a more quantitative basis by calculating the matrix elements of the tensor force $T_o^{(1)}$ (eq. 3.5a) between coupled basis states $|(LS)JM\rangle$ in a classical manner and showing that they are equal to the quantum-mechanical ones (eqs. 3.7,3.8) in the limit of large L.

Since we are only interested in the reduced matrix elements of $T_0^{(1)} = (\underline{S}.\hat{\underline{R}})^2 - \frac{1}{3}S^2$, we can simplify the problem by considering the state in which the projection of $\underline{L}$ on the z-axis takes its maximum value of $M_L = L$.

The function describing the orbital motion of the alpha particle about the core then varies as $\sin^{L}\Theta e^{iL\Phi}$ (with Θ and Φ polar angles for the position of the cluster). So, we can take the orbit of the alpha particle to be essentially localized in the xy plane in the limit of large L. The vector model of the various angular momenta is shown in Fig. 5c.

To find the average value of $T_o^{(1)}$, we consider Fig. 5d. The angle between $\underline{S}$ and $\underline{R}$ is labelled ω, with $\underline{R}$ lying in the xy plane. Then $\underline{S}$ is projected onto the xy plane, meeting it at a point B, such that the length AB is the projection of $\underline{S}$ on the z-axis (M_s) and the angle $A\hat{O}B$ is labelled θ. We label the angle between OB and $\underline{R}$ by ϕ, and find the point C on $\underline{R}$ such that the angle $O\hat{B}C$ is $\pi/2$. We can then write;

$$(\underline{S}.\hat{\underline{R}})^2 - \tfrac{1}{3}\underline{S}^2 = \underline{S}^2\left(\cos^2\omega - \tfrac{1}{3}\right) \qquad (3.16)$$

To take the scalar product $\underline{S}.\hat{\underline{R}}$ we see from Fig. 5d that $OA\cos\theta$ is the component of OA lying in the xy plane, and $OA\cos\theta\cos\phi$ is the component parallel to $\underline{R}$. Since the other components of OA are perpendicular to $\underline{R}$ we have

$$OA\cos\omega = OA\cos\theta\cos\phi \qquad (3.17)$$

$$\cos\omega = \cos\theta\cos\phi \qquad (3.18)$$

To take the average value of $T_o^{(1)}$ we now use the relations

$$\langle\cos^2\phi\rangle = 1/2 \qquad (3.19)$$

$$\langle\cos^2\theta\rangle = \frac{S(S+1) - M_s^2}{S(S+1)} \qquad (3.20)$$

and then from eq. 3.16

$$\left\langle(\underline{S}.\hat{\underline{R}})^2 - \tfrac{1}{3}\underline{S}^2\right\rangle = \left\langle\underline{S}^2\left(\cos^2\theta\cos^2\phi - \tfrac{1}{3}\right)\right\rangle \qquad (3.21)$$

$$= \frac{1}{6}S(S+1) - \frac{1}{2}M_s^2 \qquad (3.22)$$

We know that M_s, the projection of $\underline{S}$ on the z-axis, can only take the values 0 and ±1. The value $M_s=0$ corresponds to the core being oriented so that its symmetry axis is more or less in the xy plane, whilst $M_s=\pm1$ tends to align the symmetry axis with the z-axis. As the orbit of the alpha cluster lies essentially in the xy plane, setting $M_s=0$ produces a situation like Fig. 5b, and $M_s=\pm1$ produces the orbit shown in Fig. 5a. We now have the three relations;

$$\text{If } M_s=\pm1 \quad (\text{i.e. } J=L\pm1) \qquad \langle T_o^{(1)}\rangle = -\frac{1}{6} \tag{3.23a}$$

$$\text{If } M_s=0 \quad (\text{i.e. } J=L) \qquad \langle T_o^{(1)}\rangle = \frac{1}{3} \tag{3.23b}$$

For an attractive interaction between cluster and core we see that there will be a reduction in the energies of states with J=L, because of the greater amount of core material encountered by the cluster in its orbit, whilst for states having J=L±1, the energy will be increased, because less core material is encountered. This provides a physical picture of the effects of the tensor force in various states, and we note that eqs. 3.23 are the same as the high-L limits of the equivalent quantum mechanical quantities of eq. 3.8. Another interesting feature is that $\langle T_o^{(1)}\rangle$, as given in eq. 3.22, vanishes for $S=\frac{1}{2}$ ($M_s=\pm\frac{1}{2}$), indicating that there is no observable quadrupole moment for a state having spin $S=\frac{1}{2}$. We now proceed to the microscopic description of the ^{14}N-α system, to justify these phenomenological and classical ideas more rigorously.

3.4 Semimicroscopic Treatment of $^{18}F = {}^{14}N+\alpha$.

3.4.1 The Microscopic Model.

The formalism for the decomposition $^{18}F = {}^{14}N+\alpha$ is exactly the same as that for the case $^{19}F = {}^{15}N+\alpha$ dealt with in the last chapter, except that the number of core nucleons, A_1, is now understood to be 14. We write the full Hamiltonian, split it up to describe cluster, core and relative motion and write its eigenfunctions as sums of product states in an exactly analogous manner to that in eqs. 2.3, 2.4 and 2.5. That is,

$$H = \sum_{i=1}^{A_1+A_2} \frac{p_i^2}{2m_n} + \sum_{i<j} V_{ij} \qquad (3.24)$$

$$H \approx H_{A_1} + H_{A_2} + H_{rel} \qquad (3.25)$$

$$\Psi_{JM} = \phi(\underline{A}_2) \sum_{M'(M'')} \langle SM'LM'' | JM \rangle \phi_{SM'}(\underline{A}_1) \psi_{LM''}(\underline{R}) \qquad (3.26)$$

The Pauli principle is similarly treated by choosing the real part of the phenomenological optical potential (to include some of the effects of exchange of nucleons between cluster and core) as the cluster-nucleon potential from which to build up the effective cluster-core potential V_{Cc}, and restricting the quantum numbers of relative motion to obey eq. 1.13 and so exclude redundant states

$$2N+L = \sum_{i=1}^{A_2} (2n_i + l_i) \geq 2A_2 \quad (=8 \text{ in this case}) \qquad (3.27)$$

The only difference is how we write the ground state wavefunction of the ^{14}N core. We choose to approximate this as two p-shell holes in the ^{16}O closed shell $|0\rangle$ coupled to spin S=1 and isospin T=0. These

holes may therefore have angular momenta $j_1, j_2 = \frac{1}{2}, \frac{3}{2}$ and the analogue of eq. 2.6 can be written as:

$$|^{14}N; S\epsilon(1) M\rangle = \sum_{\substack{j_1 \leq j_2 \\ m_1,(m_2), m_t}} C_{j_1 j_2} (1+\delta_{j_1 j_2})^{-\frac{1}{2}} \langle j_1 m_1 j_2 m_2 | SM\rangle \langle \tfrac{1}{2} m_t \tfrac{1}{2} -m_t | 00\rangle b^{\dagger}_{j_1 m_1 m_t} b^{\dagger}_{j_2 m_2 - m_t} |0\rangle \qquad (3.28)$$

with symbols as defined for eq. 2.6, and in addition amplitudes for finding two holes with angular momenta j_1 and j_2 are included. To obtain values for the coefficients $C_{j_1 j_2}$ we have recourse to some work on the p-shell nuclei by Cohen and Kurath.[44]) Several fits were made to well-determined energy levels of nuclei in the mass range A=5 to A=15 and a series of two-particle matrix elements $\langle (j_1 j_2) ST | V | (j_3 j_4) ST\rangle$ deduced. (V is the residual interaction). In fact, it was found that excluding data from the A=6,7 nuclei resulted in better reproduction of the spectra for the remaining p-shell nuclei, so we have made use of this particular series of matrix elements (the (8-16)2BME fit). These can readily be converted to two-hole matrix elements and the energies for $j=\frac{1}{2}$ and $j=3/2$ holes evaluated.. To obtain the energies and wavefunctions of the S=1, T=0 states which may be formed in ^{14}N it is necessary to diagonalize a 3x3 matrix (since there are three combinations of $j_1 j_2$ which can couple to the required spin and isospin) to find the eigenvalues and associated eigenvectors. On doing this, three energy eigenvalues of 27.73, 31.63 and 43.01 MeV are found. This lowest value of 27.73 MeV is the difference in binding energy between the ground states of ^{14}N and ^{16}O. Knowing the lowest eigenvalue we can use it to calculate the associated normalized eigenvector, and hence the two-hole amplitudes appropriate to the ground state of ^{14}N. We find

$$C_1 = C_{\frac{1}{2}\frac{1}{2}} = 0.9495 \; ; \; C_2 = C_{\frac{1}{2}\frac{3}{2}} = 0.3127 ; \; C_3 = C_{\frac{3}{2}\frac{3}{2}} = -0.0270 \qquad (3.29)$$

Finally, we use the same form of the alpha-nucleon force, containing central and vector spin-orbit terms as in the last chapter eq. 2.7, from which to build an effective ^{14}N-α potential.

3.4.2 The Effective Cluster-Core Potential.

We make a tensor decomposition of the radial function U_c and U_{LS} as in eqs. 2.8 and 2.10, and write the relative orbital angular momentum between alpha and hole as in Appendix II of chapter 2. It is immediately apparent that since this expression only contains $\underline{L}$ and $\underline{P}$ to first order it is clear that the momentum and angular momentum tensors (eqs. 3.5b,c) will not appear in the final interaction. We then seek to write the cluster-nucleon interaction as a sum of dot products of rank-K spherical tensors in alpha and nucleon coordinates as in eq. 2.13.

$$V_{\alpha n}^{(i)} = \sum_K f_K(r_i, R)\, A_K(\underline{\alpha}) \cdot \overline{T}_K(\underline{\Omega}_i) \qquad (3.30)$$

Equations 2.14,15,16,17,18 then follow through as before, except that the core spin, S is 1 instead of $\frac{1}{2}$, and we sum over 14 instead of 15 core nculeons. In other words, we are trying to write the cluster-core potential as

$$V_{Cc} = \sum_K F_K(R)\, A_K(\underline{\alpha}) \cdot S_K \qquad (3.31)$$

where

$$F_K(R) = \frac{\left\langle \phi_{S=1}(^{14}N; \underline{\Omega}_j) \left\| \sum_{i=1}^{14} f_K(r_i, R)\, \overline{T}_K(\underline{\Omega}_i) \right\| \phi_{S=1}(^{14}N; \underline{\Omega}_j) \right\rangle}{\langle S=1 \| S_K \| S=1 \rangle} \qquad (3.32)$$

Recalling that P,T-invariance arguments and the linear appearance of $\underline{P}$ and $\underline{L}$ in our model, only permit terms in the potential V_{Cc} which are central or of the form $\underline{L}.S$ or $T_o^{(1)}$ (eq. 3.5a) we note that when K=1 the vector $A_1(\underline{\alpha})$ must be proportional to $\underline{L}$ (the angular momentum of the alpha particle) and when K=2, $A_2(\underline{\alpha})$ must be proportional to $T_2(\hat{\underline{R}},\hat{\underline{R}}) = \sqrt{\frac{2}{3}}C_2(\hat{\underline{R}})$ (eq. 3.4).

3.4.3 The Reduced Matrix Elements of $T_K(\underline{n}_i)$.

Since the core spin is 1 in this case it is possible to have K=2 in addition to 0 and 1 as were encountered in the ^{15}N-α calculation. This spin of 1 leads to a small quadrupole deformation of ^{14}N (the quadrupole moment is +0.01 barns [45]) and the phenomenological model was originally based on the idea that the orbiting alpha would interact with this deformation. Even if the interation between the ^{14}N density and alpha is independent of spin there can be a tensor interaction induced between cluster and core. However, we note that a sum of single-particle interactions will not give rise to such a force if the spin S=1 is built up from two single-particle orbits having $j=\frac{1}{2}$, since in this case there is no quadrupole deformation.

We again write $T_K(\underline{n}_i)$ as formed from tensors of ranks k_1 and k_2 in the nucleon space and spin coordinates respectively and proceed to evaluate reduced matrix elements of T_K between ^{14}N ground state wave functions which we approximate by two p-shell holes coupled to an inert ^{16}O core. By explicitly writing in the isospin Clebsch-Gordan coefficients in eq. 3.28 we obtain the ^{14}N ground state wavefunction in neutron-proton formalism as

$$|^{14}N;S(=1)M\rangle = \sum_{j_1 j_2} C(j_1 j_2) \left| \left(j_1^{-1}(n)\, j_2^{-1}(\rho)\right) SM \right\rangle \qquad (3.33)$$

where the new coefficients, $C(j_1 j_2)$, are related to those of eq. 3.29 by

$$C\left(\tfrac{1}{2},\tfrac{1}{2}\right) = C_1 \; ; C\left(\tfrac{1}{2},\tfrac{3}{2}\right) = -C\left(\tfrac{3}{2},\tfrac{1}{2}\right) = \frac{1}{\sqrt{2}} C_2 \; ; \; C\left(\tfrac{3}{2},\tfrac{3}{2}\right) = C_3 \qquad (3.34)$$

and the coupled two-hole states are given by

$$\left|\left(j_1^{-1}(n)\, j_2^{-1}(\rho)\right) SM\right\rangle = \sum_{m_1 (m_2)} \langle j_1 m_1 j_2 m_2 | SM \rangle \, b^{\dagger}_{j_1 m_1}(n)\, b^{\dagger}_{j_2 m_2}(\rho) \, |0\rangle \qquad (3.35)$$

Since the tensors T_K are all isoscalar we may write the reduced matrix element of interest in the form;

$$\langle {}^{14}N;S(=1) \| T_K \| {}^{14}N;S(=1)\rangle = \langle {}^{14}N;S(=1) \| T_K(n) + T_K(\rho) \| {}^{14}N;S(=1)\rangle \qquad (3.36)$$

to which we may apply a standard formula [24]) to write the right hand side as

$$= 2 \sum_{j_1 j_1' j_2} C(j_1 j_2)\, C(j_1' j_2)\, \alpha(S K j_1 j_1') \begin{Bmatrix} S & S & K \\ j_1 & j_1' & K \\ j_2 & j_2 & 0 \end{Bmatrix} \langle j_1^{-1} \| T_K \| j_1'^{-1} \rangle \qquad (3.37)$$

where we again define $\alpha(abcd) = \sqrt{(2a+1)(2b+1)(2c+1)(2d+1)}$, and particle-hole conjugation can be applied to the single-hole reduced matrix element as in section 2.3.3 to obtain

$$\langle j_1^{-1} \| T_K \| j_1'^{-1} \rangle = \langle 0 \| T_K \| 0 \rangle \, \delta_{j_1 j_1'} \, \delta_{K0} \, \overline{\langle j_1 \| \tilde{T}_K \| j_1' \rangle} \qquad (3.38)$$

(c.f. eq. 2.20) with $\tilde{T}_K$ the time-reversed tensor $(\mathcal{T}^{-1} T_K \mathcal{T})^{\dagger}$ and $\mathcal{T}$ the time-reversal operator. Again the core expectation value is purely central (hence the δ_{K0}) and represents an $^{16}0$-α potential, to which is added a 2 hole-alpha potential. So we obtain

$$\langle {}^{14}N;S(-1)\|T_K\|{}^{14}N;S(-1)\rangle = \langle 0\|T_K\|0\rangle\delta_{K0} - 2\sum_{j_1 j_1' j_2} C(j_1 j_2)C(j_1' j_2)\alpha(SKj_1 j_2)\begin{Bmatrix} S & S & K \\ j_1 & j_1' & K \\ j_2 & j_2 & 0 \end{Bmatrix}\langle j_1\|\tilde{T}_K\|j_1'\rangle \quad (3.39)$$

We decompose the hole contributions into their space and spin components to find

$$\langle {}^{14}N\|T_K\|{}^{14}N\rangle_{hh} = -2C_{KK_1K_2}\langle \ell\|\tilde{R}_{K_1}\|\ell\rangle\langle s\|\tilde{S}_{K_2}\|s\rangle \quad (3.40)$$

where

$$C_{KK_1K_2} = \sum_{j_1 j_1' j_2} C(j_1 j_2)C(j_1' j_2)\alpha(SKj_1 j_2)\alpha(j_1' K\ell s)\begin{Bmatrix} S & S & K \\ j_1 & j_1' & K \\ j_2 & j_2 & 0 \end{Bmatrix}\begin{Bmatrix} j_1 & j_1' & K \\ \ell & \ell & K_1 \\ s & s & K_2 \end{Bmatrix} \quad (3.41)$$

and $\ell=1$, $s=\frac{1}{2}$ for the reduced single particle matrix elements. We now use the symmetry properties of the 9j symbol to interchange the first two columns of both 9j symbols in eq. 3.41. Since j_1 and j_1' are merely dummy indices, the value of the sum must be unchanged, so the argument of the phase factor introduced by the manipulation, $(-1)^{\beta}$, must be an even integer. Now $\beta = 2[S+K+j_1+j_1'+j_2+\ell+s]+(K+k_1+k_2)$, and since the expression in square brackets contains an even number of half-integral angular momenta (j_1, j_1', j_2, s) and the integers (S, K, ℓ), the sign change is simply $(-1)^{K+k_1+k_2}$, as in the ${}^{19}F = {}^{15}N+\alpha$ calculation. So $K+k_1+k_2$ must be an even integer, and identical arguments concerning the behaviour of $T_K(R_{k_1}, S_{k_2})$ under parity and time reversal transformations allow the removal of the time-reversed operators from eq. 3.40 to yield

$$\langle {}^{14}N\|T_K\|{}^{14}N\rangle_{hh} = 2(-1)^{1+K}\langle \ell\|R_{k_1}\|\ell\rangle\langle s\|S_{k_2}\|s\rangle C_{KK_1K_2} \quad (3.42)$$

Had the calculation concerned the interaction between an alpha and two p-shell particles we would have obtained a result exactly like eq. 3.42 but without the phase $(-1)^{1+K}$.

We now consider the possible combination of tensor ranks (K,k_1,k_2) with the new possibility of K=2, and find that the evenness of $K+k_1+k_2$ allows

SCALAR	(0,0,0)	(0,1,1)	
VECTOR	(1,0,1)	(1,2,1)	(1,1,0)
TENSOR	(2,2,0)	(2,1,1)	

The combination (1,1,0) is again barred because $\underline{\ell}_i$ never occurs without $\underline{s}_i$, so the remaining allowed terms indicate that contributions from the following tensors are possible

SCALAR	1	$\underline{\ell}.\underline{s}$
VECTOR	$\underline{s}$	$T_1(C_2(\hat{\underline{r}}),\underline{s})$
TENSOR	$C_2(\hat{\underline{r}})$	$T_2(\underline{\ell},\underline{s})$

We can now pick out such terms from the tensor deompositions of $U_c(|\underline{r}-\underline{R}|)$ and $U_{LS}(|\underline{r}-\underline{R}|)\underline{\ell}_{rel}.\underline{s}$ to obtain a cluster-core potential of the form;

$$V_{Cc} = V_0(R) + V_1(R)\underline{L}.\underline{S} + V_2(R)T_0^{(1)} \qquad (3.43)$$

The coupling of the two holes to form spin-1 states is taken care of by the coefficients $C_{Kk_1k_2}$, which can be evaluated with the aid of the 9-j symbols listed in Tables 1 and 3. These were calculated by relating them to 6-j and 3-j symbols and using algebraic expressions for the latter [46]) and then checked against standard tables. [47]) The values obtained for the various $C_{Kk_1k_2}$ are;

$$C_{000} = C_1^2 + C_2^2 + C_3^2 = 1$$

$$C_{011} = \frac{\sqrt{2}}{3}\left(C_1^2 + \frac{1}{4}C_2^2 - \frac{1}{2}C_3^2\right)$$

$$C_{101} = -\frac{1}{3}\sqrt{\frac{2}{3}}\left(C_1^2 + 2C_1C_2 - \frac{3}{2}C_2^2 - 2\sqrt{\frac{5}{2}}C_2C_3 - C_3^2\right)$$

$$C_{121} = \frac{2}{3}\sqrt{\frac{2}{3}}\left(C_1^2 - \frac{1}{4}C_1C_2 - \frac{3}{8}C_2^2 + \frac{1}{4}\sqrt{\frac{5}{2}}C_2C_3 - \frac{1}{10}C_3^2\right)$$

$$C_{220} = C_1C_2 + \frac{1}{4}C_2^2 + \frac{1}{\sqrt{10}}C_2C_3 - \frac{2}{5}C_3^2$$

$$C_{211} = -\frac{1}{6}\sqrt{10}\left(C_1C_2 - \frac{1}{2}C_2^2 + \frac{1}{\sqrt{10}}C_2C_3 + \frac{4}{5}C_3^2\right)$$

(3.44)

We note the following points concerning these sums of products of amplitudes.

i) The central terms, C_{000} and C_{011}, contain no cross-terms since a scalar operator is unable to connect states of different j.

ii) The tensor terms, C_{220} and C_{211}, contain no terms in C_1^2 since this product corresponds to both holes having $j=\frac{1}{2}$. Hence the tensor force will be small in comparison with the central term since C_1 is the dominant amplitude (see eq. 3.29).

iii) The product C_1C_3 is absent from all the terms because all the T_K are single-particle operators and can not simultaneously change both angular momenta from $\frac{1}{2}$ to 3/2 as this combination requires.

Finally, we point out that $T_0^{(1)}$ may be written as,

$$T_0^{(1)} = T_2\left(C_1(\hat{R}), C_1(\hat{R})\right) \cdot T_2(\underline{S},\underline{S}) = T_2(\hat{R},\hat{R}) \cdot T_2(\underline{S},\underline{S})$$

$$= \sqrt{\frac{2}{3}}\, C_2(\hat{R}) \cdot S_2 \qquad (3.45)$$

3.4.4 The Form Factors V_o, V_1 and V_2.

We again use the definitions of eqs. 2.24 and 2.25 for commonly occurring integrals of the p-shell radial wavefunction with components $U_{C(\ell)}(r,R)$ and $U_{LS_{(\ell)}}(r,R)$ of the tensor decomposition (eq. 2.10) i.e.

$$F_{A_{(\ell)}}(R) = \int_0^\infty U_{A_{(\ell)}}(r,R)\,|R(r)|^2\, r^2 dr \qquad (2.24)$$

and

$$F^{\pm}_{LS_{(1)}}(R) = \int_0^\infty U_{LS_{(1)}}(r,R)\,|R(r)|^2 \left(\frac{R}{r}\right)^{\pm 1} r^2 dr \qquad (2.25)$$

This time, the tensor decomposition of the central potential $U_C(|\underline{r}-\underline{R}|)$ gives two contributions to the effective cluster-core potential.

i) Taking $\mathcal{L}=0$ in eq. 2.28 corresponds to the allowed tensor rank combination (0,0,0) with $A_K(\underline{\alpha}) = 1$, $R_{k_1} = U_{C_{(0)}}(r,R)$ and $S_{k_2} = 1$. Then substitution in eq. 3.40 gives;

$$-2C_{000}F_{C_{(0)}}(R) = -2F_{C_{(0)}}(R) \qquad (3.46)$$

as the contribution to V_o (in eq. 3.42) from the central part of $V^{(i)}_{\alpha n}$.

ii) We may also set $\mathcal{L}=2$ and obtain non-vanishing results from eq. 3.42. In this case the tensor decomposition yields the term $5U_{C_{(2)}}(r,R)C_2(\hat{\underline{R}}).C_2(\hat{\underline{r}})$, which we rewrite as $5\sqrt{\frac{3}{2}}U_{C_{(2)}}(r,R)C_2(\hat{\underline{r}}).\left(\sqrt{\frac{2}{3}}C_2(\hat{\underline{R}})\right)$ for ease of comparison with the alpha operator in eq. 3.45. This corresponds to the tensor rank combination (2,2,0), and substitution in eq. 3.42 and eq. 3.32 gives a contribution to $V_2(R)$ of

$$\frac{-2.5\sqrt{\frac{3}{2}}\langle \ell \| C_2(\hat{\underline{r}}) \| \ell \rangle C_{220} F_{C_{(2)}}(R)}{\langle S(=1) \| S_2 \| S(=1) \rangle} = 6C_{220}F_{C_{(2)}}(R)$$

$$= \bar{C}_{220}F_{C_{(2)}}(R) \qquad (3.47)$$

where we have used $\langle \ell=1 \| C_2(\hat{r}) \| \ell=1 \rangle = -\sqrt{\frac{2}{5}}$ and $\langle S=1 \| S_2 \| S=1 \rangle = \sqrt{\frac{5}{3}}$

We now consider the spin-orbit part of $V_{\alpha n}^{(i)}$, treating each of the four terms separately.

(1)

i) The term $\frac{m_\alpha}{M}\underline{\ell}.\underline{s}$; like the central part of $V_{\alpha n}^{(i)}$ just dealt with, contributes to V_o and V_2. Taking $\mathcal{L}$ =0 and writing $\underline{\ell}.\underline{s}$ as $-\sqrt{3}T_o^o(\underline{\ell},\underline{s})$ (the tensor rank combination being (0,1,1)) we have the operator $-\sqrt{3}U_{LS_{(0)}}(r,R)T_o^o(\underline{\ell},\underline{s})$ to substitute in eq. 3.42, which yields:

$$2\sqrt{3}\,\frac{m_\alpha}{M}\langle \ell \| \underline{\ell} \| \ell \rangle \langle s \| \underline{s} \| s \rangle C_{o11} F_{LS_{(o)}}(R)$$

and use of $\langle J||\underline{J}||J\rangle = \sqrt{J(J+1)}$ allows the simplification

$$3\sqrt{2}\,\frac{m_\alpha}{M} C_{o11} F_{LS_{(o)}}(R) = \frac{m_\alpha}{M} \overline{C}_{o11} F_{LS_{(o)}}(R) \qquad (3.48)$$

as a contribution to V_o.

ii) For $\mathcal{L}$ =? we have the operator $5\frac{m_\alpha}{M}U_{LS_{(2)}}(r,R)C_2(\hat{\underline{R}}).C_2(\hat{\underline{r}})\underline{\ell}.\underline{s}$. We recouple the nucleon part of this to obtain $T_2(\underline{Q},\underline{s})$ where $\underline{Q}$ = $Q_1(C_2(\hat{\underline{r}}),\ell)$ (see Appendix VI) and write the alpha operator as $\sqrt{\frac{2}{3}}C_2(\hat{R})$. In this form the tensor rank combination is (2,1,1) and including the factor $-\sqrt{\frac{3}{5}}$ introduced by the recoupling gives an operator

$$-5\sqrt{\frac{3}{2}}\sqrt{\frac{3}{5}}\,\frac{m_\alpha}{M}U_{LS_{(2)}}(r,R)T_2(\underline{Q},\underline{s}).\left(\sqrt{\tfrac{2}{3}}C_2(\hat{\underline{R}})\right)$$

We note that $\underline{Q}$ has the same matrix elements between p-states as $\underline{\ell}/\sqrt{10}$, so use of eq. 3.42 and eq. 3.32 gives a contribution to V_2 of

$$\frac{2\frac{15}{\sqrt{10}}\frac{m_\alpha}{M}\langle \ell \| \underline{Q} \| \ell \rangle \langle s \| \underline{s} \| s \rangle C_{211} F_{LS_{(2)}}(R)}{\langle S \| S_2 \| S \rangle} = \frac{9}{\sqrt{10}}\frac{m_\alpha}{M} C_{211} F_{LS_{(2)}}(R)$$

$$= \frac{m_\alpha}{M}\overline{C}_{211} F_{LS_{(2)}}(R) \qquad (3.49)$$

(2) The contributions to V_1 from $\frac{m_n}{M}\underline{L}.\underline{s}$ follow exactly the same scheme as in the ^{15}N-α case. We may have $\mathcal{L}=0,2$ producing operators $U_{LS_{(0)}}(r,R)\underline{L}.\underline{s}$ and $5U_{LS_{(2)}}(r,R)C_2(\hat{\underline{R}}).C_2(\hat{\underline{r}})\underline{L}.\underline{s}$ corresponding to the rank combinations (1,0,1) and (1,2,1).

i) For $\mathcal{L}=0$. we have $A_K(\underline{\alpha}) = \underline{L}, R_{k_1} = U_{LS_{(0)}}(r,R)$, $S_{k_2} = \underline{s}$, so the contribution to V_1 is; (from eqs. 3.42 and 3.32)

$$\frac{2\frac{m_\alpha}{M}\langle s\|\underline{s}\|s\rangle C_{101} F_{LS_{(0)}}(R)}{\langle S\|\underline{S}\|S\rangle} = \sqrt{\frac{3}{2}}\frac{m_n}{M} C_{101} F_{LS_{(0)}}(R)$$

$$= \frac{m_n}{M}\overline{C}_{101} F_{LS_{(0)}}(R) \qquad (3.50)$$

ii) For $\mathcal{L}=2$ we recouple $C_2(\hat{\underline{R}})$ and $\underline{L}$ as in appendix III to obtain an effective alpha operator $\underline{L}/\sqrt{10}$. The resulting contribution to V_1 is

$$\frac{2\frac{5}{\sqrt{10}}\frac{m_n}{M}\langle \ell\|C_2(\hat{r})\|\ell\rangle\langle s\|\underline{s}\|s\rangle C_{121} F_{LS_{(2)}}(R)}{\langle S\|\underline{S}\|S\rangle} = -\sqrt{\frac{3}{2}}\frac{m_n}{M} C_{121} F_{LS_{(2)}}(R)$$

$$= -\frac{m_n}{M}\overline{C}_{121} F_{LS_{(2)}}(R) \qquad (3.51)$$

(3) The term $-\frac{m_\alpha}{M}\underline{R}\Lambda\underline{p}.\underline{s}$ is found to contribute to V_o and V_2 as follows. Setting $\mathcal{L}=1$ gives an operator $-3\frac{m_\alpha}{M}U_{LS_{(1)}}(r,R).C_1(\hat{\underline{R}}).C_1(\hat{\underline{r}})R\Lambda\underline{p}.\underline{s}$ and we can combine $C_1(\hat{\underline{R}})$ with $\underline{R}$ to make an alpha coordinate tensor of rank 0 or 2 (rank 1 is forbidden by symmetry considerations). In the nucleon coordinates, $C_1(\hat{\underline{r}})$ is combined with $\underline{p}$ to make $\underline{\ell}$, so the rank combinations are (0,1,1) and (2,1,1).

i) The scalar term (see appendix IV) comes from recoupling the operator to $-\frac{m_\alpha}{M}\frac{R}{r}U_{LS_{(1)}}(r,R)\underline{\ell}.\underline{s}$. Writing $\underline{\ell}.\underline{s} = -\sqrt{3}T^o_o(\underline{\ell},\underline{s})$ and using eq. 3.42 yields a contribution to V_o of

$$-2\sqrt{3}\frac{m_\alpha}{M}\langle \ell\|\underline{\ell}\|\ell\rangle\langle s\|\underline{s}\|s\rangle C_{011}F^{+}_{LS_{(1)}}(R) = -3\sqrt{2}\frac{m_\alpha}{M}C_{011}F^{+}_{LS_{(1)}}(R)$$

$$= -\frac{m_\alpha}{M}\overline{C}_{011}F^{+}_{LS_{(1)}}(R) \qquad (3.52)$$

ii) We may also recouple $C_1(\hat{\underline{R}})$ and $\underline{R}$ to a rank-2 tensor and obtain a contribution to V_2. When we do this, the operator becomes $\sqrt{\frac{3}{2}}\frac{m_\alpha}{M}\frac{R}{r}U_{LS_{(1)}}(r,R)C_2(\hat{\underline{R}}).T_2(\underline{\ell},\underline{s})$ (see appendix VII). Taking the alpha operator as $\sqrt{\frac{2}{3}}C_2(\hat{\underline{R}})$ and using eqs. 3.32 and 3.42 yields

$$\frac{-2.\frac{3}{2}\frac{m_\alpha}{M}\langle \ell\|\underline{\ell}\|\ell\rangle\langle s\|\underline{s}\|s\rangle C_{211}F^{+}_{LS_{(1)}}(R)}{\langle S\|S_2\|S\rangle} = -\frac{9}{\sqrt{10}}\frac{m_\alpha}{M}C_{211}F^{+}_{LS_{(1)}}(R)$$

$$= -\frac{m_\alpha}{M}\overline{C}_{211}F^{+}_{LS_{(1)}}(R) \qquad (3.53)$$

(4) The final term, $-\frac{m_n}{M}\underline{r}\wedge\underline{P}.\underline{s}$ gives two contributions to $V_1(R)$ in an analogous fashion to the equivalent term in the ^{15}N-α calculation. We set $\mathcal{L}=1$, recouple $C_1(\hat{\underline{R}})$ and $\underline{P}$ to $\underline{L}$ and $C_1(\hat{\underline{r}})$ and $\underline{r}$ to a scalar or a rank-2 tensor proportional to $C_2(\hat{\underline{r}})$. Thus the rank combinations are (1,0,1) and (1,2,1) and the operator $-3\frac{m_n}{M}U_{LS_{(1)}}(r,R)C_1(\hat{r}).C_1(\hat{R})\underline{r}\wedge\underline{P}.\underline{s}$ is rewritten in the form

$$-\frac{m_n}{M}\frac{r}{R}U_{LS_{(1)}}(r,R)\underline{L}.\left\{\underline{s}+\sqrt{\frac{5}{2}}T_1(C_2(\hat{r}),\underline{s})\right\}$$

This gives a contribution to V_1 of

$$-\frac{m_n}{M}\left\{C_{101}+\sqrt{\frac{5}{2}}\langle l\|C_2(\hat{r})\|l\rangle C_{121}\right\}\langle s\|\underline{s}\|s\rangle \bar{F}_{LS_{(1)}}(R)$$
$$\langle s\|\underline{S}\|s\rangle$$

$$= -\frac{m_n}{M}\left\{\sqrt{\frac{3}{2}}C_{101}-\sqrt{\frac{3}{2}}C_{121}\right\}\bar{F}_{LS_{(1)}}(R)$$

$$= -\frac{m_n}{M}\left(\bar{C}_{101}-\bar{C}_{121}\right)\bar{F}_{LS_{(1)}}(R) \qquad (3.54)$$

Collecting all these terms together, we have form factors;

$$V_0(R)=\langle 0\|T_K\|0\rangle\delta_{K0}-2\bar{F}_{C_{(0)}}(R)+\frac{m_\alpha}{M}\left[F_{LS_{(0)}}(R)-F^{+}_{LS_{(1)}}(R)\right]\bar{C}_{011} \qquad (3.55)$$

(The first term is the ^{16}O-α central potential)

$$V_1(R)=\frac{m_n}{M}\left[F_{LS_{(0)}}(R)-\bar{F}_{LS_{(1)}}(R)\right]\bar{C}_{101}-\frac{m_n}{M}\left[F_{LS_{(2)}}(R)-\bar{F}_{LS_{(1)}}(R)\right]\bar{C}_{121} \qquad (3.56)$$

$$V_2(R)=\bar{F}_{C_{(2)}}(R)\bar{C}_{220}+\frac{m_\alpha}{M}\left[F_{LS_{(2)}}(R)-F^{+}_{LS_{(1)}}(R)\right]\bar{C}_{211} \qquad (3.57)$$

We note that the alpha-nucleon spin-orbit force contributes to all three form factors, whereas the central term is only present in V_o and V_2. Hence, the inclusion of the spin-orbit term was necessary to calculate V_1 and so to check the phenomenological assumption of its smallness. Clearly, the cluster-core spin-orbit force will be small for the same reasons as in the $^{19}F = {}^{15}N+\alpha$ (all its terms involve the strength of the spin-orbit part of $V^{(i)}_{\alpha n}$ and are multiplied by m_n/M) and in fact it turns out that if we set the amplitudes $C_1=1$, $C_2=0$,

C_3=0 we get exactly the ^{15}N-α form factors; eqs. 2.34 and 2.35.

3.4.5 Choice of p-Shell Wave Functions and α-Nucleon Potential.

To produce analytic expressions for the form factors we find it convenient to follow the prescription of the last chapter and use oscillator wave functions to describe the p-shell holes, which have a radial part

$$R(r) = \sqrt{\frac{8}{3\sqrt{\pi}}}\frac{r}{b}e^{-r^2/2b^2} \qquad (2.36)$$

Also, from the many parametrizations of the central alpha-nucleon potential (including Woods-Saxon, exponential, difference of two Yukawas and Gaussian forms) we choose the Gaussian. In addition to the considerations of analyticity outlined earlier, if we follow the normal convention and write the spin-orbit form-factor as $V(r) \propto \frac{1}{r}\frac{du}{dr}$, this is also a Gaussian and the radial integrals $F_{LS_{(\ell)}}(R)$ are identical to the corresponding ones for the central potential, $F_{C_{(\ell)}}(R)$. On this occasion the central part of $V_{\alpha n}$ is very important, so we take its strength and width from the fit to scattering data of Batty and Friedman [28], and fix the strength of the spin-orbit term by considering the splitting of the $P_{3/2}$-$P_{1/2}$ doublet of resonances in ^{5}He as described in section 2.3.5. As we shall ultimately show that the cluster-core spin-orbit potential has a practically negligible effect on the ^{18}F spectrum, this rough estimate of the spin-orbit part of $V_{\alpha n}$ is good enough for our purposes. So, we take

$$V_{\alpha n}(X) = -\left(U_c + U_{LS}\,\underline{L}\cdot\underline{S}\right)e^{-X^2/a^2} \qquad (3.58)$$

with U_C = 43 MeV, U_{LS} = 7 MeV and a = 1.9 fm. We shall also repeat the calculation of the spectrum with U_{LS} = 53.8 MeV since this strength is also proposed by Batty et al. [27]).

We are now in a position to write down analytic expressions for the form factors; and in addition to the expressions of eqs. 2.41, 2.42, and 2.43 (in which U_{LS} may be replaced by U_C where appropriate to find $F_{C_{(0)}}(R)$ and $F_{C_{(2)}}(R)$) we have one additional radial integral, $F^{+}_{LS_{(1)}}(R)$

$$F^{+}_{LS_{(1)}}(R) = -\frac{2U_{LS}}{3}\left(\frac{a^2}{a^2+b^2}\right)^{5/2}\frac{R^2}{a^2}\,e^{-\frac{R^2}{a^2+b^2}} \qquad (3.59)$$

3.4.6 The Central Potential.

It is clear from the derivation of the central form factor $V_o(R)$ in section 3.4.4 (see eq. 3.55) that we could obtain the central part of the ^{14}N-α interaction by adding the central part of the 2 hole-alpha interaction to an effective ^{16}O-α interaction. The first step in such a programme is a decision on what to take for that ^{16}O-α potential. To obtain this from a folding procedure we should take the convolution of the density of ^{16}O with an alpha-nucleon potential, leaving the precise values of the parameters open to adjustment so that they can be varied to reproduce the ground state rotational band in ^{20}Ne (we might hope to have an adjustable strength like $\bar{f}$ in eq. 1.14 which is varied from one band to another). The attraction of this folding procedure is the possibility of obtaining an analytic potential by using a Gaussian form for the alpha-nucleon interaction and an ^{16}O density obtained by summing the

densities of the 4s-shell and 12p-shell nucleons, treating them as occupying oscillator states. So, taking an alpha-nucleon potential, $-Ue^{-r^2/a^2}$, and using eq. 2.36 for the p-shell nucleon density function, and

$$R_{oo}(r) = \frac{2}{\pi^{1/4}} e^{-r^2/2b^2} \tag{3.60}$$

normalized as in eq. 2.37 for the s-shell nucleon density function (the subscripts indicating node number and orbital angular momentum) we obtain an ^{16}O-α potential of modified Gaussian form;

$$V(^{16}O-\alpha) = -U\left(\frac{a^2}{a^2+b^2}\right)^{3/2}\left\{4 + \frac{12a^2}{a^2+b^2}\left(1 + \frac{2b^2R^2}{3a^2(a^2+b^2)}\right)\right\} e^{-\frac{R^2}{a^2+b^2}} \tag{3.61}$$

The weakest link in this prescription is the treatment of the ^{16}O density, so we might hope to improve on tnis result by taking an alternative parametrization of it from electron scattering data, e.g.

$$\rho(r) = \rho_o(1 + \alpha r^2)e^{-r^2/\beta^2} \tag{3.62}$$

where $\rho_o = 0.1331$ fm^{-3}, $\alpha = 0.4667$ fm^{-2} and $\beta = 1.85$ fm [48]). Again the folding integral can be evaluated analytically to yield a modified Gaussian form;

$$V(^{16}O-\alpha) = -\rho_o U\left(\frac{a^2\beta^2\pi}{a^2+\beta^2}\right)^{3/2}\left\{1 + \frac{3\alpha a^2\beta^2}{a^2+\beta^2} + \frac{\alpha a^4 R^2}{(a^2+\beta^2)^2}\right\} e^{-\frac{R^2}{a^2+\beta^2}} \tag{3.63}$$

We can now take eqs. 3.61 and 3.63 and try to choose a and U to fit the ground state band of ^{20}Ne. We clearly hope to find that values not too different from those obtained by fitting alpha-nucleon scattering data will be required.

However, we should note that this particular band has already been fitted rather well by parametrizing the folded potential of Buck, Dover

and Vary in the symmetrized Woods-Saxon form

$$V(R) = -V_o\left(\frac{1 + \cosh R_o/a_o}{\cosh R/a_o + \cosh R_o/a_o}\right) \qquad (3.64)$$

with V_o = 176 MeV, R_o = 2.25 fm and a_o = 0.8 fm (see Fig. 6 for diagram of potential).

In fitting the simple folding potentials to the ground state band of ^{20}Ne we wish to have as few free parameters as possible, so we take the width of the alpha-nucleon potential from scattering data and choose U to give these potentials the same depth as the "cosh" potential (eq. 3.64). The three potentials are shown in Fig. 6, where we see that they are very similar in appearance, although the simple foldings are slightly wider than the cosh potential. The alpha-nucleon strengths required by eqs. 3.61 and 3.63 are 40.8 MeV and 45.6 MeV respectively (to give a depth of 176 MeV, matching the cosh potential). We point out that these strengths compare favourably with the 43.0 MeV of the potential derived from alpha-nucleon scattering data of Batty and Friedman.[28])

Visually, the two simple foldings yield potentials which are not too dissimilar from the cosh potential, but judged by their ability to reproduce the ground state band of ^{20}Ne they are decidedly inferior. This is not really so surprising when we consider that the rotational spectrum being generated involves level separations which are typically of order 1% of the depth of the central potential. It is known that different parts of the spectrum are sensitive to different parts of the potential, and clearly, if the apparently similar simple foldings differ even slightly from the more accurate cosh potential in such a region the resulting level scheme may well be substantially different. For example, the L=0 level will be particularly influenced by the behaviour of the potential near

the origin, since it has a high probability of being located thereabouts, and we find that the foldings eqs. 3.61 and 3.63 place this level too close to the 2^+, although the moment of inertia for the rest of the band is satisfactory. It is strongly suspected that this is a consequence of the different R-dependencies near the origin. Because of this sensitivity to the precise shape of the potential, similar problems will be encountered in obtaining the central part of an effective ^{14}N-α potential. It seems reasonable, therefore, to use a cosh potential which is known to reproduce the rotational centroids in ^{18}F rather well. Hence we take a central nuclear interaction of the form eq. 3.64 with V_o = 168 MeV, R_o = 2.25 fm and a_o = 0.8 fm. As mentioned in chapter 2, the use of the same values of R_o and a_o in the central part of the cluster-core potential for alpha cluster states in ^{18}F, ^{19}F and ^{20}Ne (with similar depths V_o) produces the intuitively pleasing result of near equality of the moments of inertia for the ^{14}N, ^{15}N, ^{16}O-α systems.

However, the expressions for the non-central parts of the potential, $V_1(R)$ and $V_2(R)$ are used in exactly the form given in eqs. 3.56 and 3.57 using the p-shell radial wavefunctions of eq. 2.35 and the alpha-nucleon potential of eq. 3.58. Plots of these form factors are shown in Fig. 7.

We note that $V_1(R)$ (the spin-orbit form factor) is most important near the origin and has a much smaller strength than $V_2(R)$ (a factor of 10). Also shown in Fig. 7 are the radial wavefunctions of relative motion between cluster and core for L=0,2 which indicate that $|\chi_L|^2$ is largest in a region where $V_1(R)$ is very small. Conversely $V_2(R)$ (the tensor form factor) goes to zero at the origin and is peaked in that very region where $|\chi_L|^2$ is most important, showing quite emphatically that the effects

of the spin-orbit force will be entirely negligible in comparison with those of the tensor force, which is clearly the dominant cause of the level splitting. This is precisely the result suggested in the phenomenological method, and we also see that $V_2(R)$ varies smoothly in comparison with the oscillations in $|\chi_L|^2$ as required by the qualitative justification of that model.

3.4.7 Calculation of the Spectrum.

Our approach in this case is a little different from that in the ^{19}F calculation where the splittings due to the spin-orbit force were calculated with first-order perturbation theory. This time we write down a state-dependent potential for the ^{14}N-α system, including the contributions from spin-orbit and tensor interactions, and solve the one-particle Schrödinger equation for each state of given J and L. (The condition 2N+L = 8 is applied to the quantum numbers of relative motion to obtain the lowest possible band, once the forbidden states have been excluded). So, the potential used is;

$$V_{JL} = V_0(R) + V_{COUL}(R) + \tfrac{1}{2}V_1(R)\left[J(J+1) - L(L+1) - S(S+1)\right] + V_2(R)\,\Delta(J,L) \qquad (3.65)$$

where $V_0(R)$ is given in eq. 3.64 and a Coulomb term is included in the central potential which involves treating the core as a uniformly charged sphere of radius 3 fm (3.1 fm was used for ^{15}N) and the alpha particle as a point charge. (The effect of the quadrupole Coulomb force was found to be entirely negligible). The function $\Delta(J,L)$ is given in eq. 3.8. Energies and wavefunctions can then be calculated numerically

and these wavefunctions can be used to calculate the off-diagonal matrix elements of the tensor force which produce mixing between the states of odd-J which can be formed by coupling S=1 with values of L differing by two units (e.g. 3^+ from S=1 x L=2 and from S=1 x L=4). For those higher-lying states which are quasi-bound, the procedure of continuing the potential barrier at its maximum value for larger separations is adopted, as outlined in section 2.3.6.

The spectrum, calculated in this fashion is shown in Table 4 and is displayed diagrammatically (Fig. 4b) for comparison with the phenomenological results (Fig. 4a) and experiment. As a test of the sensitivity of the results to the α-nucleon potential, a spectrum is also shown in Table 4 derived from the central depth of 53.8 MeV (a 25% increase over the 43.0 MeV used before) used by Batty et al. [27]). There is little qualitative difference in the results.

In order to facilitate a comparison of the microscopic results with the assumptions of the phenomenological model we also use our wavefunctions to obtain values of the quantities $\gamma(L,L)$ and $\gamma(L,L+2)$ (defined in eqs. 3.9 and 3.11). The former is related to the fitting parameter β of ref. [20]) by $\gamma(L,L) = -3\beta$, so we therefore tabulate values of $-\frac{1}{3}\gamma(L,L)$ for the various values of L (in Table 5) and these should be compared with the L-independent phenomenological value of $\beta = 0.65$ MeV. Since this value of β was obtained by fitting the low-lying levels in the spectrum (the 2^+,4^+ and 3^+, were used to obtain C, α and β in eq. 3.12) it is highly encouraging to see that for low values of L the microscopic calculation yields a very similar result, although an increase is noted for higher values of L.

Values of the mixing parameter $\frac{1}{3}\gamma(L,L+2)$, which was taken to be zero in the phenomenological model, are also shown in Table 5. This time there is a strong disagreement between the models, since the microscopically calculated values are very different from zero. Indeed, we note the near equality of $\gamma(L,L+2)$ and $\gamma(L,L)$.

In comparing the rival claims of the two models, we point out that since the calculated values of $-\frac{1}{3}\gamma(L,L)$ are very similar to the β of the earlier model (at least for low L), the calculated spectrum of Fig. 4b would be almost identical to that of Fig. 4a if mixing was ignored. However, in its presence the splittings of the 3_1^+-1_2^+ and 5_1^+-3_2^+ levels are greatly increased, apparently to the detriment of agreement with the experimental data. Hence, it is necessary to decide whether the off-diagonal matrix elements are so large because of our particular choice of the α-nucleon potential or whether they are an inescapable consequence of a smoothly varying form factor which can correctly reproduce the diagonal matrix elements.

We incline to the latter view that $\gamma(L,L)$ and $\gamma(L,L+2)$ must inevitably be comparable in magnitude by considering the radial wavefunction $\chi_L(R)$ for L=0 and 2 and the tensor form factor $V_2(R)$. From Fig. 7, we see that these wavefunctions are essentially in phase beyond 2.5 fm, and in fact their overlap exceeds 0.75. The tensor form factor has its maximum magnitude at around 3 fm, so the integrals for $\gamma(L,L)$ and $\gamma(L,L+2)$ are even more heavily weighted towards equality. The same is true for higher L, even for L=6 and L=8, where there is one node in one function and no nodes in the other, so the only way to obtain small mixing would be to have a different alpha-nucleon range which might be able to move the peak of $V_2(R)$ nearer to the origin where $\chi_L(R)$ and $\chi_{L+2}(R)$ are more out

of phase. However, bearing in mind that $V_2(R)$ varies as $R^2e^{-R^2/a^2+b^2}$, we see that the peak will be at $R = \sqrt{a^2+b^2}$, where b is the p-shell oscillator parameter of 1.72 fm, and so no choice of the α-nucleon range a can shift the peak into the "out of phase region" sufficiently to escape the conclusion that the off-diagonal matrix elements will be large. This inevitable result of large mixing leads us to re-examine the experimental data in the next section.

The effect of the spin-orbit force is very similar to that of the last chapter, and we again define a quantity δ_L by

$$\delta_L = \int_0^\infty V_1(R)\,|\chi_L(R)|^2\,dR \qquad (3.66)$$

whose values are listed in Table 5. The energy shift, due to the spin-orbit force, of a level of given J and L from the centroid is given by the quantity(analogous to that of eq. 2.46) $\frac{1}{2}[J(J+1)-L(L+1)-S(S+1)]\delta_L$. For the J = L±1 members of a given triplet, the splitting from this source is never greater than about 60 keV, even in the maximum case, completely justifying ignoring the spin-orbit effects in the simple phenomenological model.

3.5 Summary and Conclusions.

Those alpha cluster states which are convincingly identified experimentally are well fitted by both phenomenological and microscopic calculations. This agreement essentially reflects the justification of most of the assumptions of the earlier model (neglecting vector and tensor spin-orbit forces and taking a constant diagonal matrix element of the

tensor force of 0.65 MeV) by the microscopic one. The major difference between them concerning the tensor mixing is only really tested by those levels for which the identification of experimental candidates is not so clear cut. In particular the assignment of the 1^+ and 3^+ members of the $K^\pi = 0^+$ band (in the notation of the rotational model) is affected by the question of mixing, and will now be considered in more detail.

The phenomenological model predicts the 1^+ of the $K^\pi = 0^+$ band to lie above, but very close to the 3^+ of the $K^\pi = 1^+$ band, and so favours the experimentally located 1^+ at 3.724 MeV as the relevant alpha cluster state. Similarly, this model predicts the 3^+ of the $K^\pi = 0^+$ band to lie above but very close to the 5^+ of the $K^\pi = 1^+$ band, and hence suggests that the experimental level of $J^\pi = 1^+, 2^+$ or 3^+ at 6.803 MeV is in fact the 3^+ alpha cluster state in question. The important point to note is that the 3^+-1^+ and 5^+-3^+ splittings are very small in this model. However, when non-negligible mixing is introduced the splittings are increased considerably since in the 3^+-1^+ case the 3^+ goes down and the 1^+ up in energy, and similarly for the 5^+-3^+ pair, the 5^+ goes down and the 3^+ up. The experimental data is now reviewed to see if it can be used to resolve these apparent discrepancies.

Dealing first of all with the 1^+ member of the $K^\pi = 0^+$ band which the microscopic model predicts should lie at about 4.2 MeV, we note that the shell model predicts a 1^+ two particle ($^{16}O + (sd)^2$) state at about 4.0 MeV. There will almost certainly be some mixing between these states which will result in there being two 1^+ states which both contain consdierable 2p and 4p-2h components in the spectrum around 4 MeV. We propose these two 1^+ levels to be those seen at 3.724 MeV and 4.361 MeV. The investigation of the $^{14}N(^7Li,t)^{18}F$ reaction by Middleton et al.[34])

seems to confirm this view since the cross-sections they cite at 15° for these two levels are 0.68 mb/str and 0.45 mb/str respectively. Although not small, these values are not so large as those found for the $2^+,3^+,4^+,5^+$ members of the $K^\pi = 1^+$ band, suggesting that these two 1^+ levels are sharing the α-cluster strength. Such a sharing also seems to be in agreement with the observation of Rolfs et al. [37]) that both levels have substantial 2p-0h components. So, this interpretation appears to be consistent with the available experimental data, and the levels predicted by the microscopic cluster model and shell model fall between the two experimental candidates, as required.

The 3^+ member of the $K^\pi = 0^+$ band is far more difficult to identify. Since the microscopic cluster model calculation predicts this 3^+ to lie at around 7.0 MeV, and Middleton et al. [34]) see a level of undetermined spin and parity at 7.26 MeV in the $^{14}N(^7Li,t)^{18}F$ reaction with the large cross-section at 15° of 2.25 mb/str it is very tempting to consider this level as the alpha cluster state required. However, Sens et al. [39]) believe this state to have $J^\pi = 3^-$, and also [38]) think that the 3^+ levels at 6.30 MeV and 6.48 MeV could have 4p-2h structures. Since Rolfs et al.[37]) conclude that, should the level at 6.803 MeV turn out to have $J^\pi = 3^+$ (and not 1^+ or 2^+) its structure would be more complicated than 2p-0h, and might be 4p-2h the picture is very confused. It is clear, however, that there are at least two, and possible four, 3^+ states very close together in a region where the 3^+_2 alpha cluster state is expected, and mixing between them will almost certainly result in a sharing of the cluster strength between several levels. This conclusion is supported by the cross-sections of 1.05 mb/str and 0.55 mb/str for the 3^+ states at 6.30 MeV and 6.48 MeV found by Middleton et al. in $^{14}N(^7Li,t)^{18}F$.

A mechanism by which the 3_2^+ cluster state might appear below the 5_1^+ (as both of these latter candidates are) will be presented in Chapter 5.

Finally, we observe that there are no really good candidates at all for four cluster states predicted by the model. A second 5^+ state (having $K^\pi = 0^+$) is predicted to lie close to the 7^+ seen at 11.22 MeV, and a triplet with $J^\pi = 7^+,8^+,9^+$ is predicted to lie in the energy region 18-20 MeV. However, as mentioned previously, when the cosh potential is applied to analogous cluster states in ^{19}F and ^{20}Ne the L=8 level (a nearly degenerate doublet in ^{19}F) lies higher than the experimental candidates, which in these cases are well established. Specifically, in ^{20}Ne the model predicts an 8^+ level at about 15 MeV, whilst an 8^+ level at 11.95 MeV is strongly excited in alpha transfer reactions such as $^{16}O(^{11}B,^{7}Li)^{20}Ne$ and $^{16}O(^{13}C,^{9}Be)^{20}Ne$. Simiarly, in ^{19}F, the cosh potential gives the centroid of the $\frac{15^-}{2}$ - $\frac{17^-}{2}$ doublet at about 17 MeV while the strongly excited experimental candidates from the alpha transfer reactions [$^{15}N(^{11}B,^{7}Li)^{19}F$ and $^{15}N(^{13}C,^{9}Be)^{19}F$ for example] are seen at 12.26 and 12.65 MeV. This suggests that one should perhaps look for the $7^+,8^+,9^+$ triplet of alpha cluster states in ^{18}F at about 12 MeV above the band head; i.e. 14-15 MeV. In fact narrow peaks (indicative of high spin states) are strongly excited in $^{14}N(^{13}C,^{9}Be)^{18}F$ at 14.18 MeV and in $^{14}N(^{11}B,^{7}Li)^{18}F$ at 14.18 and 15.79 MeV which may prove to be cluster states on further investigation. A further state is selectively excited at 10.60 MeV in these reactions which is in the right region to be the predicted 5_2^+. Again, a closer experimental investigation is necessary for confirmation.

To summarize, we can confidently identify the 1^+-7^+ members of the $K^\pi = 1^+$ band predicted by the cluster model with experimentally observed

levels and can also identify the levels which share the strength of the 1^+ in the $K^\pi = 0^+$ band. However, we need more information on the spin-parity values of the higher-energy states before we can propose convincing candidates for the $8^+,9^+$ members of the $K^\pi = 1^+$ band and the $3^+,5^+,7^+$ members of the $K^\pi = 0^+$ band.

CHAPTER 4

TRINUCLEON CLUSTER STATES IN A=18 NUCLEI

4.1 Experimental Evidence for Trinucleon Cluster States in A=18 Nuclei.

In the previous two chapters it was found that alpha cluster states could be identified very well by examining the data from the relevant alpha transfer experiments. Similarly, the most striking signature of a trinucleon cluster state in an A=18 nucleus would be its strong, selective excitation in a three nucleon transfer reaction onto an A=15 target (assuming the incoming beam is sufficiently energetic). Unfortunately, very few such experiments have been performed and only a few low-lying states are well established as cluster states with known spin-parity. However, we also note that a state belonging to the lowest (2N+L=6) band of trinucleon cluster states in an A=18 nucleus will have negative parity, on account of the p-shell hole in the core. Its leading term in a shell-model expansion would be $p_{1/2}^{-1}(sd)^3$. Hence, we may also have recourse to studies of γ-decay in ^{18}F and ^{18}O as a further means of identifying those states with negative parity which decay preferentially to other better established cluster states. Although we wish to propose such states as additional possible candidates, we note that this latter method yields more negative parity states with low spin than can be accommodated

in the cluster model, and the possibility of alternative structures must be borne in mind.

4.1.1 Candidates in ^{18}F.

The first step towards identifying trinucleon cluster states in ^{18}F was made by Poletti [49]) who assigned negative parities to the J=0 level at 1.08 MeV, and the J=2 level at ?.10 MeV and suggested that they might be formed by coupling a $p_{1/2}$ hole to the first two $1/2^+$ and $5/2^+$ (triton cluster) states in ^{19}F. Some supporting evidence for these two levels and also the 4^- at 4.40 MeV is supplied by Rolfs et al. [37]) who have measured strong E2 transitions between them. They also noted the rotational energy separations (varying like J(J+1)) and suggested that the three states might belong to a $K^\pi = 0^-$ band.

The helion (^3He) transfer reaction $^{15}N(^6Li,t)^{18}F$ was performed by Lindgren et al. [50]) with an incident beam energy of 30 MeV. It is not clear whether this bombarding energy is high enough to ensure that direct transfer of three nucleons in a configuration of maximum orbital symmetry is the only important reaction mechanism. Although the final states populated are expected to have predominantly 3p-1h configurations some states which are not candidates for ^{15}N-^3He cluster structure are selected. Bearing in mind this reservation, the following states are most likely to have trinucleon cluster structue from amongst the negative parity states found by Lindgren et al. The 0^-(1.08), 2^-(2.10) and 4^-(4.40), which have already been mentioned, are strongly excited. Also, (see table 6 and Fig. 8) levels with spin-parity 1^-(3.13),

$3^-(3.79)$, $2^-(4.23)$ and $1^-(4.84)$. In all cases the energy is given in brackets in MeV after the spin-parity value. Finally, Lindgren et al. find two weak candidates; the $3^{(-)}(5.50)$ and $4^-(6.097)$ which are not so strongly excited.

Two further helion transfer experiments have recently been performed. Rae et al. [41]) have studied the $^{15}N(^{11}B,^{8}Li)^{18}F$ and $^{15}N(^{12}C,^{9}Be)^{18}F$ reactions. In both cases the beam energy was 115 MeV, so that the reaction should proceed unambiguously by transfer of three nucleons in a state of maximum orbital symmetry, resulting in the strong selective population of states of high spin in ^{18}F. Strong peaks in cross-section are observed at energies of 4.34, 6.10, 7.15 and 9.45 MeV. However, the energy resolution of the experiments is so low that the excitation at "4.34 MeV" is identified with the $4^-(4.40)$ trinucleon cluster state. In fact, of these four excitations, only this $4^-(4.40)$ level has been previously identified. The remaining three levels are tentatively assigned 5^-,7^- and 6^- respectively by comparison of their excitation energies with shell model predictions. We prefer to leave the spin values open and wait for an accurate experimental determination, since it turns out that our own calculations suggest the opposite labelling of 6^- and 7^- for the latter two states. The experimental possibilities are summarized in table 6.

4.1.2 Candidates in ^{18}O.

The experimental evidence for similar trinucleon cluster states in ^{18}O is even more sparse than in ^{18}F. Those negative parity states which have been located are found to decay predominantly to lower

lying positive parity states, and very few M1 or E2 transitions from one negative parity state to another have been measured. This makes identification of cluster states even more difficult, and we have to rely solely on selective excitations in transfer reactions and assignments of negative parity. Firstly, we consider those experiments which have been able to locate states wtih negative parity in ^{18}O. Six negative parity states were discovered by Olness et al. [51]) and subsequently confirmed by Becker et al.[52]) in studies of the reaction $^{19}F(t,\alpha\gamma)^{18}O$ as follows; $1^-(4.45)$, $3^-(5.09)$, $2^-(5.53)$, $1^-(6.19)$, $3^-(6.40)$ and $0^-(6.88)$ (see table 7 and Fig. 9) Becker et al. also tentatively proposed two further levels, $2^-(7.75)$ and $4^-(7.96)$ on a basis of a study of their γ-decays. Another experiment which was able to locate negative parity states in ^{18}O was carried out by Kaschl et al. [53]) who studied the reaction $^{19}F(d,^3He)^{18}O$ and were able to populate states up to 15 MeV excitation in ^{18}O. Five of the levels already found by Becker et al. (including the tentative $2^-(7.75)$) were populated and in addition, excitations at 11.14, 11.75 and 12.25 MeV were seen. In view of the dearth of experimental information, these 11 states are all considered as possible candidates for membership of the cluster spectrum, merely on the basis of their parity.

Trinucleon transfer experiments to populate states in ^{18}O, and tc decide which of the 11 states aleady mentioned really do have cluster structure, have only been carried out recently. Martz et al. [54]) have studied $^{15}N(^6Li,^3He)^{18}O$ with an incident beam of 40 MeV. Again it is not clear that this energy is sufficiently high to ensure that only states with a ^{15}N-t structure are heavily populated. However, four of the 11 low-lying levels were populated strongly; $1^-(4.45)$, $3^-(5.09)$,

2^-(5.52) and 1^-(6.18). Also the 2^-(6.35) is weakly populated and 5^-(8.10) very strongly excited.

Finally, Rae et al. [41]) carried out the transfer reaction $^{15}N(^{13}C,^{10}B)^{18}O$ with a 105 MeV beam with a view to finding states of high spin with a ^{15}N-t structure at higher excitation energies. Strong peaks are seen corresponding to energies in ^{18}O of 7.69, 8.50, 11.06 and 11.79 MeV. They are assigned spin-parity values of 5^-,4^-,7^- and 6^- respectively on model considerations. Again we prefer to leave the spin values open until they can be better determined and summarize the data in table 7.

4.2 Phenomenological Treatment of Trinucleon Cluster States in ^{18}F and ^{18}O. [21])

Following the successes of the BDV cluster model in describing the properties of alpha cluster states in ^{20}Ne, ^{19}F, ^{18}F and ^{18}O [13,19,20]) it is natural to extend the model to attempt to describe the trinucleon cluster states discussed in the last section. So, the phenomenological approach was applied to these states in ^{18}F, treating them as a linear combination of the decompositions $^{15}N+^{3}He$ and $^{15}O+t$, and in ^{18}O, treated as $^{15}N+t$.

The condition applied to exclude redundant states in this case will be

$$2N+L=\sum_{i=1}^{3}(2n_i+l_i)\geqslant 6 \qquad (4.1)$$

equivalent to putting the three cluster nucleons into the (sd) shell, at least, and so producing 3p-1h states in the mass 18 system. In the

cases of alpha cluster states, it was found that a folded potential parametrized in the form of eq. 2.1, produced almost perfect rotational bands with very similar moments of inertia for the various decompositions (e.g. $^{16}O+\alpha$, $^{15}N+\alpha$, $^{14}C+\alpha$). Also, it was found to be possible to treat triton cluster states in ^{19}F (the only other nucleus for which such states have been convincingly identified) with an analogous parametrization of the folded potential

$$-V_o f(R) = -V_o \frac{1+\cosh R_o/a_o}{\cosh R/a_o + \cosh R_o/a_o} \qquad (4.2)$$

with V_o = 116 MeV, R_o = 2.0 fm, a_o = 1.3 fm, and a spin-orbit term

$$V_{s.o.}(R) = V_{s.o.}\left(\frac{\hbar}{m_\pi c}\right)^2 \frac{1}{R}\left|\frac{df}{dR}\right| \underline{l}.\underline{\sigma} \qquad (4.3)$$

with $V_{s.o.}$ = -2.5 MeV for the lowest band. This strongly suggests that trinucleon cluster states in ^{18}F and ^{18}O can be treated with a central potential similar to that of eq. 4.2 (producing bands with almost equal moments of inertia to those found for the ^{19}F trinucleon cluster states) and that consideration of the possible spin-dependent interactions between cluster and core (both carry spin-$\frac{1}{2}$) may allow a description of the experimentally observed splitting from the rotational centroids. Bearing this in mind, the process of deriving a folded potential is short-circuited, and replaced by simply taking a series of rotationally spaced centroids for cluster angular momenta of L = 0, 2, 4, 6 relative to the core, according to the formula;

$$E(L) = C + A.L(L+1) \qquad (4.4)$$

where C is a band head energy and the moment of inertia parameter, A, is expected to be close to the $^{16}O+t$ value of 0.195 MeV. The introduction of non-central terms in the cluster-core potential can then split each

centroid into a quadruplet as follows. Both components carry a spin of $\frac{1}{2}$, so the total spin of the system can be 0 or 1. Coupling these two possibilities with the orbital angular momentum, L, produces a singlet with J = L x (S=0) and a triplet with J = L x (S=1). The phenomenological model then seeks to identify the terms allowed in a cluster-core potential by considering the restraints imposed by invariance under space inversion and time reversal. Then it tries to describe the very different patterns of splittings of the cluster states in ^{18}O and ^{18}F by giving matrix elements of these terms constant values, chosen to fit the well identified low lying levels in both nuclei.

In listing the possible non-central terms in the cluster-core potential we find that there are two more than in the previous cases dealt with for which at least one of the components had spin-0. In addition to the central potential, we now have three vector-vector contractions, which are

$$V_{S_c S_t} = V_{S_c S_t}(R)\, \underline{\sigma}_c \cdot \underline{\sigma}_t \qquad (4.5)$$

$$V_{LS_c} = V_{LS_c}(R)\, \underline{L} \cdot \underline{\sigma}_c \qquad (4.6)$$

$$V_{LS_t} = V_{LS_t}(R)\, \underline{L} \cdot \underline{\sigma}_t \qquad (4.7)$$

where the subscript, c, indicates a core variable; t, a trinucleon cluster variable, and $\underline{\sigma}$ are the Pauli spin matrices. Of these, we expect V_{LS_c} to be small by analogy with the findings in other cluster states in which the core carries a spin, and V_{LS_t} to be similar to the ^{16}O-t spin-orbit force. We can also build tensor forces, which will affect those states in which the spins couple to $\underline{S} = \underline{S}_t + \underline{S}_c = 1$, involving the position, momentum and angular momentum of the cluster.

By using the same considerations as in the ^{14}N-α case concerning the expected smallness of a spin-orbit force and the similarity of matrix elements of the momentum and position tensor, only the position tensor is considered in the model.

$$V_T = V_T(R)\left[(\underline{\sigma}_{s_c}\cdot\hat{\underline{R}})(\underline{\sigma}_{s_t}\cdot\hat{\underline{R}}) - \tfrac{1}{3}\underline{\sigma}_{s_c}\cdot\underline{\sigma}_{s_t}\right] \qquad (4.8)$$

All these terms may be multiplied by isospin dependent factors.

Application of the Wigner-Eckart theorem and some standard formulae for reduced matrix elements of spherical tensor operators between coupled basis states [24]) yields the following relations.

$$\langle (L'S')J \| V_{S_cS_t}(R)\,\underline{\sigma}_c\cdot\underline{\sigma}_t \| (LS)J\rangle = \delta_{SS'}\delta_{LL'}\alpha_L\left[2S(S+1)-3\right] \qquad (4.9)$$

where

$$\alpha_L = \int_0^\infty |\chi_L(R)|^2 V_{S_cS_t}(R)\,dR \qquad (4.10)$$

and this radial integral is taken to be constant in the phenomenological model, which is equivalent to assuming that $V_{S_cS_t}(R)$ is a smoothly varying function which encloses most of the strength of $\chi_L(R)$.

The core spin-orbit term, eq. 4.6, is ignored, and the cluster spin-orbit term, eq. 4.7 gives

$$\langle (L'S')J \| V_{LS_t}(R)\,\underline{L}\cdot\underline{\sigma}_t \| (LS)J\rangle = \delta_{LL'}\begin{cases} 0 & \text{for } S'=S=0 \\ \xi_L\sqrt{L(L+1)} & \text{for } S'=1, S=0 \\ \tfrac{1}{2}\xi_L\left[J(J+1)-L(L+1)-2\right] & \text{for } S'=S=1 \end{cases} \qquad (4.11)$$

where

$$\xi_L = \int_0^\infty |\chi_L(R)|^2 V_{LS_t}(R)\,dR \qquad (4.12)$$

By similar reasoning, the radial integral, ξ_L, is taken to be constant. Finally,

$$\langle (L'S')J \| V_T \| (LS)J \rangle = \delta_{LL'} \delta_{SS'} \delta_{S1} \beta_L \Delta(J,L) \qquad (4.13)$$

where $\Delta(J,L)$ is as defined in eqn. 3.8

$$\beta_L = 2 \int_0^\infty |\chi_L(R)|^2 V_T(R) dR \qquad (4.14)$$

and the Kronecker delta, $\delta_{LL'}$, indicates that tensor mixing will be ignored.

Using these expressions it is possible to write down analytic expressions for the energies of the states of odd J, and the elements of a 2x2 matrix which must be diagonalized to obtain the energies of the even J states. This introduces five free parameters for each of the T=0 and T=1 sets of states, although two of these ten quantities are band heads, and we expect A and ξ_L to be the same for both isospins, so there are only six parameters free to fit the energy differences of the spectra. (A, ξ_L, and a β_L and α_L for each isospin) Various fits with different constraining relations were performed by Buck et al. [21]) to obtain the parameters shown in table 9 and the spectra of Figs. 8a, 9a. The fit E of ref. [21]) involved the most severe restriction of parameters. An interesting consequence of this procedure was the strong empirical suggestion that the tensor strength parameter, β_L, should be the same for both T=0 and T=1, whilst the spin-spin parameter, α_L, should be of equal magnitude but opposite sign for the differing isospins. Thus, it is proposed that this behaviour of the spin-spin term may be due to an isospin exchange term in the spin-spin potential of the form

$$V_{\sigma\tau} = \tfrac{1}{2} V_{S_c S_t}(R) \underline{\sigma}_c \cdot \underline{\sigma}_t \left[1 + \underline{\tau}_c \cdot \underline{\tau}_t \right] \qquad (4.15)$$

where $\underline{\sigma}$ and $\underline{\tau}$ are the Pauli spin and isospin matrices respectively.

It can be seen from Figs. 8 and 9 that the fits B1 and B2 of Buck et al. [21]) (which give the best reproduction of the trinucleon spectra of all the five fits performed) are able to account for the low lying states very well and predict additional levels in the regions where strong excitations are seen in three-nucleon transfer reactions. Unfortunately, the spin-parity values of these higher lying states are not known and are only assigned by Rae et al. [41]) on the basis of comparison of the observed energies with shell model predictions (these J^{π} values are bracketed in tables 6 and 7). We prefer not to label the states at all, until more data is available. Once again, there is a need to try to justify the assumptions and account for the magnitudes of fitting parameters used in this phenomenological treatment on a more microscopic level. We therefore extend the semi-microscopic model which was used for the ^{15}N-α and ^{14}N-α systems to this problem to see if it can provide a greater insight or justification of the earlier model.

4.3 Semimicroscopic Treatment of Trinucleon Cluster States in ^{18}F and ^{18}O.

4.3.1 The Microscopic Model.

The many-body Hamiltonian, H, for a system of A_1+A_2 nucleons is split up to describe the cluster (containing $A_2=3$ nucleons), the core (containing $A_1=15$ nucleons) and relative motions, as in chapters 2

and 3. We also write the eigenfunctions of that Hamiltonian as sums of product states in a similar way. Thus

$$H = \sum_{i=1}^{A_1+A_2} \frac{p_i^2}{2m_n} + \sum_{i<j} V_{ij} \qquad (4.16)$$

$$H \approx H_{A_1} + H_{A_2} + H_{rel} \qquad (4.17)$$

$$\Psi_{JM} = \sum_{M',M'',M'''} \langle S_t M' L M'' | \underline{J}_1 M'+M'' \rangle \phi_{S_t M'}(\underline{A}_2) \psi_{LM''}(\underline{R}) \langle J_1 M'+M'' S_c M''' | JM \rangle \phi_{S_c M'''} \qquad (4.18)$$

(where the isospin summation has been suppressed). In this case there is the additional complication that both cluster and core carry spins (S_t and S_c respectively). For the microscopic calculation it is found to be most convenient to couple the cluster spin $\underline{S}_t$ with the orbital angular momentum $\underline{L}$ to obtain an intermediate angular momentum $\underline{J}_1$ and then to couple this with the core spin $\underline{S}_c$ to obtain the final angular momentum $\underline{J}$. This is to be contrasted with the coupling scheme preferred in the phenomenological model where the two spins are coupled, $\underline{S}_t + \underline{S}_c = \underline{S}$, and then the final $\underline{J}$ is produced by combining this $\underline{S}$ with $\underline{L}$. Of course, this is just a matter of convenience in the particular model being dealt with, and does not affect the final results.

An effective cluster-core potential, V_{Cc} in H_{rel}, is built up by summing a nucleon-trinucleon potential over all 15 core nucleons, and ideally the real part of an optical potential should be used to include some of the effects due to exchange of core nucleons with those in the cluster. Also, as mentioned in the last section, the quantum numbers

of relative motion of the system are restricted, sc that the cluster is placed in the (sd) shell and redundant states are excluded.

$$2N+L=\sum_{i=1}^{3}(2n_i+l_i)\geq 6 \qquad (4.1)$$

This condition allows relative orbital angular momenta L = 0,2,4,6 corresponding to 3,2,1,0 nodes in the radial wavefunction.

The core is either ^{15}N or ^{15}O in their respective ground states and will be approximated as a $p_{1/2}$ hold in the ^{16}O closed shell $|0\rangle$, as in the ^{15}N-α calculation of Chapter 2. Therefore, we write the core wavefunction $\phi_{S_c M}(\underline{A}_1)$ as

$$|^{15}A;\underline{S}_c(=\tfrac{1}{2})M_1,\underline{T}_c(=\tfrac{1}{2})M_T\rangle = b^{\dagger}_{\frac{1}{2}M\frac{1}{2}M_T}|0\rangle \qquad (4.19)$$

All the symbols are defined in eq. 2.6. Finally, we need to decide which terms to include in the nucleon-trinucleon potential from which the effective cluster-core potential V_{Cc} is to be built. The terms used to fit scattering data are not a good guide in this case, since very few double polarization experiments (which would exhibit the full range of spin-dependent effects) have been performed, and many authors simply use central terms to fit the data obtained from unpolarized beams and targets. (See for example, refs. 55 and 56). Indeed, we note that all the terms allowed in the final cluster-core potential (see section 4.2) are also possible in the nucleon-trinucleon potential, with a possible isospin-dependent multiplier $\underline{\tau}_n.\underline{\tau}_t$ (subscripts n and t for nucleon and trinucleon respectively). With one eye on the final result, and noting that de Shalit and Walecka [57]) were able to fit the seven P-wave excited states of the alpha particle which are found between 20 and 30 MeV with a potential of this form, we opt for the following;

$$V_{nt}^{(i)}(x) = U_c(x) + U_{\tau\tau}(x)\,\underline{\tau}_n\cdot\underline{\tau}_t + U_{ss}(x)\,\underline{\sigma}_n\cdot\underline{\sigma}_t + U_{s\tau}(x)\left[\underline{\sigma}_n\cdot\underline{\sigma}_t\right]\left[\underline{\tau}_n\cdot\underline{\tau}_t\right]$$

$$+ U_{LS_n}(x)\,\underline{l}_{rel}\cdot\underline{\sigma}_n + U_{LS_t}(x)\,\underline{l}_{rel}\cdot\underline{\sigma}_t \qquad (4.20)$$

which also includes all the vector-vector contractions discussed in section 4.2, and the notation is explained there. We note that tensor terms are also possible, but omit them for simplicity and because there is no evidence for them yet.

4.3.2 The Effective Cluster-Core Potential.

In this section we build up an effective cluster-core potential by summing the nucleon-trinucleon interaction over all 15 core nucleons as in previous sections. However, there are additional complications this time in that the cluster carries a spin and there is isospin-dependence to consider. Taking the potential of eq. 4.20 (and using the expression $\underline{l}_{rel}\cdot\underline{s}$ of eq. 2.12, derived in Appendix II) we make tensor decompositions of all the radial functions $U_A(X)$ (see Appendix 1)

$$U_A(|\underline{r}_i - \underline{R}|) = \sum_{\ell} (2\ell+1)\, U_{A_{(\ell)}}(r_i,R)\, C_\ell(\hat{\underline{R}})\cdot C_\ell(\hat{\underline{r}}_i) \qquad (4.21)$$

with

$$U_{A_{(\ell)}}(r_i,R) = \frac{1}{2}\int_{-1}^{1} U_A(|\underline{r}_i - \underline{R}|)\, P_\ell(\cos\theta)\, d(\cos\theta) \qquad (4.22)$$

where $\underline{r}_i, \underline{R}$ are nucleon and trinucleon position vectors (relative to the core centre) and $\cos\theta = \hat{\underline{r}}_i\cdot\hat{\underline{R}}$. It is our aim to rewrite the nucleon-

trinucleon potential as a sum of scalar contractions of rank-K spherical tensors in the various space-spin coordinates of nucleon and trinucleon (denoted in general by $\underline{n}_i$ and $\underline{t}$) multiplied by another scalar contraction of rank-K' spherical tensors in their respective isospin-coordinates. So. we want to produce a potential;

$$V_{nt}^{(i)} = \sum_{\substack{\text{All tensors of} \\ \text{all ranks } K,K'}} f_{KK'}(r_i,R)\left[A_K(\underline{t})\cdot B_K(\underline{n}_i)\right]\left[C_{K'}(\underline{t})\cdot D_{K'}(\underline{n}_i)\right] \qquad (4.23)$$

where $A_K, B_K,$ are rank-K tensors in the space-spin coordinates (of the appropriate particle) and $C_{K'}, D_{K'}$ are rank K' tensors in isospace (and in our formulation of the model can only be the unit operator, 1, or the isospin vector operator $\underline{\tau}$, see (4.20)). All difficulties in writing the potential in this form have already been encountered in the systems dealt with previously. Such an interaction will give a contribution to the energy of

$$\left\langle \phi_{S_c T_c}^{(\text{core},\underline{n}_j)} \Phi_{LS_tT_t}^{I}(\underline{R})\left((LS_t)J_1S_c\right)J_2(T_cT_t)T \middle| \sum_{i=1}^{15} V_{nt}^{(i)} \middle| \phi_{S_cT_c}^{(\text{core},\underline{n}_j)} \Phi_{LS_tT_t}^{I}(\underline{R})\left((LS_t)J_1S_c\right)J_2(T_cT_t)T \right\rangle \qquad (4.24)$$

and Φ is formed by coupling the cluster spin S_t to its orbital angular momentum L

$$\left|\Phi_{LS_t}^{I}(J_1,M)\right\rangle = \sum_{M'M''} \langle S_tM'LM'' | J_1M'+M''\rangle \phi_{S_tM'}\psi_{LM''}(\underline{R}) \qquad (4.25)$$

where the isospin part of the wavefunction has been suppressed. We now integrate over the nucleon coordinates to obtain

$$\left\langle \Phi_{LS_tT_t}^{I}(\underline{R})\left((LS_t)J_1S_c\right)J_2(T_cT_t)T \middle| \sum_{K,K'} \left[A_K(\underline{t})\cdot N_K(\underline{n}_j)\right]\left[C_{K'}(\underline{t})\cdot M_{K'}(\underline{n}_j)\right] \middle| \Phi_{LS_tT_t}^{I}(\underline{R})\left((LS_t)J_1S_c\right)J_2(T_cT_t)T \right\rangle \qquad (4.26)$$

with

$$N_K^Q M_{K'}^{Q'} = \frac{\left\langle \phi_{\xi_c T_c}^{(\text{core}, \Omega_d)} S_c(m_s+Q), T_c(m_t+Q') \middle\| \sum_{i=1}^{15} f_{KK'}(r_i, R) B_K^Q(\Omega_i) D_{K'}^{Q'}(\Omega_i) \middle\| \phi_{\xi_c T_c}^{(\text{core}, \Omega_d)} S_c m_s T_c m_t \right\rangle S_K^{Q\,(\text{core})} T_{K'}^{Q'\,(\text{core})}}{\left\langle S_c(=\tfrac{1}{2}), T_c(=\tfrac{1}{2}) \middle\| S_K^{(\text{core})} T_{K'}^{(\text{core})} \middle\| S_c(=\tfrac{1}{2}) T_c(=\tfrac{1}{2}) \right\rangle} \tag{4.27}$$

where the triple bars indicate reduced matrix elements in both space-spin and isospin spaces. So

$$N_K^Q M_{K'}^{Q'} = F_{KK'}(R) S_K^{Q\,(\text{core})} T_{K'}^{Q'\,(\text{core})} \tag{4.28}$$

Now, we have written the interaction in terms of induced operators in the spaces of the core spin and isospin and may write the cluster-core interaction as

$$V_{Cc} = \sum_{K,K'} F_{KK'}(R) \left(A_K^{(t)} \cdot S_K^{(\text{core})} \right) \left(C_{K'}^{(t)} \cdot T_{K'}^{(\text{core})} \right) \tag{4.29}$$

All the manipulations necessary to express the nucleon-trinucleon potential in the form (4.23) have already been performed, and we see that the isospin terms are particularly simple since each term in (4.20) is either isospin-independent or contains the scalar product $\underline{\tau}_n \cdot \underline{\tau}_t$, which is already in the form desired. Just as the only possible values of K' are 0,1 (indicating that the trinucleon isospin operator, $C_{K'}(\underline{t})$, is either the unit operator or $\underline{\tau}_t$) because the core isospin is 1/2, so the only values of K are 0,1 since the spin of the core is 1/2. However, the possible terms corresponding to K = 0,1 are now a little different from those encountered in the ^{15}N-α system, because we must take the

cluster spin into account. In this case the trinucleon space-spin operator, $A_K(\underline{t})$ can be proportional to the following terms. For K=0, it can be proportional to the unit operator or to $\underline{L}.\underline{S}_{\underline{t}}$, whilst for K=1 it may be proportional to $\underline{S}_{\underline{t}}$, $\underline{L}$ or $\{(\underline{\sigma}_{\underline{t}}.\hat{\underline{R}})\hat{\underline{R}}-\frac{1}{3}\sigma_t\}$. The symmetry arguments concerning which ranks, K, can appear, in terms of the nucleon space tensor, rank k_1, and spin tensor, rank k_2, turn out to be identical to those in section 2.3.3 where the ^{15}N-α system is dealt with.

4.3.3 The Reduced Matrix Elements of $B_K(\underline{n}_i)\ D_{K'}(\underline{n}_i)$.

As before we consider the space-spin tensor $B_K(\underline{n}_i)$ to be formed by combining a spatial tensor of rank-k_1, R_{k_1}, with a spin tensor of rank-k_2, S_{k_2}. We wish to evaluate reduced matrix elements of $B_K D_{K'}$ between core ground state wavefunctions, treated as a $p_{1/2}$ hole in an inert ^{16}O core.

$$\langle {}^{15}A, S_c(\tfrac{1}{2}), T_c(\tfrac{1}{2}) \| B_K D_{K'} \| {}^{15}A, S_c(\tfrac{1}{2}), T_c(\tfrac{1}{2}) \rangle = \langle (j_1 T)^{-1} \| B_K D_{K'} \| (j_1 T)^{-1} \rangle \quad (4.30)$$

where $|(j_1 T)^{-1}>$ is a hole with intrinsic angular momentum $\frac{1}{2}$ and isospin $\frac{1}{2}$. Application of particle-hole conjugation to write this as a single particle reduced matrix element gives

$$\langle (j_1 T)^{-1} \| B_K D_{K'} \| (j_1 T)^{-1} \rangle = \langle 0 \| B_K D_K \| 0 \rangle \delta_{K0} \delta_{K'0} - \langle j_1 T \| \widetilde{B_K D_{K'}} \| j_1 T \rangle \quad (4.31)$$

where $\widetilde{B_K D_{K'}}$ is the time reversed operator $(\mathcal{T}^{-1} B_K D_{K'} \mathcal{T})^\dagger = (\mathcal{T}^{-1} B_K \mathcal{T}\, \mathcal{T}^{-1} D_{K'} \mathcal{T})^\dagger$ and $\mathcal{T}$ is the time reversal operator. The core expectation value will contribute only for scalars, in both spaces (as signified by the Kronecker symbols) but in addition to a purely

central term there is an additional contribution from the spin-orbit force $\underline{L}.\underline{\sigma}_t$ (which does not contain any core variables) which is a new feature occurring because the cluster carries a spin. The contribution from the hole can be split up into space, spin and isospin components [24]) yielding

$$\langle {}^{15}A \| B D_{K K'} \| {}^{15}A \rangle_h = -\alpha(j_1 K \ell s) \begin{Bmatrix} j_1 & j_1 & K \\ \ell & \ell & k_1 \\ s & s & k_2 \end{Bmatrix} \langle \ell \| \tilde{R}_{k_1} \| \ell \rangle \langle s \| \tilde{S}_{k_2} \| s \rangle \langle T \| \tilde{D}_{K'} \| T \rangle \tag{4.32}$$

with $\alpha(abcd) = \sqrt{(2a+1)(2b+1)(2c+1)(2d+1)}$, $j_1 = \frac{1}{2}$ (the value of the core spin, S_c, since only one hole is involved). As in the ^{15}N-α case, interchanging the first two columns of the Wigner 9-j symbol shows that $K+k_1+k_2$ is even (since $j_1=\frac{1}{2}$, $s=\frac{1}{2}$ and $\ell=1$). Also if $K'=0$, $k_1=0$ or $k_2=0$ we have unit operators, and for $K'=1$, $k_1=1$ or $k_2=1$ we have operators which change sign under time reversal (since they are proportional to $\underline{r}$, $\underline{\ell}$ or $\underline{s}$). These considerations allow us to remove the time reversal operators and rewrite (4.32) in the form;

$$\langle {}^{15}A \| B D_{K K'} \| {}^{15}A \rangle_h = (-1)^{1+K+K'} \alpha(j_1 K \ell s) \begin{Bmatrix} j_1 & j_1 & K \\ \ell & \ell & k_1 \\ s & s & k_2 \end{Bmatrix} \langle \ell \| R_{k_1} \| \ell \rangle \langle s \| S_{k_2} \| s \rangle \langle T \| D_{K'} \| T \rangle \tag{4.33}$$

The rank combinations are the same as in section 2.3.3 for K, k_1 and k_2. Namely,

SCALAR	(0,0,0)	(0,1,1)	
VECTOR	(1,0,1)	(1,2,1)	(1,1,0)

The central and core spin-orbit terms are exactly analogous to those dealt with in section 2.2.3. The central term only giving a (0,0,0) combination and the core spin-orbit giving all combinations except

(1,0,1) because $\underline{s}$ never occurs without $\underline{\ell}$. The spin-spin term $(\underline{\sigma}_n.\underline{\sigma}_t)$ will give combinations (1,0,1) and (1,2,1), and the term $(\underline{\sigma}.\hat{\underline{r}})\hat{\underline{r}}-\frac{1}{3}\underline{\sigma}$ corresponds to the allowed rank combination (1,2,1). The cluster spin-orbit term has $k_2=0$, and so only (0,0,0) and (1,1,0) are possible rank combinations. To summarize, the possible operators are;

SCALAR	1,	$\underline{\ell}.\underline{s}$
VECTOR	$\underline{s}$	$T_1(C_2(\hat{\underline{r}}),\underline{s})$

We now proceed to build up an effective cluster core potential of the form,

$$V_{Cc} = V_0(R) + V_{\tau\tau}(R)\underline{\tau}_c.\underline{\tau}_t + V_{SS}(R)\underline{\sigma}_c.\underline{\sigma}_t + V_{ST}(R)[\underline{\sigma}_c.\underline{\sigma}_t][\underline{\tau}_c.\underline{\tau}_t]$$
$$+V_{LS_c}(R)\underline{L}.\underline{\sigma}_c + V_{LS_t}(R)\underline{L}.\underline{\sigma}_t + V_{T_{ENS}}(R)\left[(\underline{\sigma}_c.\hat{\underline{R}})(\underline{\sigma}_t.\hat{\underline{R}})-\tfrac{1}{3}\underline{\sigma}_c.\underline{\sigma}_t\right]$$
$$+V_{\tau T_{ENS}}(R)(\underline{\tau}_c.\underline{\tau}_t)\left[(\underline{\sigma}_c.\hat{\underline{R}})(\underline{\sigma}_t.\hat{\underline{R}})-\tfrac{1}{3}\underline{\sigma}_c.\underline{\sigma}_t\right] \qquad (4.34)$$

4.3.4 The Form Factors $V_o, V_{\tau\tau}, V_{SS}, V_{ST}, V_{LS_c}, V_{TENS}$ and $V_{\tau TENS}$.

We use the definitions of the radial integrals given in (2.24) and (2.25)

$$F_{A_{(\ell)}}(R) = \int_0^\infty U_{A_{(\ell)}}(r,R)\,|R_{(\ell)}|^2\,r^2dr \qquad (4.35)$$

$$F^{\pm}_{A_{(\ell)}}(R) = \int_0^\infty U_{A^{(\pm)}_{(\ell)}}(r,R)\,|R_{(\ell)}|^2\,r^2dr \qquad (4.36)$$

and proceed with a tensor decomposition of the various $U_A(X)$, as before.

1) The central part of the nucleon-trinucleon potential, $U_c(X)$, will

only contribute to $V_o(R)$, exactly as in section 2.3.4. So, using (4.27) to obtain this term we find it to be

$$\langle \text{CORE} \| U_{C_{(0)}}(r,R) \| \text{CORE} \rangle = -F_{C_{(0)}}(R) \qquad (4.37)$$

2) The isospin dependent term, $U_{\tau\tau}(X)\underline{\tau}_n.\underline{\tau}_t$, contributes similarly since the isospin operators factor out trivially, affecting the sign change under time reversal and yielding a term proportional to $\underline{\tau}_c.\underline{\tau}_t$. So the contribution to $V_{\tau\tau}(R)$ is;

$$\langle \text{CORE} \| U_{\tau\tau_{(0)}}(r,R) \| \text{CORE} \rangle = F_{\tau\tau_{(0)}}(R) \qquad (4.38)$$

3) The spin-spin term, $U_{SS}(X)\underline{\sigma}_n.\underline{\sigma}_t$, is a little more complicated

i) If we take $\mathcal{L}=0$ in (4.21), it is able to produce a term proportional to $\underline{\sigma}_c.\underline{\sigma}_t$. In this case the nucleon operator is $U_{SS_{(0)}}(r,R)\underline{\sigma}_n$, to be dotted with $\underline{\sigma}_t$, so we have tensor ranks $K'=0$, $K=1$, $k_1=0$, $k_2=1$ and the contribution to $V_{SS}(R)$ is;

$$\frac{\langle \text{CORE} \| U_{SS_{(0)}}(r,R)\underline{\sigma}_n \| \text{CORE} \rangle}{\langle S_c \| \underline{S}_c \| S_c \rangle} = \alpha\left(\tfrac{1}{2}\|\tfrac{1}{2}\right) \begin{Bmatrix} \frac{1}{2} & \frac{1}{2} & 1 \\ 1 & 1 & 0 \\ \frac{1}{2} & \frac{1}{2} & 1 \end{Bmatrix} \frac{\langle \ell \| U_{SS_{(0)}}(r,R) \| \ell \rangle \langle s \| \underline{\sigma}_n \| s \rangle}{\langle S_c \| \underline{S}_c \| S_c \rangle}$$

The 9j here, and in subsequent cases is listed in Table 1, and is $-\frac{1}{18}$ so the contribution to $V_{SS}(R)$ is

$$-\frac{1}{3}F_{SS_{(0)}}(R) \qquad (4.39)$$

ii) We may also take $\mathcal{L}=2$ in (4.21) to obtain the operator

$$5U_{SS_{(2)}}(r,R)\,\underline{\sigma}_n.\underline{\sigma}_t\,C_2(\hat{R}).C_2(\hat{r})$$

Using Appendix III with $\underline{L}$ replaced by $\underline{\sigma}_t$ and $\underline{s}$ by $\underline{\sigma}_n$, we see that the part of this operator of interest to us is

$$5U_{SS_{(2)}}^{(r,R)}\left(-\frac{3}{\sqrt{10}}\right)\left[(\underline{\sigma}_t\cdot\hat{\underline{R}})\hat{\underline{R}}-\frac{1}{3}\underline{\sigma}_t\right]\circ T_1\left(C_2(\hat{\underline{r}}),\underline{\sigma}_n\right)$$

Hence, we get a contribution to the tensor form factor $V_{TENS}(R)$ on using (4.27) with $K'=0, K=1, k_1=2, k_2=1$; of

$$\frac{\langle \text{CORE}\|B_K D_{K'}\|\text{CORE}\rangle}{\langle S_c\|\underline{S}_c\|S_c\rangle}=\frac{-15}{\sqrt{10}}\alpha\left(\tfrac{1}{2}\|\tfrac{1}{2}\right)\begin{Bmatrix}\frac{1}{2} & \frac{1}{2} & 1\\ 1 & 1 & 2\\ \frac{1}{2} & \frac{1}{2} & 1\end{Bmatrix}\frac{\langle \ell\|U_{SS_{(2)}}^{(r,R)}C_2(\hat{\underline{r}})\|\ell\rangle\langle s\|\underline{\sigma}_n\|s\rangle}{\langle S_c\|\underline{S}_c\|S_c\rangle}$$

$$=2F_{SS_{(2)}}(R)\quad \text{contributing to } V_{TENS}(R) \tag{4.40}$$

4) The term $U_{ST}(X)[\underline{\sigma}_n\cdot\underline{\sigma}_t][\underline{\tau}_n\cdot\underline{\tau}_t]$ is very similar to this last one, with the isospin dependence factoring out and then giving a $\underline{\tau}_c\cdot\underline{\tau}_t$ dependence as in the case of $U_{\tau\tau}(X)\underline{\tau}_n\cdot\underline{\tau}_c$. So, we get the same results as for $U_{SS}(X)\underline{\sigma}_n\cdot\underline{\sigma}_t$ with an extra sign change and an isospin factor. A contribution to $V_{ST}(R)$ of

$$\frac{1}{3}F_{ST_{(0)}}(R) \tag{4.41}$$

and a contribution to an isospin dependent tensor, $V_{\tau TENS}(R)$, of

$$-2F_{ST_{(2)}}(R) \tag{4.42}$$

5) $U_{LS_n}(X)\underline{\ell}_{rel}\cdot\underline{\sigma}_n$ gives exactly the same contributions as the $\underline{\ell}_{rel}\cdot\underline{s}$ term in the ^{15}N-α calculation; A contribution to $V_o(R)$ of

$$\frac{m_t}{M}\left[F_{LS_{n(0)}}(R)-F^{+}_{LS_{n(1)}}(R)\right] \tag{4.43}$$

where $M = m_t+m_n$, and a contribution to $V_{LS_c}(R)$ of

$$\frac{m_n}{M}\left[F^{-}_{LS_{n(1)}}(R)-\frac{2}{3}F_{LS_{n(2)}}(R)-\frac{1}{3}F_{LS_{n(0)}}(R)\right] \tag{4.44}$$

5) All the tensor recoupling for the final term $U_{LS_t}(X)\underline{\ell}_{rel}\cdot\underline{\sigma}_t$ has already been done in earlier calculations, and we merely have to use these results. We write $\underline{\ell}_{rel}$ as in Appendix II to obtain four terms;

$$\underline{\ell}_{rel}=\left\{\frac{m_t}{M}(\underline{\ell}+\underline{L})-\frac{m_n}{M}(\underline{R}\wedge\underline{p}+\underline{r}\wedge\underline{P})\right\} \tag{4.45}$$

i) We may take $\mathcal{L}=0$ in (4.21) to obtain a contribution to $V_{SS}(R)$ from $\frac{m_t}{M}\underline{\ell}.\underline{\sigma}_t$ of;

$$\frac{\langle \text{CORE}\|\|B_K D_{K'}\|\|\text{CORE}\rangle}{\langle S_c\|\underline{S}_c\|S_c\rangle}=\frac{m_t}{M}\alpha\left(\tfrac{1}{2}\|\tfrac{1}{2}\right)\begin{Bmatrix}\frac{1}{2} & \frac{1}{2} & 1\\ 1 & 1 & 1\\ \frac{1}{2} & \frac{1}{2} & 0\end{Bmatrix}\langle \ell\|U_{LS_t(0)}(r,R)\underline{\ell}\|\ell\rangle$$

$$=\frac{4}{3}\frac{m_t}{M}F_{LS_{t(0)}}(R) \tag{4.46}$$

We may also take $\mathcal{L}=2$, and obtain the operator $5\frac{m_t}{M}U_{LS_t}{}_{(2)}(r,R)C_2(\hat{\underline{R}}).C_2(\hat{\underline{r}})\underline{\ell}.\underline{\sigma}_t$. The term of interest in this recoupling is then (see Appendix III)

$$-5\frac{m_t}{M}\frac{3}{\sqrt{10}}U_{LS_{t(2)}}(r,R)\left\{(\underline{\sigma}_t.\hat{\underline{R}})\hat{\underline{R}}-\tfrac{1}{3}\underline{\sigma}_t\right\}.T_1\left(C_2(\hat{\underline{r}}),\underline{\ell}\right)$$

giving a contribution to the tensor form factor, $V_{TENS}(R)$ of

$$-\frac{15}{\sqrt{10}}\frac{m_t}{M}\alpha\left(\tfrac{1}{2}\|\tfrac{1}{2}\right)\begin{Bmatrix}\frac{1}{2} & \frac{1}{2} & 1\\ 1 & 1 & 1\\ \frac{1}{2} & \frac{1}{2} & 0\end{Bmatrix}\frac{\langle \ell\|U_{LS_{(2)}}(r,R)T_1(C_2(\hat{\underline{r}}),\underline{\ell})\|\ell\rangle}{\langle S_c\|\underline{S}_c\|S_c\rangle}$$

$$=-2\frac{m_t}{M}F_{LS_{t(2)}}(R) \tag{4.47}$$

ii) The term $\frac{m_n}{M}\underline{L}.\underline{\sigma}_t$ can only contribute to $V_{LS_t}(R)$ with $\mathcal{L}=0$. Then we have

$$\langle \text{CORE}\|\|B_K D_{K'}\|\|\text{CORE}\rangle=-\frac{m_n}{M}\alpha\left(\tfrac{1}{2}0|\tfrac{1}{2}\right)\begin{Bmatrix}\frac{1}{2} & \frac{1}{2} & 0\\ 1 & 1 & 0\\ \frac{1}{2} & \frac{1}{2} & 0\end{Bmatrix}\langle \ell\|U_{LS_{t(0)}}(r,R)\|\ell\rangle$$

$$=-\frac{m_n}{M}F_{LS_{t(0)}}(R) \tag{4.48}$$

iii) The term $-\frac{m_t}{M}\underline{R}_\Lambda\underline{P}.\underline{\sigma}_t$, with $\mathcal{L}=1$ in (4.21) can be recoupled to give,

$$-\frac{m_t}{M}U_{LS_{t(1)}}(r,R)\frac{\underline{R}}{r}\left\{\underline{\ell}.\underline{\sigma}_t-\frac{3}{2}\underline{\ell}.\left[(\underline{\sigma}_t.\hat{\underline{R}})\hat{\underline{R}}-\tfrac{1}{3}\underline{\sigma}_t\right]\right\}$$

which give contributions to $V_{SS}(R)$ and $V_{TENS}(R)$ respectively. The nucleon parts of these two operators differ by the factor -3/2, so we only need to find the reduced matrix element of $\underline{\ell}$.

$$\frac{\langle \text{CORE}\|B_kD_{k'}\|\text{CORE}\rangle}{\langle S_c\|\underline{S}_c\|S_c\rangle}=-\frac{m_t}{M}\alpha\left(\tfrac{1}{2}\|\tfrac{1}{2}\right)\begin{Bmatrix}\frac{1}{2} & \frac{1}{2} & 1\\ 1 & 1 & 1\\ \frac{1}{2} & \frac{1}{2} & 0\end{Bmatrix}\frac{\langle \ell\|\frac{R}{r}U_{LS_{t(1)}}(r,R)\underline{\ell}\|\ell\rangle}{\langle S_c\|\underline{S}_c\|S_c\rangle}$$

$$=-\frac{4}{3}\frac{m_t}{M}F^{+}_{LS_{t(1)}}(R) \qquad (4.49)$$

to $V_{SS}(R)$ and hence

$$2\frac{m_t}{M}F^{+}_{LS_{t(1)}}(R) \qquad (4.50)$$

to $V_{TENS}(R)$.

iv) The final term $-\frac{m_n}{M}\underline{r}_\Lambda\underline{P}.\underline{s}_t$ contributes to $V_{LS_t}(R)$ when $\mathcal{L}=1$. The final operator obtained is $-\frac{m_n}{M}U_{LS_{t(1)}}(r,R)\frac{r}{R}\underline{L}.\underline{s}_t$

$$\langle \text{CORE}\|B_kD_{k'}\|\text{CORE}\rangle=\frac{m_n}{M}\alpha\left(\tfrac{1}{2}0\|\tfrac{1}{2}\right)\begin{Bmatrix}\frac{1}{2} & \frac{1}{2} & 0\\ 1 & 1 & 0\\ \frac{1}{2} & \frac{1}{2} & 0\end{Bmatrix}\langle \ell\|\frac{r}{R}U_{LS_{t(1)}}(r,R)\|\ell\rangle$$

$$=\frac{m_n}{M}\overline{F_{LS_{t(1)}}}(R) \qquad (4.51)$$

Collecting all these terms together we obtain the following contributions from the hole-trinucleon interaction.

$$V_0(R)=-F_{C_{(0)}}(R)+\frac{m_t}{M}\left[F_{LS_{n(0)}}(R)-F^{+}_{LS_{n(1)}}(R)\right] \qquad (4.52)$$

$$V_{SS}(R)=-\frac{1}{3}F_{SS_{(0)}}(R)+\frac{4}{3}\frac{m_t}{M}\left[F_{LS_{t(0)}}(R)-F^{+}_{LS_{t(1)}}(R)\right] \qquad (4.53)$$

$$V_{ST}(R) = \frac{1}{3}F_{ST_{(0)}}(R) \tag{4.54}$$

$$V_{TENS}(R) = 2F_{SS_{(0)}}(R) - 2\frac{m_t}{M}\left[F_{LS_{t(2)}}(R) - F^{+}_{LS_{t(1)}}(R)\right] \tag{4.55}$$

We also obtain an isospin dependent tensor of the form

$$V_{2\,TENS}(R)\left[(\underline{\sigma}_t\cdot\hat{\underline{R}})(\underline{\sigma}_c\cdot\hat{\underline{R}}) - \tfrac{1}{3}\underline{\sigma}_c\cdot\underline{\sigma}_t\right](\underline{\tau}_t\cdot\underline{\tau}_c) \tag{4.56}$$

with

$$V_{2\text{-}TENS}(R) = -2F_{ST_{(2)}}(R) \tag{4.57}$$

$$V_{LS_c}(R) = \frac{m_n}{M}\left[F^{-}_{LS_{n(1)}}(R) - \frac{2}{3}F_{LS_{n(2)}}(R) - \frac{1}{3}F_{LS_{n(0)}}(R)\right] \tag{4.58}$$

$$V_{LS_t}(R) = \frac{m_n}{M}\left[F^{-}_{LS_{t(1)}}(R) - F_{LS_{t(0)}}(R)\right] \tag{4.59}$$

We observe that the central and core spin-orbit form factors are identical in form to the equivalent quantities in the ^{15}N-α case. The spin-spin form factor contains contributions both from spin-spin and cluster spin-orbit terms in the nucleon-trinucleon potential, and introducing an isospin-dependence to this latter spin-spin force necessarily produces an isospin dependent tensor force between cluster and core. We can now add these contributions to an ^{16}O-trinucleon potential (containing central and cluster spin-orbit terms) to obtain an effect 15 nucleon-trinucleon potential.

4.4.1 Combination of Microscopic and Phenomenological Calculations.

In the last section an effective cluster-core potential for a 15 nucleon-3 nucleon system was derived from a nucleon-trinucleon potential. Ideally we would now like to take an optical potential which fits nucleon-trinucleon scattering data and calculate expressions for the various form factors in eqs. (4.52)-(4.59). However, the scattering data available at present is inadequate to uniquely determine all the spin and isospin dependent terms which are present in (4.20), and it will be necessary to wait until more experiments with polarized beams and targets have been performed and analysed to carry through this scheme in the same way as was done for the alpha-cluster systems. The necessary polarization data is gradually being extracted (see for example, ref. 58) and optical potentials with more spin-dependent terms are being produced [59]. So, we may hope that an effective nucleon-trinucleon potential will be abailable in the future to allow a semimicroscopic calculation to be carried out in the same spirit as for the systems dealt with in Chapters 2 and 3.

In the meantime we can combine the semimicroscopic formulae with the earlier phenomenology to produce another fit to the data, but with fewer free parameters. This can come about as follows. The microscopic treatment shows that the following three terms in the nucleon-trinucleon potential

$$U_{SS}(x)\,\underline{\sigma}_n.\underline{\sigma}_t + U_{ST}(x)\left[(\underline{\sigma}_n.\underline{\sigma}_t)(\hat{\underline{r}}_n.\hat{\underline{r}}_t)\right] + U_{LS_t}(x)\,\underline{l}_{nt}.\underline{\sigma}_t \qquad (4.60)$$

give rise to similar terms in the cluster-core potential and also a tensor and isospin dependent tensor interaction. So, we can take the geometries of the three radial terms to be the same as in the central part of the optical potential which fits elastic nucleon-trinucleon

scattering (in the absence of polarization) and then choose the strengths of these terms to try and reproduce the spectrum. In fact, there is a further constraint we can apply to the strength of the spin-orbit term.. There are three excited states of the alpha particle (at about 20 MeV excitation) which have isospin-0 and are split solely by a spin-orbit force (see Fig. 10). Hence, we can constrain the spin-orbit strength to reproduce this splitting, leaving only the strengths of $U_{SS}(X)$ and $U_{ST}(X)$ free to produce the same effects as the phenomenological parameters α,β and ξ. (see section 4.2) This will enable us to check that the strengths required are "reasonable", and since we have a relation between α,β and ξ, to check the consistency of the phenomenological values assigned to them (table 9). Also, we have not produced an isospin exchange term microscopically in the effective cluster-core potential akin to the empirical $(1+\underline{\tau}_1.\underline{\tau}_2)(\underline{\sigma}_1.\underline{\sigma}_2)$(see eq. 4.15) of the phenomenological model, so we may be able to get some insight into whether this effect arises from a fortuitous combination of form factors, rather than as a symmetry requirement.

To produce this new fit we retain the phenomenological assumption of perfect rotational spacing of the L-centroids with a moment of inertia parameter A = 0.195 MeV. We then use cluster-core radial wavefunctions appropriate to the ^{16}O-t system to evaluate the parameters α,β and ξ of eqs. (4.10), (4.11) and (4.12), noting that in this calculation α and β will have isospin-dependent components. To evaluate the terms $V_A(R)$ (see eqs. (4.52)-(4.59)) we approximate the nucleon-trinucleon radial terms $U_A(X)$(see eq. 4.20) by Gaussian forms so that we can combine them with oscillator wavefunctions for the p-shell hole in ^{16}O, to obtain analytic expressions for the $V_A(R)$. We then get the four expressions $F_o(R)$, $F_2(R)$, $F_1^{\pm}(R)$ given in eqs. 2.41, 2.42, 2.43

and 3.48, and choose the strengths of U_{SS} and U_{ST} (eq. 4.20) to reproduce the 1^-(4.449 MeV)-0^-(6.860 MeV) separation in ^{18}O and the 0^-(1.080 MeV)-1^-(3.133 MeV) separation in ^{18}F (see Figs. 8,9). We then have a nucleon-trinucleon potential with which to calculate the rest of the spectrum, and as a reasonability check, we also calculate the splitting of the seven P-wave excited states of the alpha-particle at around 20 MeV excitation [57]) (see Fig. 10).

4.4.2 Details of Fit of Trinucleon Cluster States in ^{18}O and ^{18}F.

The procedure is to choose a width for the Gaussian forms used in the $U_A(X)$, fit the spin-orbit strength by comparison with the T=0 P-wave excited states of the alpha particle at around 20 MeV, then choose strengths for U_{SS} and U_{ST} to reproduce the 0^--1^- splittings mentioned in the last section since we know that these are due solely to spin-spin forces (possibly isospin-dependent) as the levels in question have L=0 and are unaffected by spin-orbit and tensor forces. So, to carry out this prescription we take the optical potentials of Drigo and Pisent [55]) and De Vries et al. [56]) and replace their central Woods-Saxon terms, which describe unpolarized nucleon-trinucleon scattering, by Gaussians with widths chosen to give the same radius for a fall of the potential to 1/e of its maximum value. Of course this is a rather gross approximation, but since we are still free to choose the strengths to be used in conjunction with this radial form, it should be possible to obtain the values of the integrals we require without too great a loss in accuracy. It should thus be borne in mind that the required strengths will be order of magnitude guides to the values needed in an optical nucleon-trinucleon potential rather than precise

predictions. In fact the optical potentials of Drigo and Pisent and De Vries et al. suggest different Gaussian widths, but the corresponding cluster state energies resulting only differ by typically 0.1 MeV. For our purposes, the spectrum resulting from the replacement of a Woods-Saxon form with a Gaussian indicates that any loss of accuracy is outweighed by the benefits of analytic expressions in the various tensor decompositions. We also note that Sherif [59]) has a central term in his optical potential whose geometry is identical to that of De Vries et al. The Gaussian width parameters obtained were;

Drigo/Pisent $a = 2.65$ fm

De Vries et al. $a = 2.23$ fm

and the strengths;

Drigo/Pisent $U_{SS}=5.49, U_{ST}=-5.22, U_{LS_t}=-0.46, U_{LS_n}=-1.38$ MeV

DeVries et al. $U_{SS}=8.22, U_{ST}=-7.71, U_{LS_t}=-0.56, U_{LS_n}=-1.68$ MeV

So, we are seeking to use a nucleon-trinucleon potential of the form

$$V_{nt}^{(i)}(x) = \left\{U_c + U_{\tau\tau}\underline{\tau}_n\cdot\underline{\tau}_t + U_{ss}\underline{\sigma}_n\cdot\underline{\sigma}_t + U_{st}(\underline{\sigma}_n\cdot\underline{\sigma}_t)(\underline{\tau}_n\cdot\underline{\tau}_t) + U_{LS_n}\underline{\ell}_{rel}\cdot\underline{\sigma}_n + U_{LS_t}\underline{\ell}_{rel}\cdot\underline{\sigma}_t\right\} e^{-\frac{x^2}{a^2}} \qquad (4.61)$$

to build up an effective cluster-core potential. Since we shall only be concerned with the T=0 trinucleon cluster states in ^{18}F and the T=1 states in ^{18}O, the contributions of the first two terms in (4.61) are absorbed into the band head, and the central part of the cluster-core potential is written

$$E(L) = C + AL(L+1) \qquad (4.62)$$

A=0.195 MeV, C(^{18}O) = 5.05 MeV, C(^{18}F) = 2.58 MeV. The spin-dependent terms are then calculated from the formulae derived in section 4.3 from

the potential of eq. 4.61. The derived cluster spin-orbit term will also contain a contribution from the ^{16}O-t interaction, to which the hole-trinucleon contribution must be added.

The resulting spectra are shown in Figs. 8b and 9b, and the calculated energies listed in table 8. In addition, parameters α', α'_T, β', β'_T, ξ'_t and ξ'_c are calculated for comparison with the parameters of Buck et al. [21]) shown in table 10. We define

$$\alpha' = \int_0^\infty |\chi_L(R)|^2 V_{SS}(R)\, dR \tag{4.63}$$

$$\alpha'_T = \int_0^\infty |\chi_L(R)|^2 V_{ST}(R)\, dR \tag{4.64}$$

$$\beta' = 2\int_0^\infty |\chi_L(R)|^2 V^{(R)}_{TENS}\, dR \tag{4.65}$$

$$\beta'_T = 2\int_0^\infty |\chi_L(R)|^2 V^{(R)}_{\vec{c}\,TENS}\, dR \tag{4.66}$$

$$\xi'_t = \int_0^\infty |\chi_L(R)|^2 V_{LS_t}(R)\, dR \tag{4.67}$$

$$\xi_n = \int_0^\infty |\chi_L(R)|^2 V_{LS_n}(R)\, dR \tag{4.68}$$

To compare these with the expressions listed in table 8 we note the following relations;

^{18}O	^{18}F
$\alpha = \alpha' + \alpha'_T$	$\alpha = \alpha' - 3\alpha'_T$
$\beta = \frac{1}{3}(\beta' + \beta'_T)$	$\beta = \frac{1}{3}(\beta' - 3\beta'_T)$
$\xi_t = \xi'_t$	$\xi_t = \xi'_t$

The phenomenological assumption is that $\xi'_n = 0$. These parameters are listed in table 10. The values of α for the two nuclei are necessarily

very close to the equivalent fitting parameter of Buck et al. [20]) because of the way the strengths of the non-central terms in the nucleon-trinucleon potential were chosen. We also note that there is very little variation of α with cluster angular momentum, and that it is very similar for both ^{18}F and ^{18}O, but not necessarily equal and opposite. The core spin-orbit force is very small, and the cluster spin-orbit parameters are essentially equal to those for the ^{16}O-t system. The only difference from the purely phenomenological model is in the tensor force. This is larger than expected from the phenomenology and mimics the spin-spin force in changing sign from ^{18}F to ^{18}O. The spin-spin and tensor forces are actually closely related, and by choosing the strengths of U_{SS} and U_{ST} in the nucleon-trinucleon potential as we have done (i.e. to reproduce the 0^--1^- splittings in ^{18}F and ^{18}O which are expected to be due solely to the spin-spin force) we automatically fix the tensor force (with and without isospin dependence) between the 15-nucleon core and the 3-nucleon cluster. This is because the spin-spin force between cluster and core is essentially given by integrals involving the $\mathcal{L}=0$ components of a tensor decomposition of $U_{SS}(R)$ and $U_{ST}(R)$ and p-wave oscillator functions. (There is a small modification due to the spin-orbit force in the nucleon-trinucleon system which can also lead to a spin-spin force between cluster and core). Similarly, the tensor force between cluster and core is given by integrals involving the $\mathcal{L}=2$ components of a tensor decomposition of $U_{SS}(R)$ and $U_{ST}(R)$. So, choosing the strengths and geometries of $U_{SS}(R)$ and $U_{ST}(R)$ to produce the required spin-spin force between cluster and core determines the tensor force also, and the latter appears with an isospin dependence in the same way as the former. Depsite this difference the calculated spectra do not differ greatly from the phenomenological ones. The low-lying levels,

for which there are good experimental candidates, are well reproduced, and higher levels are predicted to lie in the vicinity of states which are selectively excited in three nucleon transfer reactions. The two Gaussians used for the nucleon-trinucleon potential geometries which have substantially different widths, produce the same level ordering. Indeed very few levels differ by more than 0.1 MeV in the two cases. However, it should be remembered that the strengths used for the non-central terms are to be regarded as order of magnitude guides rather than precise values.

Finally, as a check on the nucleon-trinucleon potentials, the seven P-wave excited states of the alpha particle at around 20 MeV are caluclated and shown in Fig. 10 (the isospin term $U_{\tau\tau}(X)\underline{\tau}_n.\underline{\tau}_t$ is needed to reproduce the splitting of these states, and strengths of 6.22 MeV for a = 2.65 fm and 8.92 MeV for a = 2.23 fm are used). Of course, the T=0 levels are fitted well, since their splitting is simply due to the spin orbit force. Of the T=1 levels, the 0^--2^- splitting is well fitted for the same reason. The two 1^- levels are rather badly fitted, but we note that even "realistic" potentials have difficulties with this spectrum [60]) and conclude that it serves as a good guide to the nucleon-trinucleon spin-orbit force, but is not very helpful for the other terms.

4.5 Summary and Conclusions.

The results of the semimicroscopic work are encouraging in that the low-lying regions of the spectra of trinucleon cluster states in ^{18}F and ^{18}O can be reproduced satisfactorily with a few reasonable assumptions concerning the strengths of non-central terms in a

nucleon-trinucleon potential. It is clear that the nucleon-trinucleon potential we have used can, and will be, improved as more detailed scattering data, which are sensitive to the spin-dependence of the interaction, particularly any tensor forces, which we have ignored, become available. Such information will allow the calculation to be carried through again with the kind of optical potential which was so successful in building up a ^{14}N-α potential from a nucleon-alpha interation, and we expect a corresponding improvement in the cluster spectra in ^{18}F and ^{18}O to result.

Some idea of the validity of the nucleon-trinucleon potential used can be obtained by calculating the splittings of certain excited states of the alpha particle with it (Fig. 10). This is encouraging but indicates that there are certainly some deficiencies inherent, and it may be that the inclusion of tensor forces (possibly isospin-dependent) is necessary. At any rate, the present potential is giving a reasonable description of this splitting, does not have excessively large strengths or widths, and is adequate for giving some further insight into the phenomenological treatment.

Firstly, we find that the core spin-orbit force is negligibly small, as assumed by Buck et al.[21]) and that the cluster spin-orbit force is very similar to that in the ^{16}O-t system. The more important question concerns the "origin" of the empirical isospin exchange term on the spin-spin force suggested in ref. 21) (see eq. 4.15). According to the calculation presented this does not arise from some symmetry requirement, but from a combination of form factors giving more or less equal strengths to the radial factors multiplying$(\underline{\sigma}_c.\underline{\sigma}_t)$and $(\underline{\sigma}_c.\underline{\sigma}_t)(\underline{\tau}_c.\underline{\tau}_t)$ in the cluster-core potential. In essence this "equality" is also present in the nucleon-trinucleon force, and furthermore leads to a similar

apparent isospin exchange term in the tensor part of the cluster-core interaction. This causes the spectra we calculate to differ in detail from those of the phenomenological model,but the low-lying levels, for which there are good experimental candidates, are not radically changed. It is hoped that the spin-parity values of those states excited strongly in three nucleon transfer to ^{15}N will soon be determined, to see how the middle parts of the predicted spectra compare with reality, and hence whether there is any evidence for mixing with states of different structure, or for core excitations. The highest levels are included in the diagrams (Figs. 8,9), but bearing in mind that the free triton and helion only have binding energies of about 8 MeV we feel that a more sophisticated calculation is necessary to deal with the states having these quantum numbers.

CHAPTER 5

CORE POLARIZATION IN THE $^{14}N+\alpha$ SYSTEM

5.1 Introduction.

The motivation behind the work in this thesis is to put the phenomenological treatments of cluster states in light nuclei, so successfully presented by Buck and his collaborators[13,14,19,20,21], on a more microscopic footing. This programme has been carried out, with encouraging results for alpha cluster states in ^{18}F and ^{19}F in chapters 2 and 3, and for trinucleon cluster states in ^{18}O and ^{18}F in chapter 4. The most successful of these semi-microscopic calculations has been the one dealing with alpha cluster states in ^{18}F, using the cluster-core decomposition $^{18}F = {}^{14}N+\alpha$, where many of the assumptions made in the phenomenological approach were vindicated, and in addition the importance of tensor mixing between cluster states of odd J in ^{18}F was realized (see Fig. 4). Although a good description of these states was thus obtained, some problems still remained. In particular, the treatment we have used inevitably places the state with $J^\pi = 3^+$ formed by coupling an orbital angular momentum of the alpha particle of L=4 with the ^{14}N spin of S=1 above the state with $J^\pi = 5^+$ from that same coupling, whilst the experimental situation strongly implies the reverse ordering (see Fig. 4). So, some further refinements of the microscopic calculation are called for.

One possibility is that the ^{14}N core may not be identical to a free ^{14}N nucleus in its ground state. In treating the ^{14}N core as two

p-shell holes in an inert $^{16}0$ core coupled to spin S=1 and isospin T=0, in chapter 3, it was found that three states with these quantum numbers could be formed. Hence, in a naive cluster model we might expect to see three sets of rotational bands formed by coupling an alpha particle, with various orbital angular momenta, to each of these states of ^{14}N having S=1. In the absence of mixing between them, only that band based on the ground state 1^+ of ^{14}N would be strongly excited in alpha transfer reactions, since excitation of the other bands would require a two-step process such as Coulomb excitation of the ^{14}N target followed by the transfer of a four-nucleon cluster, for which the probability would be very small. The configuration of the two holes in a given state of ^{14}N can be labelled by the amplitudes for which they have angular momenta $\frac{1}{2}\frac{1}{2}$, $\frac{1}{2}\frac{3}{2}$ and $\frac{3}{2}\frac{3}{2}$ (coupled to S=1), i.e. the coefficients c_1, c_2 and c_3 of eq. 3.29. In addition, the tensor force between cluster and core also depends on these coefficients, as can be seen from eq. 3.44 and 3.57. It is thus possible to visualise a situation in which the amplitudes c_1,c_2 and c_3 change in such a way as to increase the energy of the ^{14}N core, but also change the strength of the tensor force, so as to produce a state of lower total energy. In other words, the tensor force between cluster and core could mix the bands based on the three 1^+ states of ^{14}N, by polarizing the core so that its actual state could be written as a linear combination of the three 1^+ states seen in free ^{14}N. Since the lower two 1^+ states in ^{14}N are roughly 4 MeV apart, mixing between them might be a significant effect in the cluster states, and its inclusion in a calculation of the cluster spectrum of ^{18}F would represent a considerable improvement on the earlier calculations which take the core to be in its free ground state.

The effects of the mixing just mentioned might be apparent in the alpha transfer reactions to ^{14}N. Those cluster states in ^{18}F with very large components of ground state ^{14}N in their core would be very strongly selected, whilst those with sizeable mixing, and hence smaller ground state components, would be seen with corresponding smaller cross-sections. So, it is not expected that those cluster states whose cores differed very much from ground state ^{14}N would show up strongly in alpha transfer. However, it might be possible to see these states by measuring branching ratios for electromagnetic decay from a high lying state with a given core configuration to two(or more) lower lying states with mixed core configurations. The kind of process envisaged is illustrated schematically in Fig. 11. The 7^+ at 11.22 MeV and 5^+ at 6.57 MeV are seen strongly in alpha transfer to ^{14}N and so, must have cores which look very much like ground state ^{14}N. Since ^{14}N has an excited 1^+ state at 3.9 MeV we might expect there to be a 5^+ state (formed by coupling an alpha particle with L=4 to this excited ^{14}N core) at around 10 MeV. If the cores are not identically equal to the 1^+ states in free ^{14}N, but contain admixtures of them, the 7^+ might be able to decay to both 5^+ levels with a measurable branching ratio. (See Fig. 11). In addition to making its presence feld in the cross-sections for alpha transfer and electromagnetic transition rates between cluster states, core mixing might also noticeably affect the excitation energies of some states. In particular, this might bring the relative positions of the 5^+ and 3^+ levels at around 6.5 MeV into closer agreement with experiment (see Fig. 4). It was mentioned at the beginning of this section, that if the ^{14}N core is taken to have the same configuration as a free ^{14}N nucleus in its ground state, the level with $J^\pi = 3^+$ (from the

coupling L=4 x S=1) inevitably lies above the level with $J^\pi = 5^+$ (from the same coupling). However, if we consider a second band based on the excited state of ^{14}N at 3.95 MeV having $J^\pi = 1^+$, there will be a state at about 7.5 MeV having $J^\pi = 3^+$ from the coupling L=2 x S=1 in that higher lying band. Since the ground state band 3_2^+ lies at about 7 MeV, there may well be large mixing between these 3^+ states, resulting in one of them having an energy below the 5^+ level at 6.57 MeV. With these possibilities in mind we proceed to consider the effect of core polarization in the system $^{14}N+\alpha$, although we still treat ^{14}N as 2 p-shell holes in an inert ^{16}O core, coupled to spin S=1 and isospin T=0.

5.2 Core Polarization.

As mentioned in the last section, treating the ^{14}N core as two p-shell holes in an inert ^{16}O core allows three states with quantum numbers $(S^\pi,T) = (1^+,0)$ to be formed. It is then possible to form three rotational bands by coupling an alpha particle in various orbits to each of these states. In this section we consider how the tensor interaction between cluster and core can result in polarization of the ^{14}N core and hence a mixing of these bands. We simplify the problem a little by neglecting the cluster-core spin-orbit force, and also the contribution to the cluster-core tensor force which arises from the alpha-nucleon spin-orbit force, since these terms were both found to be very small in section 3.4. This amounts to taking the tensor form factor of eq. 3.57 to be given by $6C_{220}F_{c_{(2)}}(R)$ (where C_{220} is defined in eq. 3.44 and $F_{c_{(2)}}(R)$ in eqs. 2.24 and 2.10). The neglected terms could be included in our treatment in an analogous way to the tensor force, but it is felt that no significant changes result from this extra effort.

Initially we will consider those cluster states in ^{18}F which have even values of J, since only one value of the orbital angular momentum of the alpha particle, L, can be coupled with the core spin, S=1, to produce them, (e.g. J=2 from L=2 x S=1) so the extra problem of mixing of different L-values does not arise here. We can now find a Hamiltonian matrix for even J alpha cluster states in ^{18}F by combining the matrix elements of the residual interaction in the p-shell of Cohen and Kurath[44] with the expression for the tensor interaction between cluster and core derived in Chapter 3. The residual interaction is presented as a series of matrix elements $(CK)_{ij} = \langle (j_1 j_2)_i ST | H_o | (j_3 j_4)_j ST \rangle$, where $j_1 j_2 = \frac{1}{2}, \frac{3}{2}$ and couple to a total angular momentum S, with isospin T, in the p-shell and H_o is the effective Hamiltonian. For a core spin of 1, we thus obtain a 3x3 matrix whose eigenvalues give the energy of the core and whose eigenvectors yield amplitudes c_1, c_2 and c_3 for finding the hole angular momenta combinations $\frac{1}{2}\frac{1}{2}, \frac{1}{2}\frac{3}{2}$ and $\frac{3}{2}\frac{3}{2}$ respectively. Originally the eigenvector corresponding to the lowest eigenvalue of this matrix was used to evaluate the various factors in eq. 3.44. However, we now notice that the tensor force between cluster and core given ineqs. 3.8 and 3.9 with $V_2(R) = 6C_{220}F_{c_{(2)}}(R)$ can be written as

$$(C_1\ C_2\ C_3)\begin{pmatrix} 0 & 1/2 & 0 \\ 1/2 & 1/4 & 1/2\sqrt{10} \\ 0 & 1/2\sqrt{10} & -2/5 \end{pmatrix}\begin{pmatrix} C_1 \\ C_2 \\ C_3 \end{pmatrix}\Delta(J,L)\int_0^\infty 6F_{c_{(2)}}(R)\,|\chi_L(R)|^2\,dR \qquad (5.1)$$

Hence, we can write a Hamiltonian matrix for the whole system by adding the tensor matrix

$$T = \begin{pmatrix} 0 & 1/2 & 0 \\ 1/2 & 1/4 & 1/2\sqrt{10} \\ 0 & 1/2\sqrt{10} & -2/5 \end{pmatrix}\Delta(J,L)\int_0^\infty 6F_{c_{(2)}}(R)\,|\chi_L(R)|^2\,dR \qquad (5.2)$$

to the 2 p-shell hole matrix of Cohen and Kurath, and in addition adding the energy of the centroid of the triplet of states associated with a

given L to the diagonal terms. Then, the resulting 3x3 matrix can be diagonalised to give three energy eigenvalues and three associated eigenvectors.

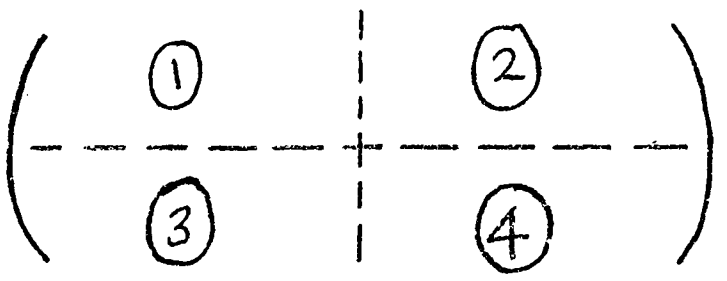
This yields eigenvectors in the $|j_1 j_2>$ basis, but it would be more interesting to have them as a linear combination of ground, first and second excited $(1^+,0)$ states of ^{14}N. We can do this by performing a unitary transformation on the matrix. The unitary matrix is constructred in the standard way from the normalized eigenvectors of the original Cohen and Kurath matrix. The energies of the L-centroids to be added to the diagonal elements can be taken from the cosh potential (eq. 3.64 with V_o = 168 MeV), pure rotational spacing or experiment. As an example of the kind of results obtained we consider those states with J=2.

The matrix to be diagonalized has elements $H_{ij} = (CK)_{ij} + T_{ij} + E(CENTROID)\delta_{ij}$. We take the energy of the centroid appropriate to a state with L=2 from the experimental spectrum of ^{18}F. (We use 3.38 MeV which represents the effect of the central part of the cluster-core interaction). The unitary matrix used to transform H so that its eigenvectors contain linear combinations of ground first and second excited $(1^+,0)$ states of ^{14}N (henceforth referred to as $|0>$,$|1>$ and $|2>$ respectively) is formed from the eigenvectors of the matrix (CK). Upon diagonalization the energies and normalized eigenvectors which result are;

STATE	ENERGY (MeV)	CORE EIGENVECTOR
2^+_1	2.70	$0.98\|0> + 0.20\|1> + 0.00\|2>$
2^+_2	7.67	$-0.20\|0> + 0.98\|1> + 0.00\|2>$
2^+_3	19.81	$-0.00\|0> - 0.00\|1> + 1.00\|2>$

The energies corresponding to pure |0>, |1> and |2> core states would have been 2.90, 7.47 and 19.81 MeV respectively. The general features of a small mixing between ground and first excited $(1^+,0)$ states of ^{14}N with negligible mixing of the second excited state, resulting in energy shifts of about 0.2 MeV are repeated for the other states of even J. Table 11 lists the calculated energies of all alpha cluster states below 20 MeV belonging to the 2N+L = 8 band of ^{18}F, and the spectrum is illustrated, with the effects of band mixing, in Fig. 12.

We have thus found that the effects of band mixing due to polarization of the ^{14}N core only produce minor changes in the energies and wave-functions of the even-J alpha cluster states in ^{18}F. However, when we consider states of odd-J there is the additional complication that two different values of L may be mixed together in each state. For example, a $J^\pi = 3^+$ state may contain a mixture of the two couplings L=2 x S=1 and L=4 x S=1. So, in forming the matrix, H, for odd values of J it is necessary to take into account two values of L, and hence a 6x6 matrix will be produced. If we partition this matrix into four 3x3 submatrices the elements can be found as follows:



The submatrices 1 and 4 are formed exactly as for the even-J 3x3 matrices, with elements for the lower L-value going into submatrix 1 and elements for the higher L-value going into submatrix 4. That is to say, we take the matrix elements of the residual interaction listed by Cohen and Kurath, add the tensor matrix of eq. 5.2 (the radial integral and $\Delta(J,L)$ will differ for the two L-values in question) and add the energy

of the appropriate L-centroid to the diagonal terms. Since the tensor force can connect states of equal J, and L differing by two units, the elements in submatrices 2 and 3 will be non-zero. In fact, the tensor force between states of different L can be written as

$$(C_1' \; C_2' \; C_3') \begin{pmatrix} 0 & 1/2 & 0 \\ 1/2 & 1/4 & 1/2\sqrt{10} \\ 0 & 1/2\sqrt{10} & -2/5 \end{pmatrix} \begin{pmatrix} C_1 \\ C_2 \\ C_3 \end{pmatrix} \frac{\sqrt{(L+1)(L+2)}}{2L+3} \int_0^\infty 6 F_{c_{(2)}}(R) \chi^*_{L+2}(R) \chi_L(R) \, dR \qquad (5.3)$$

so, the matrix to be inserted in submatrix 2 (and also in submatrix 3 since it is symmetric) is

$$T' = \begin{pmatrix} 0 & 1/2 & 0 \\ 1/2 & 1/4 & 1/2\sqrt{10} \\ 0 & 1/2\sqrt{10} & -2/5 \end{pmatrix} \frac{\sqrt{(L+1)(L+2)}}{2L+3} \int_0^\infty 6 F_{c_{(2)}}(R) \chi^*_{L+2}(R) \chi_L(R) \, dR \qquad (5.4)$$

We now have the prescription for writing down the 6x6 matrices for the alpha cluster states of odd-J, and diagonalization of these matrices will produce energies and eigenvectors (in the $|j_1 j_2(L)>$ basis for the core) of the remaining cluster states in ^{18}F of interest.

Again it is desirable to make a unitary transformation so that we obtain eigenvectors in a basis which illustrates the $(1^+,0)$ components mixed in the core and also the L-mixing. The required 6x6 unitary matrix is obtained by putting the 3x3 matrix of eigenvectors of the Cohen and Kurath matrix (CK) in submatrices 1 and 4 ,and putting the zero 3x3 matrix in submatrices 2 and 3 . We have the added bonus now of being able to evaluate the mixing of orbital angular momenta, while the core remains in a pure state ($|0>$,$|1>$ or $|2>$), separately. We can form a 2x2 matrix by selecting the elements of the transformed 6x6 matrix which correspond to $<0L|H|0L>$, $<0L'|H|0L'>$, $<0L|H|0L'>$ and $<0L'|H|0L>$ for example (and similarly for states based on the core

being represented by a pure $|1\rangle$ or $|2\rangle$ state). Diagonalization of the 2x2 sub-matrices gives the mixing of different Ls within a given band, without any band mixing which is what was calculated in Chapter 3 for a ground state core. Diagonalization of the whole matrix gives the full effects of mixing, and the two stages mentioned are illustrated in Fig. 12. The eigenvectors for the various cluster states are given in Table 12.

We note the following points which emerge from the diagonalization.

i) The matrix for J=1 when transformed into the $|0L\rangle$, $|1L\rangle$, $|2L\rangle$ basis has zero elements for $H_{12}, H_{13}, H_{23}, H_{21}, H_{31}, H_{32}$. Hence submatrix 1 of the 6x6 matrix is diagonal. This is because this submatrix corresponds to L=0, and the tensor force contains a factor $\frac{L}{2L+3} = \Delta(10)$, which vanishes for L=0, so the off-diagonal matrix elements also vanish. This illustrates another advantage of applying the unitary transformation from the $|j_1 j_2\rangle$ basis; the size of the tensor matrix elements responsible for the mixing becomes apparent.

ii) The band based on the pure first excited $(1^+,0)$ state of ^{14}N exhibits practically zero splitting into triplets. Only when band mixing is introduced does any splitting become apparent (Fig. 12). This is because the amplitudes, c_1, c_2 and c_3 for the two-hole combinations to spin S=1 for the first excited $(1^+,0)$ state in ^{14}N are such that C_{220} (see eq. 3.44) is very small.

iii) The most interesting aspect in the lower part of the spectrum is the way in which the 3_2^+ state falls below the 5_1^+ state when band mixing is introduced (Fig. 12). This happens because the 3^+ state based on the ground state of ^{14}N with L=4 is very close in energy to the 3^+ state based on the first excited $(1^+,0)$ state of ^{14}N (at 3.9 MeV) with L=2. Ignoring all mixing we can write.

$$3_2^+;|0,4\rangle \approx C+20\alpha+\tfrac{5}{7}\beta_4 \qquad (5.5a)$$

$$3_3^+;|1,2\rangle \approx (C+3.9)+6\alpha+\tfrac{2}{7}\beta_2' \qquad (5.5b)$$

where α is the moment of inertia parameter ($\simeq$0.2 MeV) and C is the band head for the ground state band. Also β_4 = 0.73 MeV (from Table 5) and $\beta_2' \simeq 0$ as discussed in point (ii). Hence, the difference in energies, with no mixing is approximately 0.6 MeV. Although the matrix elements of the effective Hamiltonian between these two states are not particularly large, this fortuitous near degeneracy results in large mixing, and the 3_2^+ state lying below the 5_1^+ which is in agreement with the ordering of the best experimental candidates. The fact that these two 3^+ states are strongly mixed also indicates that the cross-section observed in alpha transfer onto ^{14}N for them will probably be smaller than that found for the other, purer cluster states (although kinematic considerations must also be taken into account)

5.3 Electric Quadrupole Transitions Between Cluster States.

It has been shown by Buck et al.[20]) that the allowed M1 transitions between alpha cluster states in ^{18}F are very small and that the electric quadrupole transitions are large. In this section we recalculate the B(E2) values for these states to see if the modifications of the wave functions due to core excitation produce significant changes, and also consider the possibility of locating those cluster states based primarily on excited states of the ^{14}N core by measuring the branching ratios for

decays from high lying states to them and to states based primarily on ground state cores. An expression for the B(E2) value for a transition from a state of angular momentum J_i to one of J_f is given in ref. 20 and discussed in Appendix VIII. It is

$$B(E2;J_i\to J_f)=\frac{2J_f+1}{2J_i+1}\left|\langle J_f(lL_f)\|Y_2\|J_i(lL_i)\rangle\right|^2\beta_2^2\left[\int_0^\infty r^2 U^*_{J_fL_f}(r)\,U_{J_iL_i}(r)\,dr\right]^2 \tag{5.6}$$

where $\beta_2=\dfrac{A_1^2Z_2+A_2^2Z_1}{(A_1+A_2)^2}=\dfrac{14}{9}$ for alpha cluster states in ^{18}F (5.7)

and

$$\langle J_f(lL_f)\|Y_2\|J_i(lL_i)\rangle=(-1)^{J_f+L_f+1}\sqrt{\frac{(2J_i+1)(2L_i+1)5}{4\pi}}\,W(L_fL_iJ_fJ_i;2l)\,\langle 20L_i0|L_f0\rangle \tag{5.8}$$

A_1 is the number of core nucleons, A_2 the number of cluster nucleons, Z_1 the charge on the core and Z_2 the charge on the cluster. In addition, the $U_{JL}(r)$ are radial wavefunctions for the motion of the alpha particle about the core. In arriving at this formula the quadrupole moment of the ^{14}N core has been ignored because it is known to be very small (0.01 barns [45]).

Using these formulae with our calculated wavefunctions, we find the B(E2) values shown in table 14, in Weisskopf units. The angular momentum coupling coefficients needed are listed in table 13 and the Weisskopf unit is taken to be [61])

$$B_W(E\lambda)=\frac{(1.2)^{2\lambda}}{4\pi}\left(\frac{3}{\lambda+3}\right)^2 A^{\frac{2\lambda}{3}}\ (fm)^{2\lambda}$$

$$B_W(E2)=\frac{(1.2)^4}{4\pi}\left(\frac{3}{5}\right)^2(A_1+A_2)^{4/3}\simeq\frac{0.747}{4\pi}(A_1+A_2)^{4/3}\ (fm)^4 \tag{5.9}$$

Table 14 shows that small differences from the values of Buck et al. [30]) occur, but in most cases the predicted value is consistent with the experimental measurement. The only major change is for the 3^+(3.357 MeV) → 2^+(2.524 MeV) transition, for which unfortunately the experimental measurement is so uncertain as to preclude any firm conclusions being drawn.

Finally, we consider the branching ratio for E2 transitions from the 7^+ state at 11.22 MeV to the 5^+ at 6.57 MeV and the 5^+ predicted to lie at 9.54 MeV. It had been hoped that if such a branching ratio was measurable it could be used to locate those alpha cluster states which are not heavily populated in alpha transfer to ^{14}N. However, a calculation (ignoring all other competing decay modes) yields a ratio of 4.7×10^{-5}. When we note that in addition all three levels are above the alpha emission threshold in ^{18}F, (so the number of decays to the 5^+ at 9.54 MeV will be far smaller even than the calculated ratio suggests)we conclude that this mechanism will not provide a means of experimentally locating those alpha clusters states based primarily on excited cores. Despite this negative result we still derive worthwhile benefits from the inclusion of core polarization, since we can now conclude that the predicted spectrum of cluster states based on a chiefly ground state core is in excellent agreement with the best experimental candidates (discussed in Section 3.1 and displayed in Fig. 12), and good agreement is obtained between measured and predicted electromagnetic (E2) transitions between them (without using effective charges).

APPENDIX I

TENSOR DECOMPOSITION OF $U(|\underline{r}-\underline{R}|)$

Any scalar function of the separation distance of two points, $\underline{r}$ and $\underline{R}$, may be expanded in terms of the modified spherical harmonics $C_\ell(\theta_1,\phi_1)$ and a function of the two scalar lengths r, R as follows

$$U(|\underline{r}-\underline{R}|) = \sum_{\ell}^{!} (2\ell+1)\, U_\ell(r,R)\, C_\ell(\hat{\underline{R}}).C_\ell(\hat{\underline{r}}) \qquad (I.1)$$

$\hat{\underline{R}}$ and $\hat{\underline{r}}$ being unit vectors parallel to $\underline{R}$ and $\underline{r}$.

$$U(|\underline{r}-\underline{R}|) = \sum_{\ell,m}^{!} 4\pi\, U_\ell(r,R)\,(-1)^m\, Y_\ell^m(\hat{\underline{R}})\, Y_\ell^{-m}(\hat{\underline{r}}) \qquad (I.2)$$

and using the spherical harmonic addition theorem in the form

$$P_n(\cos\gamma) = \frac{4\pi}{2n+1} \sum_{m=-n}^{n}{}^{!} (-1)^m Y_n^m(\theta_1,\phi_1)\, Y_n^{-m}(\theta_2,\phi_2) \qquad (I.3)$$

gives

$$U(|\underline{r}-\underline{R}|) = \sum_{\ell}^{!} (2\ell+1)\, U_\ell(r,R)\, P_\ell(\cos\gamma) \qquad (I.4)$$

where $\cos\gamma = \hat{\underline{r}}.\hat{\underline{R}}$. Now multiply both sides by $P_{\ell'}(\cos\gamma)$ and integrate over solid angle.

$$\int_{-1}^{1} U(|\underline{r}-\underline{R}|)\, P_\ell(\cos\gamma)\, d(\cos\gamma) = 2U_\ell(r,R) \qquad (I.5)$$

where the orthonormality property of the Legendre polynomials has been used:

$$\int_{-1}^{1} P_\ell(\cos\theta)\, P_{\ell'}(\cos\theta)\, d(\cos\theta) = \left(\frac{2}{2\ell+1}\right)\delta_{\ell\ell'} \qquad (I.6)$$

So, the expansion I.1 is possible with $U_\ell(r,R)$ given by

$$U_\ell(r,R) = \frac{1}{2}\int_{-1}^{1} U(|\underline{r}-\underline{R}|)\, P_\ell(\cos\gamma)\, d(\cos\gamma) \qquad (I.7)$$

APPENDIX II

THE RELATIVE ORBITAL ANGULAR MOMENTUM OF HOLE AND CLUSTER

We assume that the core remains fixed in space and take its centre as the origin of our coordinate system. Then, considering the hole and cluster to have masses, position vectors and momenta of $m, M, \underline{r}, \underline{R}, \underline{p}, \underline{P}$ respectively we evaluate the relative orbital angular momentum. With a fixed core, the centre of mass of the hole-cluster system will orbit the origin, (the core centre) whilst the hole and core orbit their centre of mass. We now show that the total angular momentum of the system can be separated in this manner.

$$\underline{L}_{TOT} = (\underline{r} \wedge \underline{p}) + (\underline{R} \wedge \underline{P}) \qquad \text{(II.1)}$$

by definition

$$(m+M)\,\underline{R}_{CM} = m\underline{r} + M\underline{R}$$

$$\therefore \quad (m+M)\,\underline{V}_{CM} = m\underline{v} + M\underline{V}$$

$$\therefore \quad \underline{L}_{CM} = (m+M)\,\underline{R}_{CM} \wedge \underline{V}_{CM}$$

$$\underline{L}_{CM} = \frac{(m\underline{r} + M\underline{R}) \wedge (m\underline{v} + M\underline{V})}{(m+M)} \qquad \text{(II.2)}$$

$$\underline{L}_{REL} = m(\underline{r} - \underline{R}_{CM}) \wedge \underline{v} + M(\underline{R} - \underline{R}_{CM}) \wedge \underline{V}$$

$$\underline{L}_{REL} = \frac{mM}{m+M}\left(\underline{r} \wedge \underline{v} + \underline{R} \wedge \underline{V} - \underline{R} \wedge \underline{v} - \underline{r} \wedge \underline{V}\right)$$

$$\underline{L}_{REL} = \frac{mM}{m+M}(\underline{r} - \underline{R}) \wedge (\underline{v} - \underline{V}) \qquad \text{(II.3)}$$

Inspection of equations II.1, II.2 and II.3 supports our initial assertion

$$\underline{L}_{TOT} = \underline{L}_{CM} + \underline{L}_{REL} \qquad \text{(II.4)}$$

It is the relative orbital angular momentum of II.3 that must be used in considering the spin-orbit force. This is an "intuitively obvious" result; vector product of relative separation and relative velocity multiplied by the reduced mass of the two components. It can also be expanded as:

$$\underline{L}_{REL} = \frac{M}{m+M}\left(\underline{1}-\underline{R}_{\wedge}\underline{P}\right) - \frac{m}{m+M}\left(\underline{L}-\underline{r}_{\wedge}\underline{P}\right) \qquad \text{(II.5)}$$

APPENDIX III

TREATMENT OF $C_2(\hat{R}).C_2(\hat{r})L.s$

We need to decouple these two scalar products and rewrite the expression as a scalar product of a rank-K tensor in the alpha coordinates with an equal rank tensor in the nucleon coordinates. (Only K=0,1 is possible in the equation (2.22) of interest because it contains the 9-j symbol $\begin{Bmatrix} \frac{1}{2} & \frac{1}{2} & K \\ 1 & 1 & k_1 \\ \frac{1}{2} & \frac{1}{2} & k_2 \end{Bmatrix}$ as can be seen by applying the triangulation condition to the first row).

$$C_2(\hat{R}).C_2(\hat{r})L.s = \sum_{\lambda,\mu} (-1)^{\lambda+\mu} C_2^{\mu}(\hat{R}) C_2^{-\mu}(\hat{r}) L^{\lambda} s^{-\lambda} \qquad \text{(III.1)}$$

Let

$$A_K^{\lambda+\mu} = \sum_{\lambda(\mu)} \langle K\lambda+\mu | 2\mu | \lambda \rangle C_2^{\mu}(\hat{R}) L^{\lambda} \qquad \text{(III.2)}$$

Then, we can apply the orthonormality property of the Clebsch-Gordan coefficients to obtain

$$C_2^{\mu}(\hat{R}) L^{\lambda} = \sum_{K,\lambda+\mu} \langle 2\mu | \lambda | K\lambda+\mu \rangle A_K^{\lambda+\mu} \qquad \text{(III.3)}$$

where we note that

$$A_1^1 = -\frac{3}{\sqrt{10}} (\hat{R}.L) \hat{R}_1^1 + \frac{1}{\sqrt{10}} L_1^1 \qquad \text{(III.4)}$$

This equation is obtained by expanding eq. III.2, writing $C_2^{\mu}(\hat{R})$ as a product of two first rank tensors like $C_1^{\nu}(\hat{R})$, and taking cognizance of the non-commutativity of L^{λ} and $C_1^{\nu}(\hat{R})$where appropriate. Specifically,

$$[L_1^0, C_1^{\nu}(\hat{R})] = \nu C_1^{\nu}(\hat{R}) \qquad \text{(III.5)}$$

and

$$[L_{-1}^{\pm}, C_1^{(\lambda)}(\hat{\underline{R}})] = \mp\frac{1}{\sqrt{2}}\sqrt{2-\lambda(\lambda\pm1)}\,C_1^{(\lambda\pm1)}(\hat{\underline{R}}) \qquad \text{(III.6)}$$

Since only the K=1 term is of interest to us from eq. III.3, (as explained earlier) we are only interested in the operator III.4, and its other companion components. Furthermore, when we come to take matrix elements between α-states the term proportional to $\hat{\underline{R}}$ can only give zero as is apparent from the symmetry arguments invoked in formulating the phenomenological model. Hence, the only part of A_K in eq. III.2 of interest to us here is the remaining vector term $\frac{1}{\sqrt{10}}\underline{L}$.

APPENDIX IV

TREATMENT OF $-3C_1(\hat{\underline{R}}).C_1(\hat{\underline{r}})R_{\Lambda}\underline{p}.\underline{s}$

We wish to decouple this term and then recouple $C_1(\hat{\underline{R}})$and $\underline{R} = RC_1(\hat{\underline{R}})$ to produce the operator in the alpha coordinates. Although this operator may appear to be able to have ranks 0 or 1, only the former behaves correctly under time reversal and parity. (The rank 1 term will necessarily have the same behaviour as $\underline{R}$, which is not acceptable) Using $(\underline{a}_{\wedge}\underline{b})^{\lambda+\mu} = \frac{\sqrt{2}}{i}\sum_{\lambda}\langle 1\lambda 1\mu|1\lambda+\mu\rangle a^{\lambda}b^{\mu}$ we can write

$$-3C_1(\hat{\underline{R}}).C_1(\hat{\underline{r}})\underline{R}_{\wedge}\underline{p}.\underline{s} = -\frac{3\sqrt{2}}{i}\sum_{\alpha,\beta,\gamma}(-1)^{\alpha+\gamma}\langle 1\alpha|1\beta 1\alpha-\beta\rangle R_{\rho}^{-\alpha}s^{\alpha-\beta}C_1^{\gamma}(\hat{\underline{R}})C_1^{-\gamma}(\hat{\underline{r}}) \qquad \text{(IV.1)}$$

(see eq. IV.8) Define

$$T_Q^{\gamma-\alpha} = \sum_{\gamma,\alpha}\langle Q\gamma-\alpha|1\gamma 1-\alpha\rangle C_1^{\gamma}(\hat{\underline{R}})C_1^{-\alpha}(\hat{\underline{R}}) \qquad \text{(IV.2)}$$

The orthonormality properties of the Clebsch-Gordan coefficients then allow us to write

$$C_1^{\gamma}(\hat{\underline{R}})C_1^{-\alpha}(\hat{\underline{R}}) = \sum_{Q,\gamma-\alpha}\langle 1\gamma 1-\alpha|Q\gamma-\alpha\rangle T_Q^{\gamma-\alpha} \qquad \text{(IV.3)}$$

Only Q=0 will give a non-vanishing contribution in the interaction so the part of the operator of interest is found on setting Q=0 and hence necessarily $\gamma=\alpha$. Identifying T_o^o in eq. IV.2, we find

$$T_o^o = -\frac{1}{\sqrt{3}} \qquad \text{(IV.4)}$$

and hence the part of the nucleon operator we want is; (from IV.1)

$$A_o^o = \frac{3}{\sqrt{3}}\frac{\sqrt{2}}{i}R\sum_{\alpha,\beta}\langle 1\alpha|1\beta 1\alpha-\beta\rangle\langle 00|1-\alpha 1\alpha\rangle C_1^{-\alpha}(\hat{r})\rho^{\beta}s^{\alpha-\beta} \qquad \text{(IV.5)}$$

Using $r^{-\alpha} = rC_1^{-\alpha}(\hat{r})$ and $\langle 00|1-\alpha 1\alpha\rangle = (-1)^{1-\alpha}/\sqrt{3}$ we find

$$A_0^0 = \frac{\sqrt{2}}{i}\frac{R}{r}\sum_{\alpha,\beta}(-1)^{1-\alpha}\langle 1\alpha\,|\,|1\beta|\,\alpha-\beta\rangle r^{-\alpha}\rho^{\beta}s^{\alpha-\beta} \tag{IV.6}$$

$$A_0^0 = -\left(\frac{R}{r}\right)\underline{r}\wedge\underline{\rho}\cdot\underline{s} = -\left(\frac{R}{r}\right)\underline{\ell}\cdot\underline{s} \tag{IV.7}$$

where the last step follows from using

$$\underline{a}\wedge\underline{b}\cdot\underline{c} = \frac{\sqrt{2}}{i}\sum_{\lambda,\mu}(-1)^{\lambda}\langle 1\lambda\,|\,|1\mu|\,\lambda-\mu\rangle a^{-\lambda}b^{\mu}c^{\lambda-\mu} \tag{IV.8}$$

APPENDIX V

TREATMENT OF $-3C_1(\hat{\underline{R}}).C_1(\hat{\underline{r}})\underline{r}_\wedge\underline{P}.\underline{s}$

We wish to decouple the tensors forming this operator and recouple $C_1(\hat{\underline{R}})$ with $\underline{P}$ to make $\underline{L}$ and then recouple $C_1(\hat{\underline{r}})$ and $\underline{r} = rC_1(\hat{\underline{r}})$ to 1 or a tensor proportional to $C_2(\hat{\underline{r}})$so that this can finally be combined with $\underline{s}$ to obtain two rank-1 operators in the nucleon coordinates to be dotted with the alpha-coordinate operator $\underline{L}$. We make use of the scalar triple product formula

$$\underline{r}_\wedge\underline{P}.\underline{s} = \frac{\sqrt{2}}{i}\sum_{q,n}(-1)^q\langle 1q-n\,1n\,|1q\rangle r^{q-n}P^n_{s-q} \qquad (V.I)$$

to write the whole term in the form

$$-3C_1(\hat{R}).C_1(\hat{r})\underline{r}_\wedge\underline{P}.\underline{s} = -3\left(\frac{r}{R}\right)\frac{\sqrt{2}}{i}\sum_{\alpha,\beta,\gamma}(-1)^{\alpha+\gamma}R_1^{\gamma}C_1^{-\gamma}(\hat{r})\langle 1\alpha-\beta\,\beta\,|1\alpha\rangle C_1^{\alpha-\beta}(\hat{r})P^{\beta}_{s-\alpha} \qquad (V.2)$$

where use has been made of $\underline{r} = rC_1(\hat{\underline{r}})$ (and similarly for $\underline{R}$). Now we note that

$$(\underline{R}_\wedge\underline{P})^{\gamma+\beta} = \frac{\sqrt{2}}{i}\sum_{\gamma,\beta}\langle 1\gamma\,1\beta\,|1\gamma+\beta\rangle R_1^{\gamma}P^{\beta} \qquad (V.3)$$

So, using the orthonormality properties of the Clebsch-Gordan coefficients we obtain the term of interest

$$\frac{\sqrt{2}}{i}R_1^{\gamma}P^{\beta} = \sum_{(\gamma+\beta)}\langle 1\gamma+\beta\,|1\gamma\,1\beta\rangle L^{\gamma+\beta} \qquad (V.4)$$

We can therefore write the whole operator of eq. V.2 in the form

$$\hat{O} = -3\left(\frac{r}{R}\right)\underline{L}.\underline{V} \qquad (V.5)$$

where the vector operator $\underline{V}$ has the components given by

$$V_1^{-Q} = \sum_{\alpha,\beta} (-1)^{\alpha+\beta} \langle 1Q-\beta|\beta|1Q\rangle \langle 1\alpha-\beta|\beta|1\alpha\rangle C_1^{\beta-Q}(\hat{\underline{r}}) C_1^{\alpha-\beta}(\hat{\underline{r}}) S_1^{-\alpha} \qquad (V.6)$$

To identify $\underline{V}$, consider the component V_1^0 and use

$$C_1^{\beta}(\hat{\underline{r}}) C_1^{\alpha-\beta}(\hat{\underline{r}}) = \langle 1\beta\, 1\alpha-\beta|00\rangle T_0^0(C_1,C_1) + \langle 1\beta\, 1\alpha-\beta|2\alpha\rangle T_2^{\alpha}(C_1,C_1)$$

$$= (-1)^{\beta} \tfrac{1}{3} \delta_{\alpha,0} + \langle 1\beta\, 1\alpha-\beta|2\alpha\rangle T_2^{\alpha}(C_1,C_1) \qquad (V.7)$$

Then we can write;

$$V_1^0 = \tfrac{1}{3} \sum_{\beta} |\langle 1\beta\, 1-\beta|00\rangle|^2 S_1^0 + \sum_{\alpha,\beta} (-1)^{\alpha} \langle 1\beta\, 1\alpha-\beta|2\alpha\rangle \langle 1-\beta\, 1\beta|10\rangle \times$$

$$\times \langle 1\alpha-\beta\, 1\beta|1\alpha\rangle T_2^{\alpha}(C_1,C_1) S_1^{-\alpha} \qquad (V.8)$$

The sum over β in the second term can be found with the aid of a standard formula [31]) to give

$$-\sum_{\alpha} \sqrt{15} \langle 2\alpha\, 1-\alpha|10\rangle W(1211;11) T_2^{\alpha}(C_1,C_1) S_1^{-\alpha} \qquad (V.9)$$

We then make use of the connection between $T_2(C_1,C_1)$ and $C_2(\hat{\underline{r}})$ which is $T_2^{\mu}(C_1,C_1) = \sqrt{\frac{2}{3}}\, C_2^{\mu}(\hat{\underline{r}})$ to write

$$V_1^0 = \tfrac{1}{3} S_1^0 + \sum_{\alpha} \frac{\sqrt{10}}{6} \langle 2\alpha\, 1-\alpha|10\rangle C_2^{\alpha}(\hat{\underline{r}}) S_1^{-\alpha} \qquad (V.10)$$

and hence

$$\underline{V} = \tfrac{1}{3} \underline{S} + \frac{\sqrt{10}}{6} T_1(C_2, \underline{S}) \qquad (V.11)$$

and the whole operator is

$$\hat{O} = -\left(\frac{r}{R}\right) \underline{L} \cdot \left\{ \underline{S} + \frac{\sqrt{10}}{2} T_1(C_2, \underline{S}) \right\} \qquad (V.12)$$

APPENDIX VI

TREATMENT OF $5C_2(\hat{R}).C_2(\hat{r})\underline{\ell}.\underline{s}$

Our interest is focused on the nucleon operator $C_2(\hat{r})\underline{\ell}.\underline{s}$ which we wish to rewrite as $T_2(\underline{Q},\underline{s})$

$$C_2^{\mu}\underline{\ell}.\underline{s} = \sum_{\lambda}(-1)^{\lambda}C_2^{\mu}\ell^{\lambda}s^{-\lambda} \qquad \text{(VI.1)}$$

Define

$$Q_K^{\lambda+\mu} = \sum_{\lambda,\mu}\langle K\lambda+\mu|2\mu\lambda\rangle C_2^{\mu}\ell^{\lambda} \qquad \text{(VI.2)}$$

Only K=1 can contribute to our interation, by symmetry considerations, and this is analogous to the alpha operator of eq. III.2 and can be identified as $-\frac{3}{\sqrt{10}}(\hat{r}.\ell)\hat{r} + \frac{1}{\sqrt{10}}\ell$. Hence its reduced matrix element between two p-states, $\langle\ell=1||Q||\ell=1\rangle$ is the same as that of $\ell/\sqrt{10}$. Using the orthonormality property of the Clebsch-Gordan coefficients we can write

$$C_2^{\mu}\ell^{\lambda} = \sum_{K\lambda+\mu}\langle 2\mu\lambda|K\lambda+\mu\rangle Q_K^{\lambda+\mu} \qquad \text{(VI.3)}$$

so

$$C_2^{\mu}\underline{\ell}.\underline{s} = \sum_{K,\lambda,\mu}(-1)^{\lambda}\langle K\lambda+\mu|2\mu\lambda\rangle Q_K^{\lambda+\mu}s^{-\lambda} \qquad \text{(VI.4)}$$

with K=1, the term of interest to us is

$$= \sum_{\lambda,\mu} -\sqrt{\frac{3}{5}}\langle 1(\lambda+\mu)1-\lambda|2\mu\rangle Q_1^{\lambda+\mu}s^{-\lambda} \qquad \text{(VI.5)}$$

APPENDIX VII

TENSOR TERM ARISING FROM $-3C_1(\hat{\underline{R}}).C_1(\hat{\underline{r}})\underline{R}_\Lambda \underline{p}.\underline{s}$.

This term arose in the ^{15}N-α case where only a coupling of $C_1(\hat{\underline{R}})$ and $\underline{R}$ to a scalar was possible (see appendix IV). However, we may couple them to a rank-2 tensor in the ^{14}N-α system, so Q may take the value 2 in eq. IV.3. In this case

$$C_1^{\gamma}(\hat{\underline{R}})C_1^{-\alpha}(\hat{\underline{R}}) = \sum_{Q,\gamma-\alpha} \langle Q\,\gamma-\alpha \,|1\,\gamma|-\alpha\rangle\, T_Q^{\gamma-\alpha} \qquad \text{(IV.3)}$$

and if Q=2 we have

$$T_2^2 = C_1^1(\hat{\underline{R}})C_1^1(\hat{\underline{R}}) = \sqrt{\frac{2}{3}}\,C_2^2(\hat{\underline{R}}) \qquad \text{(VII.1)}$$

which is the alpha operator required. Then we use (IV.1) and (VII.1) to find the nucleon operator. We want to evaluate

$$-3\frac{\sqrt{2}}{i}\sum_{\alpha,\beta,\gamma}(-1)^{\alpha+\gamma}\langle 1\alpha\,|1\beta|\,\alpha-\beta\rangle\langle 2\gamma-\alpha\,|1-\alpha|\gamma\rangle R C_1^{-\gamma}(\hat{r})\rho^{\beta}s^{\alpha-\beta} \qquad \text{(VII.2)}$$

Define

$$\Gamma^{-\gamma}\rho^{\beta} = \sum_{\lambda,\beta-\gamma}\langle\lambda\,\beta-\gamma\,|1-\gamma|\beta\rangle D_\lambda^{\beta-\gamma} \qquad \text{(VII.3)}$$

so

$$D_\lambda^{\beta-\gamma} = \sum_{\beta,\gamma}\langle 1-\gamma|\beta\,|\beta-\gamma\rangle\,\Gamma^{-\gamma}\rho^{\beta} \qquad \text{(VII.4)}$$

and for λ=1, which is the only rank of interest

$$D_1^{\beta-\gamma} = \frac{i}{\sqrt{2}}\,\ell^{\beta-\gamma} \qquad \text{(VII.5)}$$

$$\text{VII.2} = -3\left(\frac{R}{r}\right)\sum_{\alpha\beta\gamma}(-1)^{\alpha+\gamma}\langle 1\alpha\,|1\beta|\,\alpha-\beta\rangle\langle 2\gamma-\alpha\,|1-\alpha|\gamma\rangle\langle 1\beta-\gamma\,|1-\gamma|\beta\rangle\,\ell^{\beta-\gamma}s^{\alpha-\beta} \qquad \text{(VII.6)}$$

The sum over 3 Clebsch-Gordan coefficients [31]) then gives

$$9W(1111;12)\left(\frac{R}{r}\right)\sum_{\alpha,\gamma}(-1)^{\alpha-\gamma}\langle 1\alpha 1-\gamma|2\alpha-\gamma\rangle l^{\alpha}_{s^{-\gamma}} \qquad \text{(VII.7)}$$

for the nucleon operator. Hence we may write the whole operator as

$$\frac{9}{6}\sqrt{\frac{2}{3}}\left(\frac{R}{r}\right)C_2(\hat{\underline{R}})\cdot T_2(\underline{l},\underline{s}) \qquad \text{(VII.8)}$$

where we have used W(1111;12) = 1/6.

APPENDIX VIII

ELECTRIC QUADUPOLE TRANSITIONS BETWEEN CLUSTER STATES.

We want to find an expression for $B(E\lambda, J_i \to J_f)$ in considering a core containing A_1 nucleons, of which Z_1 are protons, and a cluster containing A_2 nucleons, with Z_2 protons. The geometry of the system is illustrated in Fig. 13. The expression we wish to evaluate is given by [62])

$$B(E\lambda, J_i \to J_f) = \frac{(2J_f+1)}{(2J_i+1)} \left| \langle J_f \| \mathcal{M}(E\lambda) \| J_i \rangle \right|^2 \qquad \text{(VIII.1)}$$

where

$$\mathcal{M}(E\lambda, \mu) = \int \rho(\underline{r})\, r^\lambda Y_\lambda^\mu(\hat{\underline{r}})\, d\tau \qquad \text{(VIII.2)}$$

Note that the equation (5.10) contains an 'extra' factor $(2J_f+1)$ over the equivalent equation of ref. 61 on account of the different definitions of the reduced matrix element in the Wigner-Eckart theorem.

We write the factor $r^\lambda Y_\lambda^\mu(\hat{\underline{r}})$ as $\mathcal{Y}_\lambda^\mu(\underline{r})$, and hence the quadrupole operator for the cluster-core system under consideration is

$$Q_\lambda^\mu = Z_1 \mathcal{Y}_\lambda^\mu(\underline{r}_1) + Z_2 \mathcal{Y}_\lambda^\mu(\underline{r}_2) \qquad \text{(VIII.3)}$$

where

$$\underline{r}_1 = -\frac{A_2}{A_1+A_2}\underline{r} \quad \text{and} \quad \underline{r}_2 = \frac{A_1}{A_1+A_2}\underline{r}$$

(see Fig. 13). So,

$$Q_\lambda^\mu = Z_1 \mathcal{Y}_\lambda^\mu\left(-\frac{A_2}{A_1+A_2}\underline{r}\right) + Z_2 \mathcal{Y}_\lambda^\mu\left(\frac{A_1}{A_1+A_2}\underline{r}\right)$$

$$= (-1)^\lambda Z_1 \mathcal{Y}_\lambda^\mu\left(\frac{A_2}{A_1+A_2}\underline{r}\right) + Z_2 \mathcal{Y}_\lambda^\mu\left(\frac{A_1}{A_1+A_2}\underline{r}\right)$$

Now, using the fact that $\mathcal{Y}^{\mu}_{\lambda}(\underline{r})$ are homogeneous functions of x,y,z of order λ, we can immediately simplify this to

$$Q^{\mu}_{\lambda} = (-1)^{\lambda} Z_1 \left(\frac{A_2}{A_1+A_2}\right)^{\lambda} \mathcal{Y}^{\mu}_{\lambda}(\underline{r}) + Z_2 \left(\frac{A_1}{A_1+A_2}\right)^{\lambda} \mathcal{Y}^{\mu}_{\lambda}(\underline{r})$$

$$Q^{\mu}_{\lambda} = \left\{ \frac{Z_2 A_1^{\lambda} + (-1)^{\lambda} Z_1 A_2^{\lambda}}{(A_1+A_2)^{\lambda}} \right\} \mathcal{Y}^{\mu}_{\lambda}(\underline{r}) \qquad \text{(VIII.4)}$$

For the quadrupole operator, $\lambda=2$, and

$$Q^{\mu}_{2} = \left(\frac{Z_2 A_1^2 + Z_1 A_2^2}{(A_1+A_2)^2} \right) \mathcal{Y}^{\mu}_{2}(\underline{r}) = \beta_2 \mathcal{Y}^{\mu}_{2}(\underline{r}) \qquad \text{(VIII.5)}$$

$$B(E2, J_i \to J_f) = \frac{(2J_f+1)}{(2J_i+1)} \left| \langle J_f (L_f) \| Y_2 \| J_i (L_i) \rangle \right|^2 \beta_2^2 \left[\int_0^{\infty} r^2 U^{*}_{J_f L_f}(r)\, U_{J_i L_i}(r)\, dr \right]^2 \qquad \text{(VIII.6)}$$

where the reduced matrix element now refers only to the angular variables.

References

1) F. Ajzenberg-Selove, Nucl. Phys. A300 (1978) 1 and references therein.

2) B. Buck in Proceedings of the International School of Physics "Enrico Fermi" Course LXII (1974) edited by H. Faraggi and R.I. Ricci (North Holland, Amsterdam, 1976) p.29.

3) D.M. Brink, Phys. Lett. 40B (1973) 37.

4) H.S. Bradlow, W.D.M. Rae, P.S. Fisher, N.S. Go dwin, G. Proudfoot and D. Sinclair, Nucl. Phys. A314 (1979) 207.

5) M.E. Cohen, D.J. Pisano and P.D. Parker, Phys. Rev. C14 (1976) 491.

6) J.W. Toevs, Nucl. Phys. A172 (1971) 589.

7) E.C. Halbert, J.B. McGrory and B.H. Wildenthal, Phys. Rev. Letts. 20 (1968) 1112.

8) J.P. Elliott, Proc. Roy. Soc. A245 (1958) 128, 562
M. Harvey, in Advances in Nuclear Physics edited by M. Baranger and E. Vogt (Plenum,New York, 1968) Vol. 1 p.67.
D.J. Millener,D.Phil.Thesis, Oxford (1972) unpublished.

9) D.M. Brink in Proceedings of the International School of Physics "Enrico Fermi" Course XXXVI (1965) edited by C. Bloch (Academic, New York, 1966) p.247.
A. Arima, H. Horiuchi, K. Kubodera and N. Takigawa in Advances in Nuclear Physics edited by M. Baranger and E. Vogt (Plenum, New York 1972) Vol. 5, p.345.

10) H. Horiuchi and Y. Suzuki, Prog. Theor. Phys. 49 (1973) 1974.

11) D.L. Hill and J.A. Wheeler, Phys. Rev. 89 (1953) 1102.
J.J. Griffin and J.A. Wheeler, Phys. Rev. 108 (1957) 311.

12) J.A. Wheeler, Phys. Rev. 52 (1937) 1107, 1803.

13) B. Buck, C.B. Dover and J.P. Vary, Phys. Rev. C11 (1975) 1803.
J.P. Vary and C.B. Dover, Phys. Rev. Letts. 31 (1973) 1510.

14) C.B. Dover and J.P. Vary, in Lecture Notes in Physics Vol. 33, Classical and Quantum Mechanical Aspects of Heavy Ion Collisions (Springer-Verlag, Berlin, 1975) p.1.

15) A.K. Kerman, H. McManus and R.M. Thaler, Ann. Phys. 8 (1959) 551.
J. Hüfner and C. Mahaux, Ann. Phys. 73 (1972) 525.

16) K. Wildermuth and Y.C. Tang in A Unified Theory of the Nucleus (Academic, New York, 1977) p. 14.

17) S. Saito, Prog. Theor. Phys. 41 (1969) 705.

18) B. Buck, H. Friedrich and C. Wheatley, Nucl. Phys. A275 (1977) 246.

19) B. Buck and A.A. Pilt, Nucl. Phys. A280 (1977) 133.

20) B. Buck, H. Friedrich and A.A. Pilt, Nucl. Phys. A290 (1977) 205.

21) B. Buck and A.A. Pilt, Nucl. Phys. A295 (1978) 1.

22) R. Middleton, Nuclear reactions induced by heavy ions, Heidelberg (North-Holland, Amsterdam, 1969) p. 263.

23) A.A. Pilt, D.J. Millener, H. Bradlow, O. Dietzsch, P.S. Fisher, W.J. Naude, W.D.M. Rae, D. Sinclair Nucl. Phys. A273 (1976) 189.

24) D.M. Brink and G.R. Stachler in "Angular Momentum" 2nd edition (Clarendon Press, Oxford, 1968) p.148.

25) A. Bohr and B.R. Mottelson, in "Nuclear Structure" Vol.1 (W.A. Benjamin Inc., Reading, Massachusetts, 1969) p.312.

26) S. Sack, L.C. Biedenharn and G. Breit, Phys. Rev. 93 (1954) 321.

27) C.J. Batty, E. Friedman and D.F. Jackson, Nucl. Phys. A175 (1971) 1.

28) C.J. Batty, E. Friedman, Phys. Lett. 34B (1971) 7.

29) F. Ajzenberg-Selove and T. Lauritsen, Nucl. Phys. A227 (1974) 1.

30) D.F. Jackson and M. Rhoades-Brown, Nucl. Phys. A286 (1977) 354.

31) See ref. 24 p. 141.

32) W.H. Bassichis, B. Giraud, and G. Ripka, Phys. Rev. Lett. 15 (1969) 980.

33) S. das Gupta and A.B. Volkov, Phys. Rev. C6 (1972) 1893.

34) R. Middleton, L.M. Polsky, C.H. Bolbrow and K. Bethge, Phys. Rev. Lett. 21 (1968) 1398.

35) C. Rolfs, H.P. Trautvetter, R.E. Azuma and A.E. Litherland, Phys. Rev Lett. 27 (1971) 1007.

36) C.A. Davis and R. Abegg, Phys. Rev. C17 (1978) 1277.

37) C. Rolfs et al., Nucl. Phys. A199 (1973) 257,274,289,306,328.

38) J.C. Sens et al., Nucl. Phys. A199 (1973) 232, 241.

39) J.C. Sens, S.M. Refaei and A. Pape, Phys. Rev. C18 (1978) 2007.

40) M.E. Cobern and P.D. Parker, Phys. Rev. C15 (1977) 1929, Erratum: Phys. Rev. C16 (1977) 920.

41) W.D.M. Rae, N.S. Godwin, D. Sinclair, H.S. Bradlow, P.S. Fisher, J.D. King, A.A. Pilt and G. Proudfoot, Nucl. Phys. A319 (1979) 239.

42) G.R. Satchler, Oak Ridge National Laboratory Report ORNL-2861 (1960) unpublished.

43) G.R. Satchler, Nucl. Phys. 21 (1960) 116.

44) S. Cohen and D. Kurath, Nucl. Phys. 73 (1965) 1.

45) G.H. Fuller and V.W. Cohen, Nucl. Data Tables A5 (1969) 433.

46) See ref. 24 pp.36 and 43.

47) M. Rotenberg, R. Bivins, N. Metropolis, and J.K. Wooten Jr. in "The 3-j and 6-j symbols"(Crosby, Lockwood and Son Ltd., London, 1959)

48) H.R. Collard and R. Hofstadter in Landolt-Börnstein: Numerical Data and Functional Relationships in Science and Technology, edited by K.H. Hellwege and H. Schopper (Spinrger-Verlag, Berlin, 1967) Group 1, Vol. 2, p.21.

49) A.R. Pol etti, Phys. Rev. 153 (1967) 1108.

50) R.A. Lindgren, H.H. Gutbrod, H.W. Fulbright, and R.G. Markham Phys. Rev. Lett. 29 (1972) 798.

51) J.W. Olness, E.K. Warburton and J.A. Becker, Phys. Rev. C7 (1973) 2239.

52) J.A. Becker, L.F. Chase Jr., D. Kohler and R.E. McDonald, Phys. Rev. C8 (1973) 2007.

53) G.Th. Kaschl, G.J. Wagner, G. Mairle, U. Schmidt-Rohr, and P. Turek, Nucl. Phys. A155 (1970) 417.

54) L.M. Martz, S.J. Sanders and P.D. Parker in Tokyo (1977), Contributed Papers p. 177.

55) L. Drigo and G. Pisent, Nuovo Cimento 51B (1967) 419.

56) R.M. DeVries, J.L. Perrenoud and I. Slaus, Nucl. Phys. A188 (1972) 449.

57) A. de Shalit and J.D. Walecka, Phys. Rev. 147 (1966) 763.

58) G. Szaloky, F. Seiler, W. Grüebler and V. König, Nucl Phys. A303 (1978) 51.

59) H.S. Sherif, Phys. Rev. C19 (1979) 1649.

60) A. de Shalit and H. Feshbach in Theoretical Nuclear Physics Vol. 1 (John Wiley and Sons, Inc.) 1974 p.361.

61) See ref. 25 p.389.

62) See ref. 25 p.382.

TABLE 1

A list of 9-j symbols required for evaluating the terms in eq. (2.22)

$$\begin{Bmatrix} \frac{1}{2} & \frac{1}{2} & 0 \\ 1 & 1 & 0 \\ \frac{1}{2} & \frac{1}{2} & 0 \end{Bmatrix} = \frac{1}{2\sqrt{3}} \qquad \begin{Bmatrix} \frac{1}{2} & \frac{1}{2} & 0 \\ 1 & 1 & 1 \\ \frac{1}{2} & \frac{1}{2} & 1 \end{Bmatrix} = \frac{1}{3\sqrt{6}}$$

$$\begin{Bmatrix} \frac{1}{2} & \frac{1}{2} & 1 \\ 1 & 1 & 0 \\ \frac{1}{2} & \frac{1}{2} & 1 \end{Bmatrix} = -\frac{1}{18} \qquad \begin{Bmatrix} \frac{1}{2} & \frac{1}{2} & 1 \\ 1 & 1 & 2 \\ \frac{1}{2} & \frac{1}{2} & 1 \end{Bmatrix} = \frac{1}{9}$$

TABLE 2

The energies and parameters δ_L for the various models employed to describe alpha-particle cluster states in ^{19}F are compared with the experimental energies[1,23]) of states which are strongly excited in alpha transfer to ^{15}N and thought to have the spin-parity values shown. The unprimed semimicroscopic values are for the alpha-nucleon spin-orbit force of Sack et al.[26]) and the primed ones for the approximation described in the text (section 2.3.5). All energies are in MeV.

J^π	E_{EXPT}	E_{PHEN}	$E_{SEMI\ MIC}$	$E'_{SEMI\ MIC}$	δ_L	δ'_L
$\frac{1}{2}^-$	0.1099	0.19	0.19	0.19	-0.0073	-0.0122
$\frac{5}{2}^-$	1.3457	1.40	1.39	1.38	-0.0067	-0.0114
$\frac{3}{2}^-$	1.4587		1.42	1.44		
$\frac{9}{2}^-$	4.0325	4.32	4.30	4.28	-0.0055	-0.0095
$\frac{7}{2}^-$	3.9987		4.35	4.37		
1_2^{3-}	8.488	9.23	9.21	9.19	-0.0041	-0.0070
1_2^{1-}	8.957		9.26	9.28		
1_2^{7-}	12.26	16.68	16.65	16.64	-0.0032	-0.0045
1_2^{5-}	12.67		16.71	16.72		

TABLE 2

The energies and parameters δ_L for the various models employed to describe alpha-particle cluster states in ^{19}F are compared with the experimental energies[1,23]) of states which are strongly excited in alpha transfer to ^{15}N and thought to have the spin-parity values shown. The unprimed semimicroscopic values are for the alpha-nucleon spin-orbit force of Sack et al.[26]) and the primed ones for the approximation described in the text (section 2.3.5). All energies are in MeV.

J^π	E_{EXPT}	E_{PHEN}	$E_{SEMI\ MIC}$	$E'_{SEMI\ MIC}$	δ_L	δ'_L
$\frac{1}{2}^-$	0.1099	0.19	0.19	0.19	-0.0073	-0.0122
$\frac{5}{2}^-$	1.3457	1.40	1.39	1.38	-0.0067	-0.0114
$\frac{3}{2}^-$	1.4587		1.42	1.44		
$\frac{9}{2}^-$	4.0325	4.32	4.30	4.28	-0.0055	-0.0095
$\frac{7}{2}^-$	3.9987		4.35	4.37		
1_2^{3-}	8.288	9.23	9.21	9.19	-0.0041	-0.0070
1_2^{1-}	8.957		9.26	9.28		
1_2^{7-}	12.26	16.68	16.65	16.64	-0.0032	-0.0045
1_2^{5-}	12.67		16.71	16.72		

TABLE 3

A list of additional 9-j symbols required for evaluating the terms in eq. 3.41 (to be used in conjunction with Table 1)

$$\begin{Bmatrix} 1 & 1 & 0 \\ \frac{3}{2} & \frac{3}{2} & 0 \\ \frac{1}{2} & \frac{1}{2} & 0 \end{Bmatrix} = \frac{1}{\sqrt{24}} \qquad \begin{Bmatrix} \frac{3}{2} & \frac{3}{2} & 1 \\ 1 & 1 & 0 \\ \frac{1}{2} & \frac{1}{2} & 1 \end{Bmatrix} = \frac{1}{18}\sqrt{\frac{5}{2}}$$

$$\begin{Bmatrix} 1 & 1 & 0 \\ \frac{3}{2} & \frac{3}{2} & 0 \\ \frac{3}{2} & \frac{3}{2} & 0 \end{Bmatrix} = \frac{1}{4\sqrt{3}} \qquad \begin{Bmatrix} 1 & 1 & 1 \\ \frac{1}{2} & \frac{3}{2} & 1 \\ \frac{3}{2} & \frac{3}{2} & 0 \end{Bmatrix} = \frac{1}{12}\sqrt{\frac{5}{6}}$$

$$\begin{Bmatrix} 1 & 1 & 1 \\ \frac{1}{2} & \frac{1}{2} & 1 \\ \frac{3}{2} & \frac{3}{2} & 0 \end{Bmatrix} = -\frac{1}{12\sqrt{3}} \qquad \begin{Bmatrix} 1 & 1 & 1 \\ \frac{3}{2} & \frac{3}{2} & 1 \\ \frac{3}{2} & \frac{3}{2} & 0 \end{Bmatrix} = \frac{1}{6\sqrt{30}}$$

$$\begin{Bmatrix} 1 & 1 & 1 \\ \frac{1}{2} & \frac{3}{2} & 1 \\ \frac{1}{2} & \frac{1}{2} & 0 \end{Bmatrix} = \frac{1}{6\sqrt{6}} \qquad \begin{Bmatrix} \frac{1}{2} & \frac{3}{2} & 1 \\ 1 & 1 & 2 \\ \frac{1}{2} & \frac{1}{2} & 1 \end{Bmatrix} = \frac{1}{36}$$

$$\begin{Bmatrix} \frac{1}{2} & \frac{1}{2} & 1 \\ \frac{1}{2} & \frac{3}{2} & 1 \\ 1 & 1 & 0 \end{Bmatrix} = \frac{1}{9} \qquad \begin{Bmatrix} \frac{3}{2} & \frac{3}{2} & 1 \\ 1 & 1 & 2 \\ \frac{1}{2} & \frac{1}{2} & 1 \end{Bmatrix} = -\frac{1}{18\sqrt{10}}$$

$$\begin{Bmatrix} 1 & 1 & 1 \\ \frac{3}{2} & \frac{3}{2} & 1 \\ \frac{1}{2} & \frac{1}{2} & 0 \end{Bmatrix} = \frac{1}{12}\sqrt{\frac{5}{3}} \qquad \begin{Bmatrix} 1 & 1 & 2 \\ \frac{1}{2} & \frac{3}{2} & 2 \\ \frac{1}{2} & \frac{1}{2} & 0 \end{Bmatrix} = \frac{1}{\sqrt{120}}$$

$$\begin{Bmatrix} 1 & 1 & 2 \\ \frac{3}{2} & \frac{3}{2} & 2 \\ \frac{1}{2} & \frac{1}{2} & 0 \end{Bmatrix} = \frac{1}{4\sqrt{15}} \qquad \begin{Bmatrix} \frac{1}{2} & \frac{3}{2} & 2 \\ 1 & 1 & 1 \\ \frac{1}{2} & \frac{1}{2} & 1 \end{Bmatrix} = \frac{1}{12\sqrt{3}}$$

TABLE 3 (Continued)

$$\begin{Bmatrix} 1 & 1 & 2 \\ \frac{1}{2} & \frac{3}{2} & 2 \\ \frac{3}{2} & \frac{3}{2} & 0 \end{Bmatrix} = -\frac{1}{20\sqrt{6}} \qquad \begin{Bmatrix} \frac{3}{2} & \frac{3}{2} & 2 \\ 1 & 1 & 1 \\ \frac{1}{2} & \frac{1}{2} & 1 \end{Bmatrix} = \frac{1}{6\sqrt{6}}$$

$$\begin{Bmatrix} 1 & 1 & 2 \\ \frac{3}{2} & \frac{3}{2} & 2 \\ \frac{3}{2} & \frac{3}{2} & 0 \end{Bmatrix} = -\frac{1}{10}\sqrt{\frac{2}{15}}$$

TABLE 4

The semimicroscopic spectrum is given for two α-nucleon potentials with different central depths U. In both cases a spin-orbit strength of V=7.0 MeV is used and the range parameter is a=1.9 fm. The levels are given in ascending order of energy and J is the total angular momentum. All states have positive parity and we show in parentheses the L-values which are mixed in the level for odd-J states (the dominant L is given first). The K^{π} values are assigned on the basis of a comparison with experimental data where this notation is used, though we can see that it is not really appropriate to our model.

J(L,L')	K^{π}	ENERGY (MeV)	
		U = 43.0 MeV	U = 53.8 MeV
1(0,2)	1^+	1.67	1.55
2(2)	1^+	2.58	2.42
3(2,4)	1^+	3.19	3.14
1(2,0)	0^+	4.21	4.48
4(4)	1^+	5.49	5.32
5(4,6)	1^+	6.32	6.32
3(4,2)	0^+	6.92	7.13
6(6)	1^+	10.41	10.20
7(6,8)	1^+	11.49	11.53
5(6,4)	1^+	11.87	12.05
8(8)	1^+	17.97	17.72
9(8)	1^+	19.42	19.53
7(8,6)	0^+	19.65	19.83

TABLE 5

The quantity $\gamma(L,L)$ is related to the splitting produced by the tensor force by eq. 3.7, and $-\frac{1}{3}\gamma(L,L)$ should be compared with the phenomenological L-independent parameter $\beta = 0.65$ MeV. The tensor mixing of odd-J states is related to $\gamma(L,L+2)$ by eq. 3.10, and the δ_L of eq. 3.66 gives the effect of the spin-orbit force. The simple model takes $\gamma(L,L+2)$ and δ_L to be zero.

L	$-\frac{1}{3}\gamma(L,L)$ (MeV)	$-\frac{1}{3}\gamma(L,L+2)$ (MeV)	$-\delta_L$ (MeV)
0	0.62	0.61	0.0071
2	0.66	0.59	0.0068
4	0.73	0.55	0.0056
6	0.83	0.49	0.0038
8	1.02	-	0.0020

TABLE 6

Pure isospin-0 candidates for trinucleon cluster states in ^{18}F

J^π	ENERGY	
	Strong Candidates	Weak Candidates
0^-	1.080	
2^-	2.100	
1^-	3.133	
3^-	3.791	
2^-	4.226	
4^-	4.398	
1^-	4.860	
$3^{(-)}$		5.502
4^-		6.097
(5^-)	6.10	
(7^-)	7.15	
(6^-)	9.45	

The last three states are seen strongly in the three nucleon transfer work of Rae et al.[41]) but have their J^π values assigned solely on comparison with the predictions of the shell model.

TABLE 7

Candidates for trinucleon cluster states in ^{18}O (isospin 1).

J^{π}	ENERGY	
	Strong Candidates	Weak Candidates
1^-	4.456	
3^-	5.099	
2^-	5.531	
1^-	6.201	
2^-		6.351
3^-		6.404
(0^-)	6.882	
(5^-)	7.69	
2^-		7.75
4^-		7.96
5^-	8.12	
(4^-)	8.50	
(7^-)	11.06	
(6^-)	11.79	
?		12.25

TABLE 8

The energies of trinucleon cluster states in ^{18}O and ^{18}F are calculated by combining phenomenological and microscopic models as described in the text The nucleon-trinucleon potential is taken to have a Gaussian geometry, and two different widths are employed.

J^π	^{18}O ENERGY (MeV) a=2.23 fm	a=2.65 fm	J^π	^{18}F ENERGY (MeV) a=2.23 fm	a=2.65 fm
1^-	4.45	4.45	0^-	1.04	1.04
3^-	4.96	4.93	2^-	1.98	1.97
2^-	5.94	6.04	1^-	3.09	3.09
1^-	6.23	6.10	3^-	3.76	3.81
0^-	6.86	6.86	4^-	4.28	4.26
5^-	7.07	7.04	2^-	4.51	4.36
2^-	8.27	8.28	1^-	5.42	5.56
4^-	8.27	8.37	5^-	5.95	6.02
3^-	9.59	9.49	4^-	7.61	7.47
7^-	10.76	10.72	6^-	8.05	8.01
4^-	11.43	11.45	3^-	8.69	8.78
6^-	12.10	12.21	7^-	9.72	9.82
5^-	14.44	14.32	6^-	12.33	12.18
6^-	16.23	16.26	5^-	13.58	13.67

TABLE 9

The fitting parameters of Buck et al.[21]). For the definition of C,A,β,α and ξ see section 4.2, and for a description of the fitting procedures A-E see ref. 21.

NUCLEUS	PARAMETER	FIT				
		A	B	C	D	E
^{18}F	C	2.5831	2.686	2.153	2.543	2.625
	α	0.4919	0.535	0.433	0.536	0.521
	β	-0.1763	-0.190	-0.219	-0.211	-0.174
	A	0.178	0.163	0.195	0.176	0.178
	ξ	-0.180	-0.138	-0.295	-0.169	-0.186
^{18}O	C	5.052	4.968	4.713	5.113	5.105
	α	-0.602	-0.578	-0.627	-0.547	-0.521
	β	-0.068	-0.084	-0.194	-0.114	-0.174
	A	0.174	0.189	0.195	0.176	0.178
	ξ	-0.210	-0.183	-0.295	-0.169	-0.186

TABLE 10

The fitting parameters resulting from combining the microscopic and phenomenological approaches. The phenomenological model takes $\xi_c=0$. The nucleon-trinucleon potential used was taken to have two widths, and the band-head energies used were $C(^{18}O) = 5.05$ MeV and $C(^{18}F) = 2.58$ MeV. The moment of inertia parameter, A, was taken to have the ^{16}O-t value of 0.195 MeV. See eqs. (4.63)-(4.68) for definitions.

a = 2.23 fm

L	α'	α'_T	β'	β'_T	ξ'_t	ξ'_c
0	-0.324	-0.279	0.386	0.390	-0.294	-0.0030
2	-0.321	-0.279	0.408	0.413	-0.293	-0.0028
4	-0.316	-0.279	0.462	0.468	-0.292	-0.0015
6	-0.311	-0.282	0.557	0.564	-0.290	-0.0008

L	$\alpha'+\alpha'_T$	$\alpha'-3\alpha'_T$	$\frac{1}{3}(\beta'+\beta'_T)$	$\frac{1}{3}(\beta'-3\beta'_T)$
0	-0.603	0.513	0.259	-0.261
2	-0.600	0.516	0.274	-0.277
4	-0.595	0.521	0.310	-0.314
6	-0.593	0.535	0.374	-0.378
Fit B of ref.21	-0.578	0.535	-0.084	-0.190

a = 2.65 fm

L	α'	α'_T	β'	β'_T	ξ'_t	ξ'_c
0	-0.324	-0.279	0.348	0.390	-0.291	-0.0005
2	-0.322	-0.279	0.364	0.406	-0.290	-0.0002
4	-0.320	-0.281	0.402	0.448	-0.288	+0.0007
6	-0.319	-0.287	0.468	0.524	-0.286	+0.0021

L	$\alpha'+\alpha'_T$	$\alpha'-3\alpha'_T$	$\frac{1}{3}(\beta'+\beta'_T)$	$\frac{1}{3}(\beta'-3\beta'_T)$
0	-0.603	0.513	0.246	-0.274
2	-0.601	0.515	0.257	-0.285
4	-0.601	0.523	0.283	-0.314
6	-0.606	0.542	0.331	-0.368
Fit B of ref.21	-0.578	0.535	-0.084	-0.190

TABLE 11

Energies of states (MeV) when core excitation is included, with an indication of the dominant core configuration {|0>, |1> or |2>}

J	|0>	|1>	|2>
1	1.70		
2	2.70		
3	3.36		
1	3.56		
4	5.47		
3	5.87		
5	6.41		
1		6.57	
2		7.67	
1		8.15	
3		8.42	
5		9.54	
6	9.81		
4		10.57	
3		10.82	
7	11.05		
5	12.13		
7		14.50	
6		15.15	
5		15.24	
8	15.65		
1			16.42
9	17.42		
7	17.87		
3			18.03
1			18.95
2			19.81

TABLE 12

Eigenvectors of the alpha cluster states belonging to the 2N+L=8 band of ^{18}F to illustrate the mixing of the ground, first and second excited $(1^+,0)$ states of the ^{14}N core and also the mixing of different values of the orbital angular momentum of the alpha particle for final states of odd J. The basis states used are |0L>, |1L> and |2L>, and the energies in brackets are in MeV.

$1^+(1.70) = 0.936|00\rangle-0.086|10\rangle-0.004|20\rangle+0.303|02\rangle-0.153|12\rangle-0.012|22\rangle$
$1^+(3.53) = -0.258|00\rangle-0.406|10\rangle-0.020|20\rangle+0.828|02\rangle+0.288|12\rangle+0.021|22\rangle$
$1^+(6.57) = -0.026|00\rangle-0.888|10\rangle+0.010|20\rangle-0.333|02\rangle-0.317|12\rangle-0.006|22\rangle$
$1^+(8.15) = -0.235|00\rangle+0.199|10\rangle-0.010|20\rangle+0.333|02\rangle-0.891|12\rangle+0.014|22\rangle$
$1^+(16.42) = -0.015|00\rangle+0.002|10\rangle+0.761|20\rangle+0.032|02\rangle-0.002|12\rangle-0.647|22\rangle$
$1^+(18.95) = 0.013|00\rangle+0.002|10\rangle+0.648|20\rangle+0.000|02\rangle+0.002|12\rangle+0.762|22\rangle$

$2^+(2.70) = 0.980|02\rangle-0.199|12\rangle-0.013|22\rangle$
$2^+(7.67) = 0.199|02\rangle+0.980|12\rangle-0.005|22\rangle$
$2^+(19.81) = 0.013|02\rangle+0.003|12\rangle+1.000|22\rangle$

$3^+(3.36) = -0.967|02\rangle-0.004|12\rangle-0.002|22\rangle-0.200|04\rangle+0.155|14\rangle+0.014|24\rangle$
$3^+(5.87) = -0.126|02\rangle-0.623|12\rangle-0.020|22\rangle+0.754|04\rangle+0.165|14\rangle+0.014|24\rangle$
$3^+(8.42) = 0.076|02\rangle-0.774|12\rangle+0.019|22\rangle-0.567|04\rangle-0.272|14\rangle-0.010|24\rangle$
$3^+(10.82) = 0.204|02\rangle-0.114|12\rangle+0.010|22\rangle-0.265|04\rangle+0.935|14\rangle-0.010|24\rangle$
$3^+(18.03) = -0.014|02\rangle+0.003|12\rangle+0.918|22\rangle+0.032|04\rangle-0.002|14\rangle-0.395|24\rangle$
$3^+(21.51) = 0.014|02\rangle+0.001|12\rangle+0.395|22\rangle+0.004|04\rangle+0.002|14\rangle+0.918|24\rangle$

$4^+(5.47) = 0.977|04\rangle-0.212|14\rangle-0.014|24\rangle$
$4^+(10.57) = 0.212|04\rangle+0.977|14\rangle-0.006|24\rangle$
$4^+(22.77) = 0.015|04\rangle+0.003|14\rangle+1.000|24\rangle$

$5^+(6.41) = -0.982|04\rangle-0.059|14\rangle-0.005|24\rangle-0.124|06\rangle+0.128|16\rangle+0.014|26\rangle$
$5^+(9.54) = -0.008|04\rangle-0.832|14\rangle-0.015|24\rangle+0.548|06\rangle+0.084|16\rangle+0.009|26\rangle$
$5^+(12.12) = -0.098|04\rangle+0.547|14\rangle-0.027|24\rangle+0.787|06\rangle+0.266|16\rangle+0.014|26\rangle$
$5^+(15.24) = 0.160|04\rangle-0.072|14\rangle+0.012|24\rangle-0.251|06\rangle+0.952|16\rangle-0.009|26\rangle$
$5^+(21.02) = -0.013|04\rangle+0.003|14\rangle+0.966|24\rangle+0.035|06\rangle-0.003|16\rangle-0.258|26\rangle$
$5^+(25.77) = 0.013|04\rangle+0.000|14\rangle+0.258|24\rangle-0.008|06\rangle+0.001|16\rangle+0.966|26\rangle$

$6^+(9.81) = 0.972|06\rangle-0.234|16\rangle-0.015|26\rangle$
$6^+(15.15) = 0.234|06\rangle+0.972|16\rangle-0.007|26\rangle$
$6^+(27.44) = 0.017|06\rangle+0.004|16\rangle+1.000|26\rangle$

$7^+(11.05) = -0.986|06\rangle-0.105|16\rangle-0.007|26\rangle-0.077|08\rangle+0.099|18\rangle+0.012|28\rangle$
$7^+(14.50) = 0.077|06\rangle-0.937|16\rangle-0.008|26\rangle+0.338|08\rangle+0.035|18\rangle+0.005|28\rangle$
$7^+(17.87) = -0.077|06\rangle+0.328|16\rangle-0.032|26\rangle+0.897|08\rangle+0.282|18\rangle+0.017|28\rangle$
$7^+(21.39) = 0.122|06\rangle-0.052|16\rangle+0.016|26\rangle-0.270|08\rangle+0.954|18\rangle-0.008|28\rangle$
$7^+(25.56) = -0.013|06\rangle+0.003|16\rangle+0.984|26\rangle+0.038|08\rangle-0.005|18\rangle-0.174|28\rangle$
$7^+(31.68) = 0.011|06\rangle+0.000|16\rangle+0.175|26\rangle-0.012|08\rangle+0.001|18\rangle+0.984|28\rangle$

$8^+(15.65) = 0.963|08\rangle - 0.268|18\rangle - 0.018|28\rangle$
$8^+(21.43) = 0.268|08\rangle + 0.963|18\rangle - 0.010|28\rangle$
$8^+(33.88) = 0.020|08\rangle + 0.005|18\rangle + 1.000|28\rangle$

$9^+(17.42) = 0.985|08\rangle + 0.173|18\rangle + 0.010|28\rangle$
$9^+(21.11) = -0.173|08\rangle + 0.985|18\rangle - 0.001|28\rangle$
$9^+(31.76) = 0.010|08\rangle - 0.001|18\rangle + 1.000|28\rangle$

TABLE 13

Some useful angular momentum coupling coefficients for use in eq. 5.8

$W(0212{-}21) = 1/\sqrt{15}$

$W(0213;21) = 1/\sqrt{15}$

$W(2413;21) = 1/\sqrt{35}$

$W(2424;21) = -\frac{1}{3\sqrt{6}}$

$W(2435;21) = \frac{1}{3\sqrt{7}}$

$W(4657;21) = \frac{1}{\sqrt{11x13}}$

$W(6857;21) = \frac{1}{\sqrt{13x15}}$

$W(4435;21) = \frac{1}{18}\sqrt{\frac{6}{5x7x11}}$

$W(4645;21) = -\frac{1}{3\sqrt{11x15}}$

$W(2212;21) = -\frac{1}{10}\sqrt{\frac{7}{3}}$

$W(2213;21) = \frac{1}{5\sqrt{21}}$

$W(2223;21) = \frac{1}{5}\sqrt{\frac{2}{7}}$

$W(2434;21) = \frac{1}{3\sqrt{42}}$

$W(4445;21) = \frac{1}{15}\sqrt{\frac{7}{22}}$

$W(6657;21) = \frac{1}{13\sqrt{3x5x7x11}}$

$W(4434,21) = -\frac{1}{12}\sqrt{\frac{11}{5x7}}$

$W(4635;21) = \frac{1}{3\sqrt{11}}$

$\langle 2020|00\rangle = \frac{1}{\sqrt{5}}$

$\langle 2040|20\rangle = \sqrt{\frac{2}{7}}$

$\langle 2060|40\rangle = 3\sqrt{\frac{5}{11x13}}$

$\langle 2080|60\rangle = 2\sqrt{\frac{7}{5x17}}$

$\langle 2020|20\rangle = -\sqrt{\frac{2}{7}}$

$\langle 2040|40\rangle = -2\sqrt{\frac{5}{77}}$

$\langle 2060|60\rangle = -\sqrt{\frac{14}{55}}$

TABLE 14

E2 Transition Strengths in ^{18}F

INITIAL STATE		FINAL STATE		B(E2) W.U.		
J_i	E_i(MeV)	J_f	E_f(MeV)	EXPT	CALC (No mixing)	CALC (mixing)
2	2.524	1	1.701	16±8	17.75	24.14
3	3.357	1	1.701	18±4	17.75	15.41
3	3.357	2	2.524	14^{+31}_{-12}	7.2	0.042
4	5.301	2	2.524	25±7	19.49	19.49
4	5.301	3	3.357	8±4	3.90	4.09
5	6.565	3	3.357	27±6	23.4	22.52
5	6.565	4	5.301	<120	2.46	2.94

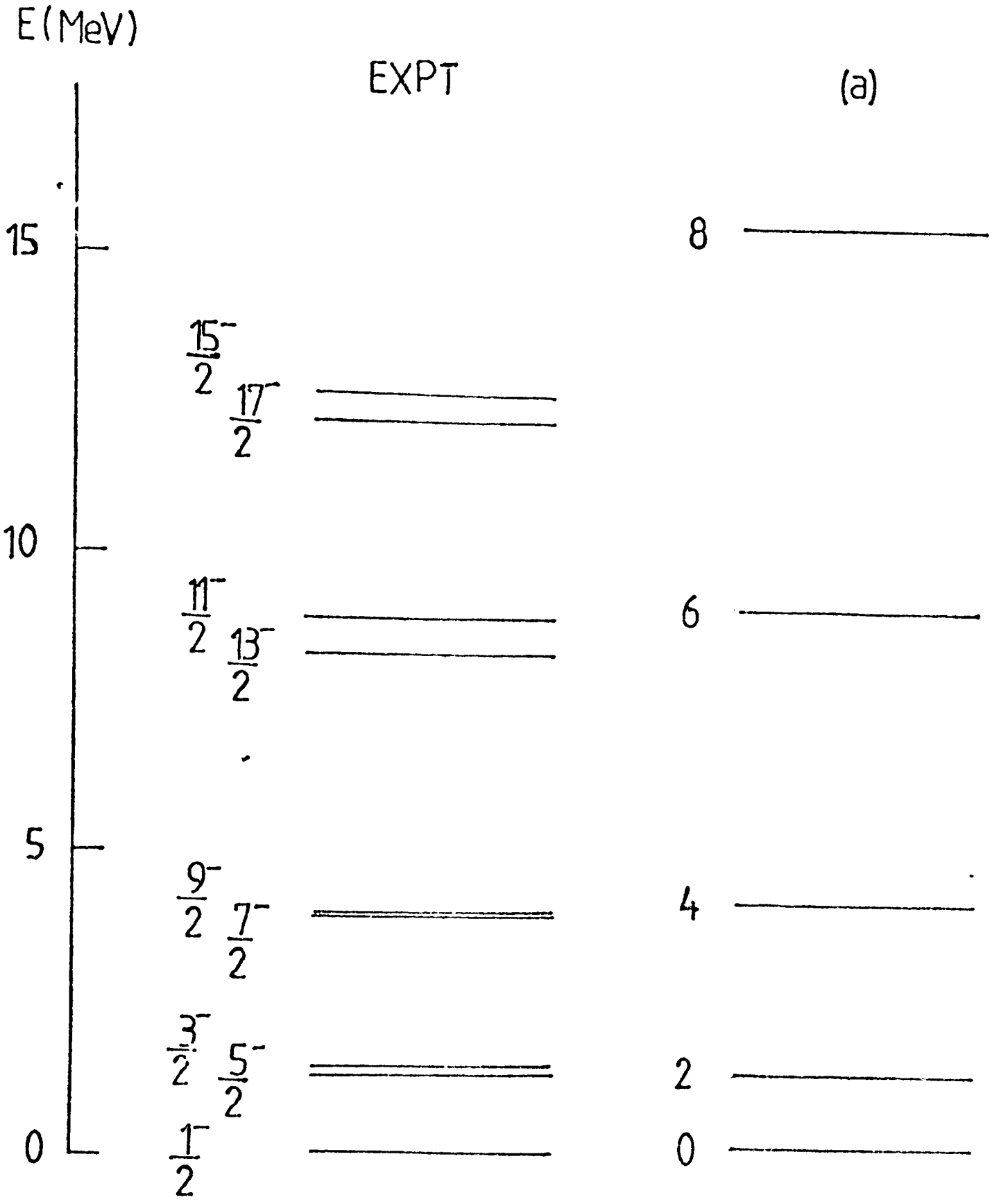


FIG. 1

Fig. 1. The predictions of the phenomenological model (a) for the energies of the lowest lying band of alpha cluster states in ^{19}F are compared with experiment. The splittings of the doublets predicted by the semimicroscopic treatment are not shown because they are so small ($\sim$ 100 keV at most).

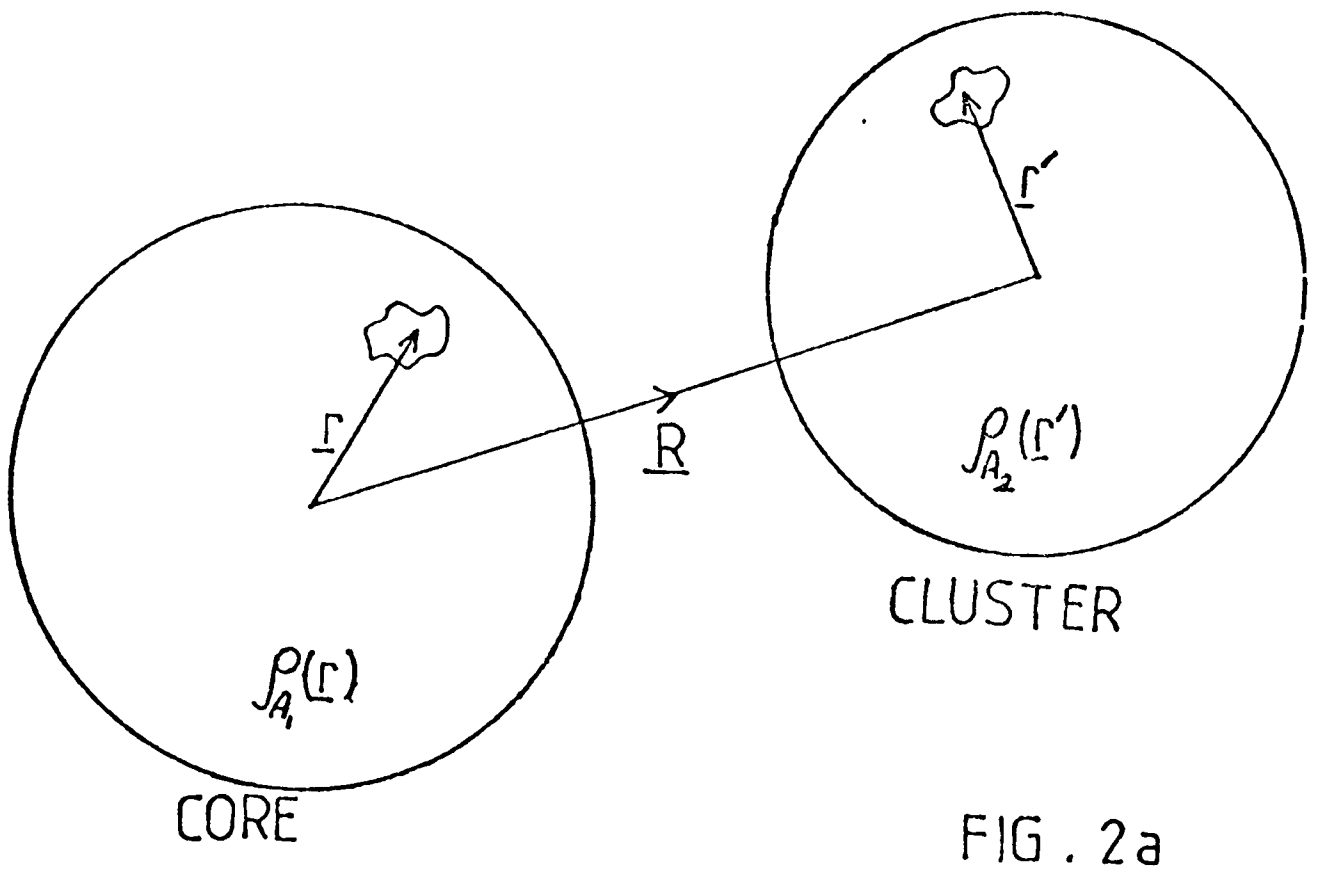


FIG. 2a

Fig. 2a. The central part of the effective cluster-core potential is formed by folding the core density $\rho_{A_1}(\underline{r})$ with the cluster density $\rho_{A_2}(\underline{r}')$ and an effective nucleon potential. The geometrical significance of $\underline{r}$, $\underline{r}'$ and $\underline{R}$ is illustrated.

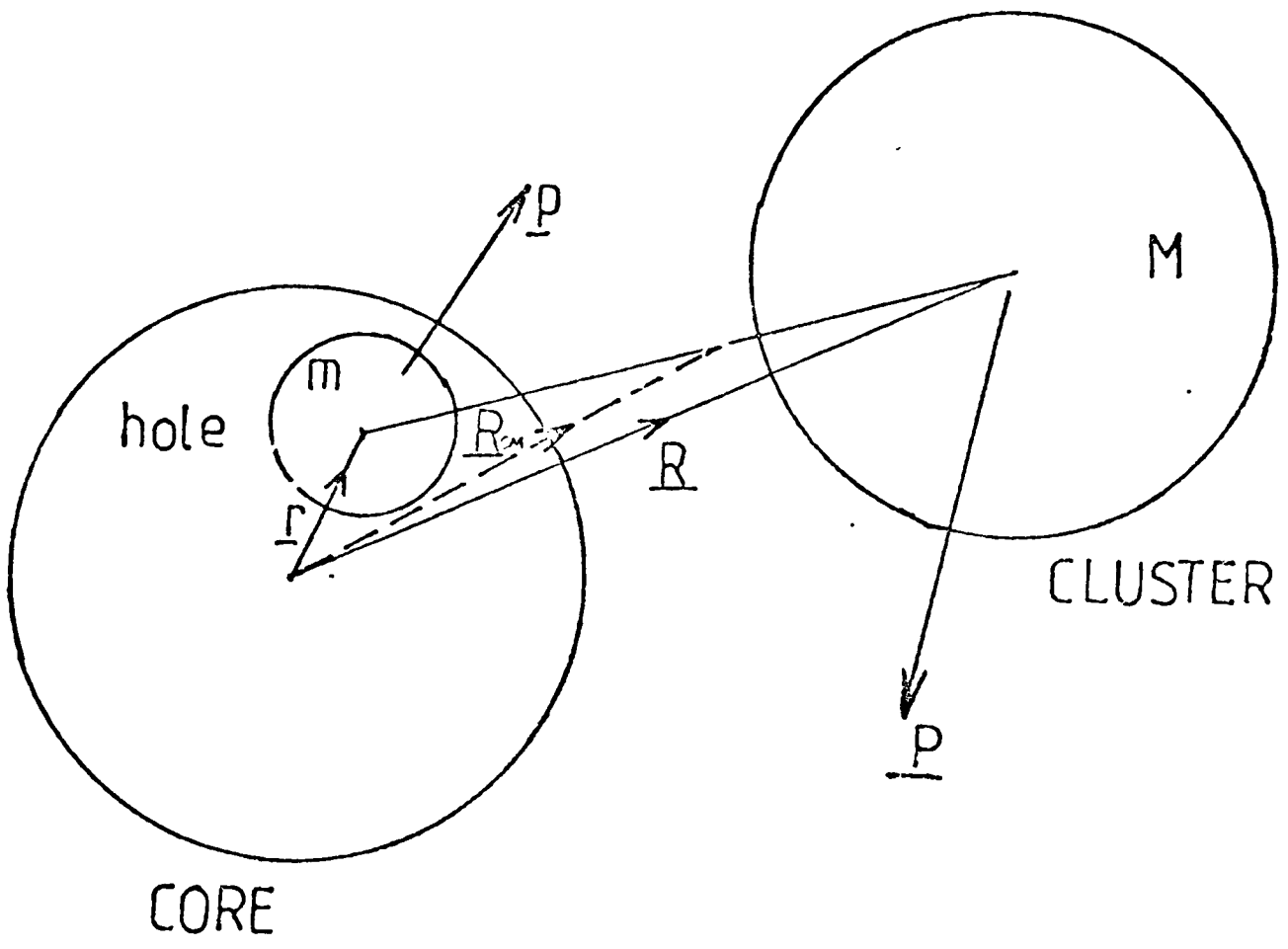


FIG. 2b

Fig. 2b. The model builds up an effective cluster-core potential by considering the interaction of particles in the core (which itself remains fixed in space) with a cluster. m,$\underline{p}$ and $\underline{r}$ are the mass, momentum and position vector of the particle (measured from the centre of the core) M,$\underline{P}$ and $\underline{R}$ are those same quantities for the cluster. $\underline{R}_{CM}$ is the position vector of the centre of mass of the particle-cluster pair.

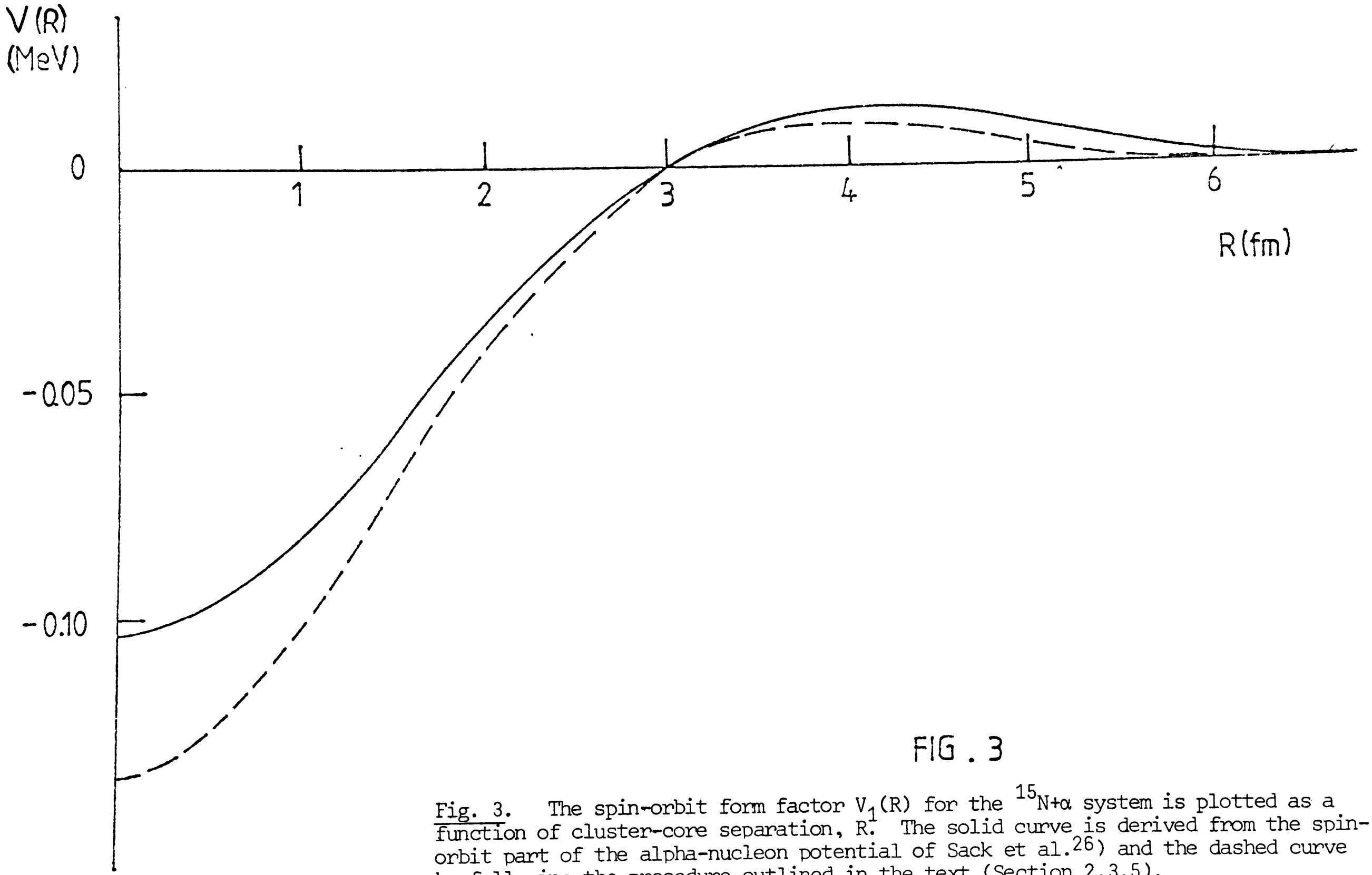


FIG. 3

Fig. 3. The spin-orbit form factor $V_1(R)$ for the $^{15}N+\alpha$ system is plotted as a function of cluster-core separation, R. The solid curve is derived from the spin-orbit part of the alpha-nucleon potential of Sack et al.[26]) and the dashed curve by following the procedure outlined in the text (Section 2.3.5).

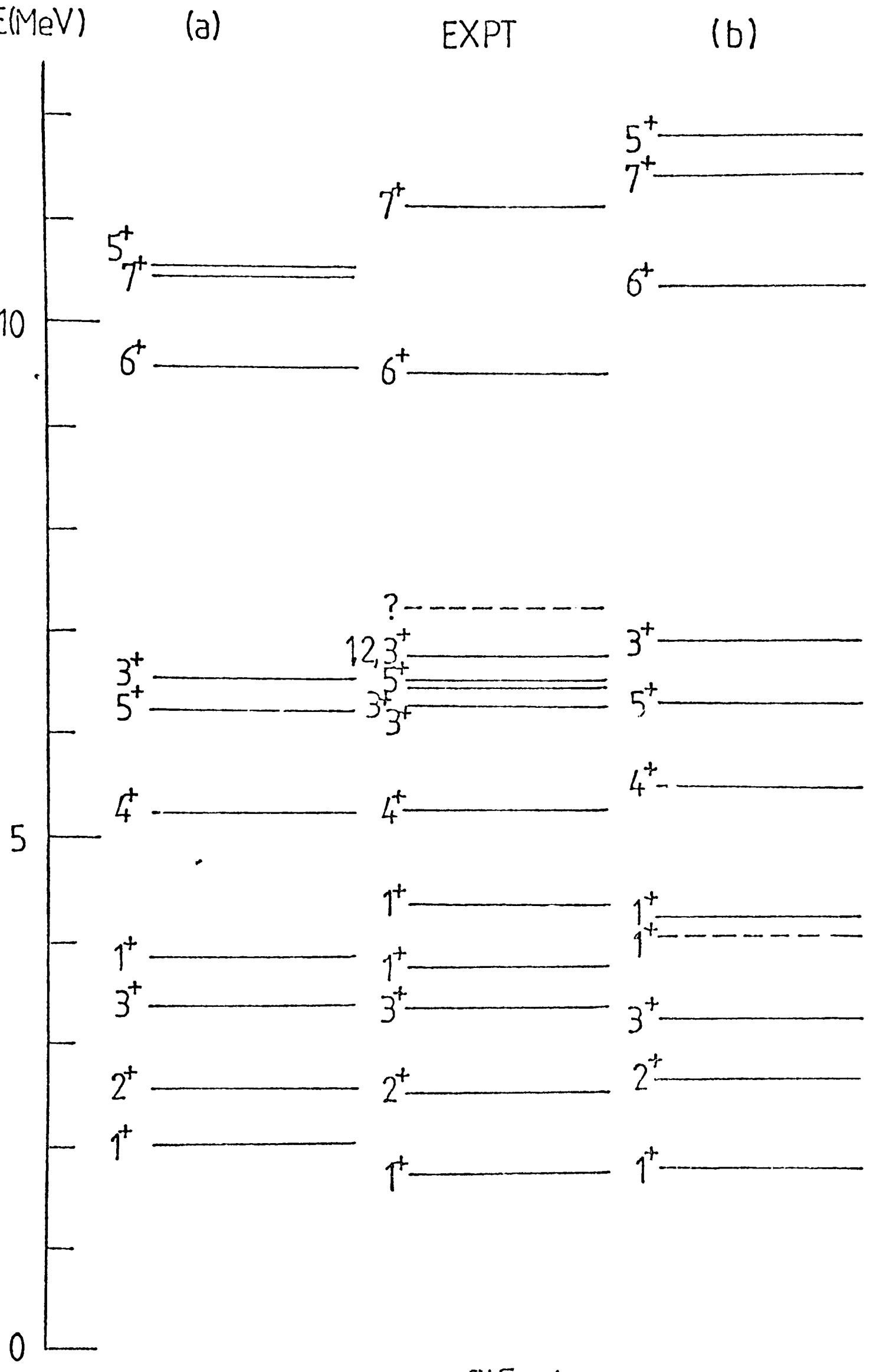


FIG. 4

Fig. 4. The semimicroscopic spectrum (b) and that of the phenomenological model (a) are compared with experiment. The dashed 1^+ level in (b) is a two-particle shell model state, whilst that in the experimental data has uncertain J^π (see text) (Energies in MeV).



FIG. 5a FIG. 5b

Fig. 5a,b. Possible classical orbits of the alpha cluster around the deformed core.

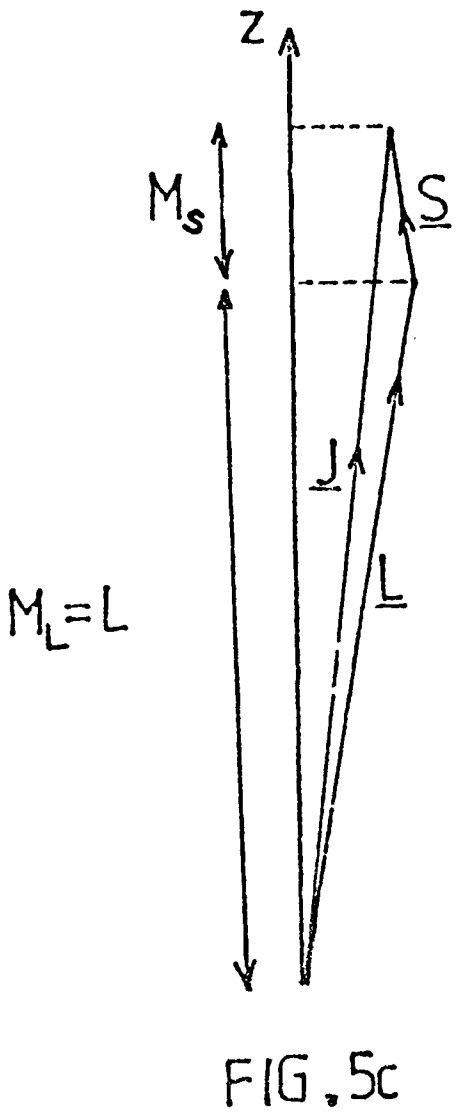


FIG. 5c

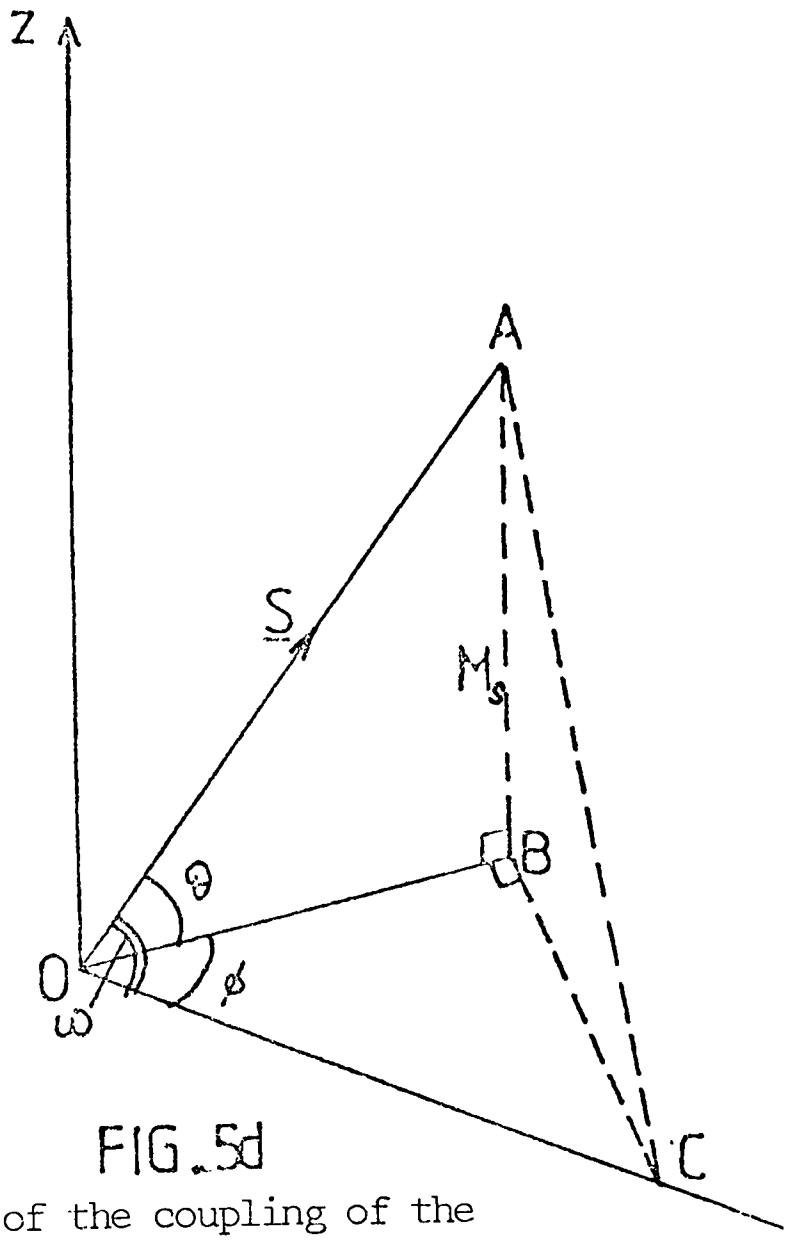


FIG. 5d

Fig. 5c . The vector model description of the coupling of the angular momenta $\underline{L}$ and $\underline{S}$ to a resultant $\underline{J}$.

Fig. 5d. Diagram to aid the classical evaluation of the average value of $(\underline{S}.\underline{R})^2 - 1/3S^2$. Points B and C are in the xy plane such that AB is parallel to the z-axis and of length M, while C is that point on $\underline{R}$ for which the angle OBC is $\pi/2$ radians.

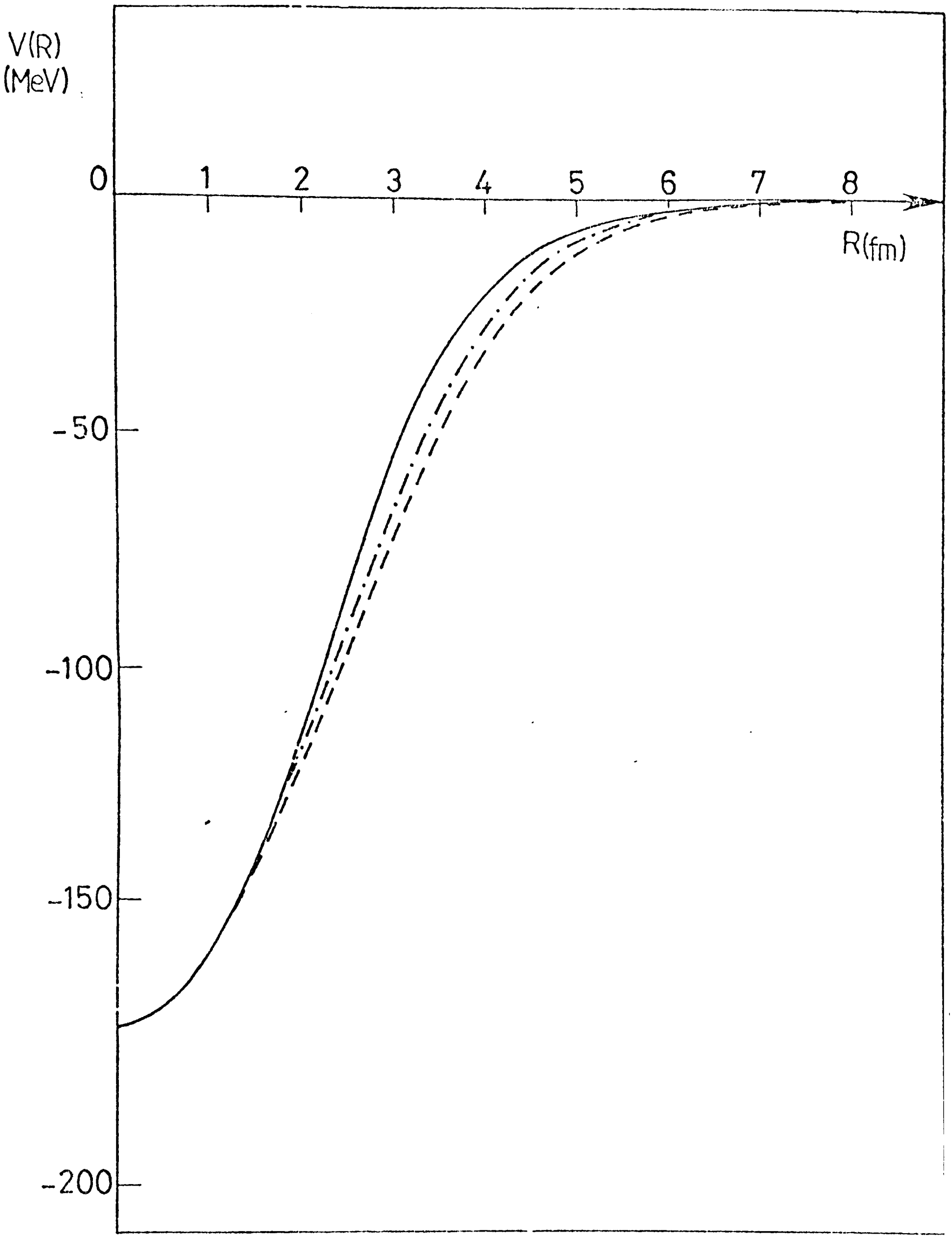


FIG. 6

Fig. 6. The folded potentials of eq. 3.61 (dashed curve) and eq. 3.63 (dash-dot curve) for the ^{16}O-α system are compared with the cosh potential of eq. 3.64 (solid curve) which gives a good fit to the ground state rotational band of ^{20}Ne (see text). In this, and the next figure, the potentials are in MeV and R in fm.

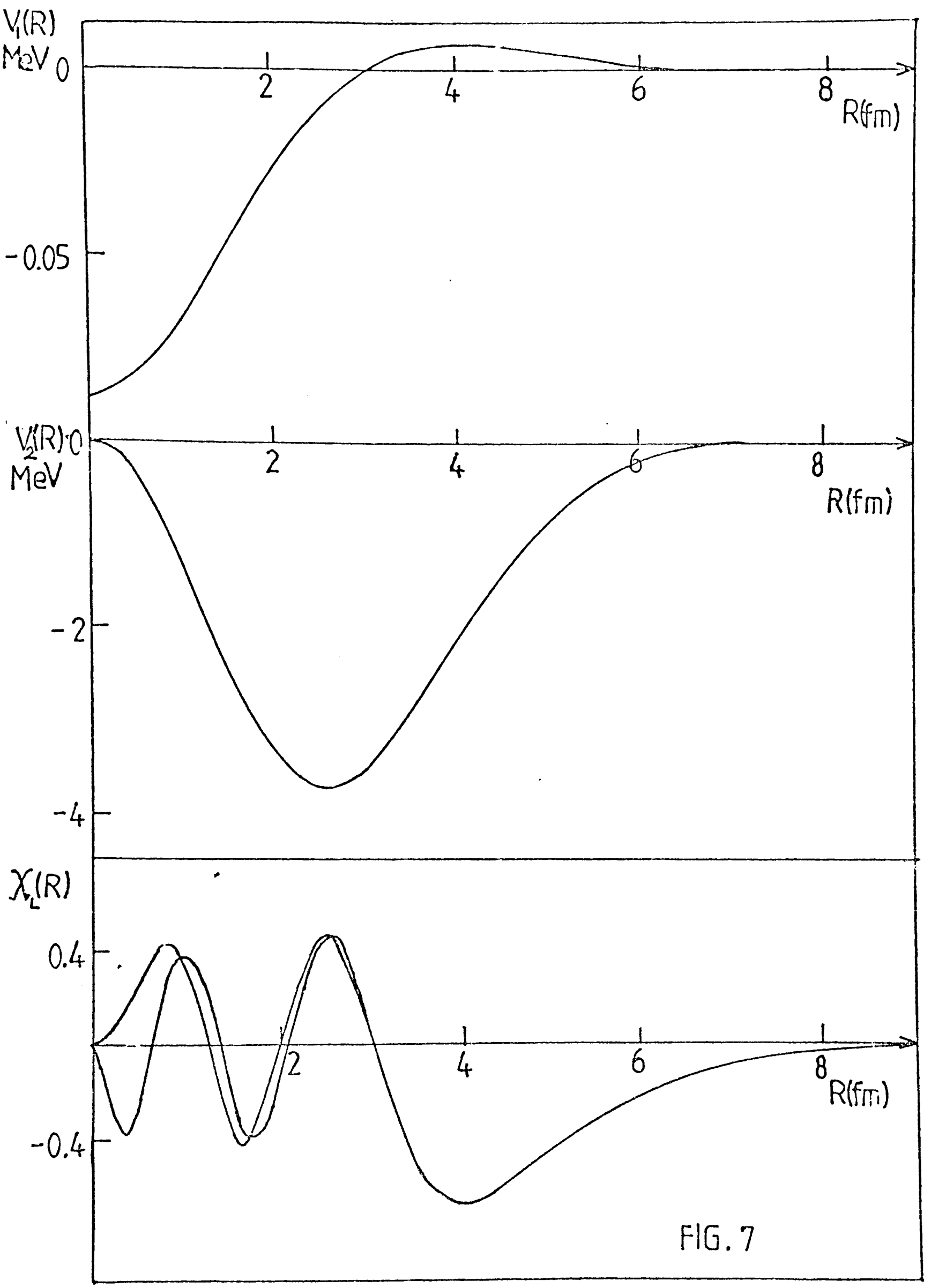


FIG. 7

Fig. 7. The spin-orbit and tensor form factors $V_1(R)$ and $V_2(R)$ eqs. 3.56 and 3.57 are shown. Also shown are the radial wavefunctions of relative motion for L=0 (4 nodes) and L=2 (3 nodes). Note that these wavefunctions are essentially in phase for $R \gtrsim 1$ fm giving rise to large off-diagonal matrix elements of the tensor force.

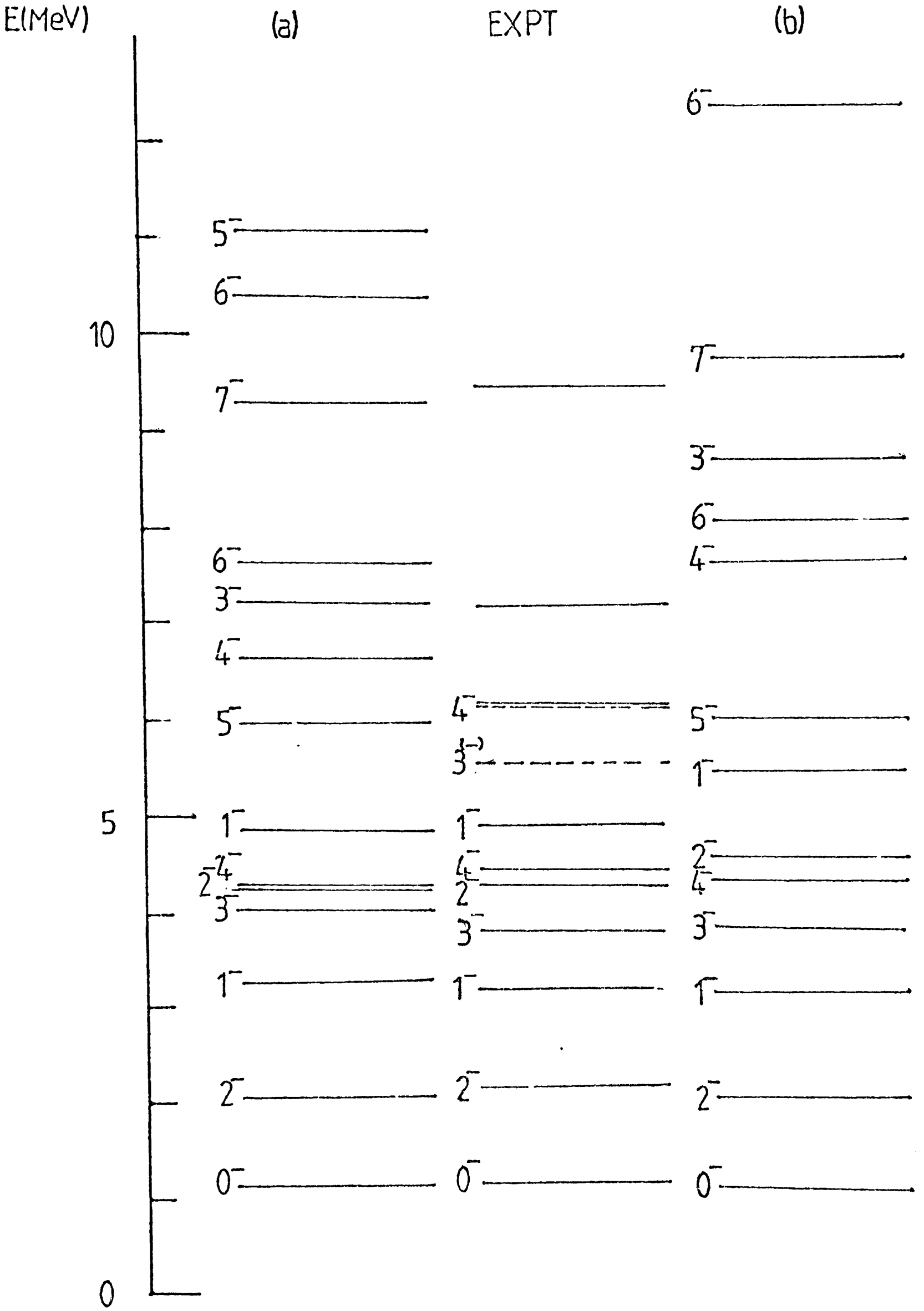


FIG. 8

Fig. 8. The phenomenological spectrum (a) (the fit B1 from ref. 21) and the semimicroscopic spectrum (b) for ^{18}F are compared with experiment. The dotted lines are tentative experimental candidates and some of the higher levels are seen strongly in ^{3}He transfer to ^{15}N, but their J^{π} values are not known.

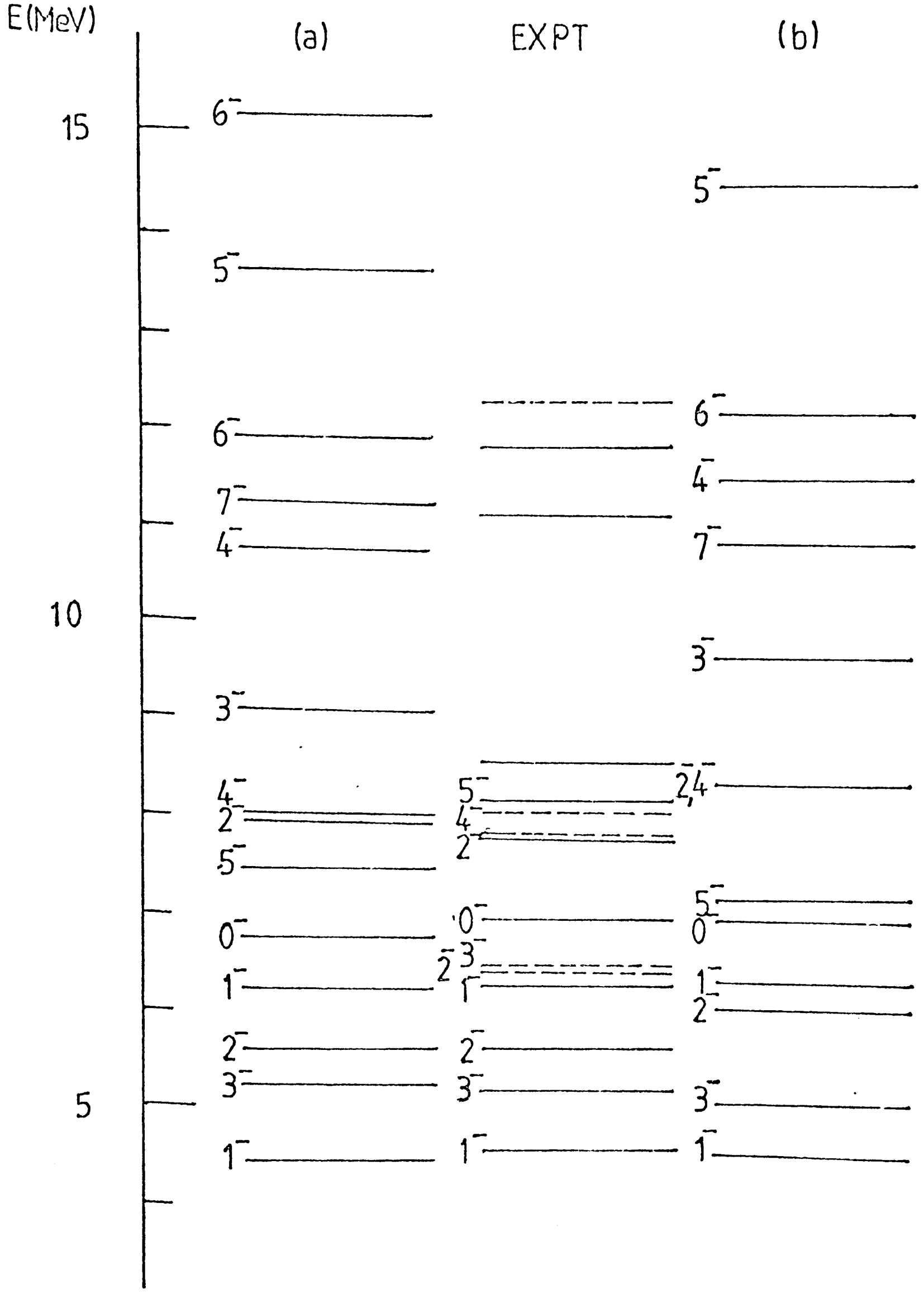


FIG. 9

Fig. 9. The phenomenological spectrum (a) (the fit B2 from ref. 21) and the semimicroscopic spectrum (b) for ^{18}O are compared with experiment.

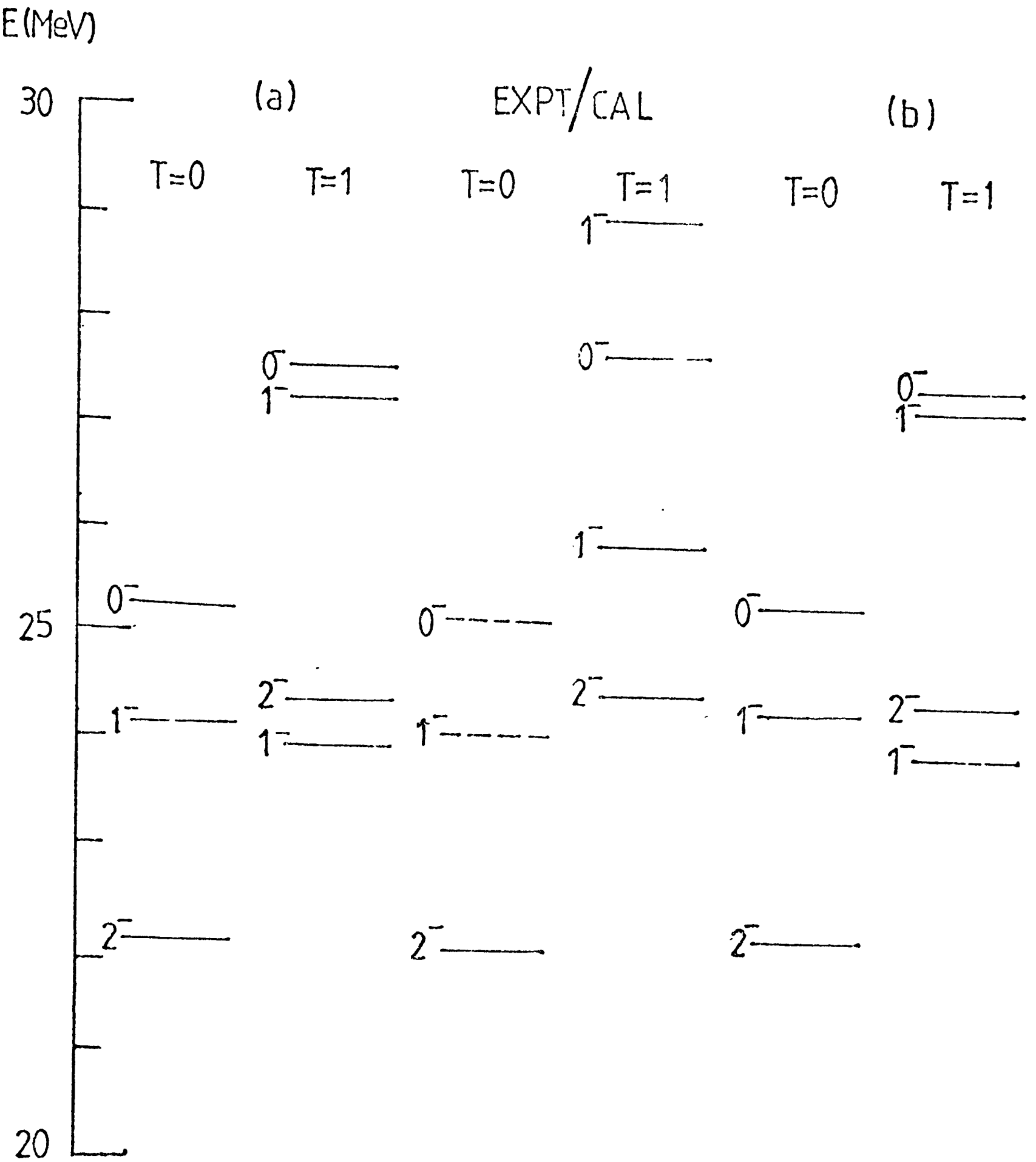


FIG 10

Fig. 10. The splittings of 7 P-wave excited states of the alpha particle predicted by the two nucleon-trinucleon potentials used are compared with experiment. The dotted levels are from the calculation of de Shalit and Walecka [57], and are not identified experimentally. Gaussian geometries were used with widths of a 2.65 fm (fit(a)) and a=2.23 fm(fit (b)). The strengths are given in the text (section 4.4.2).

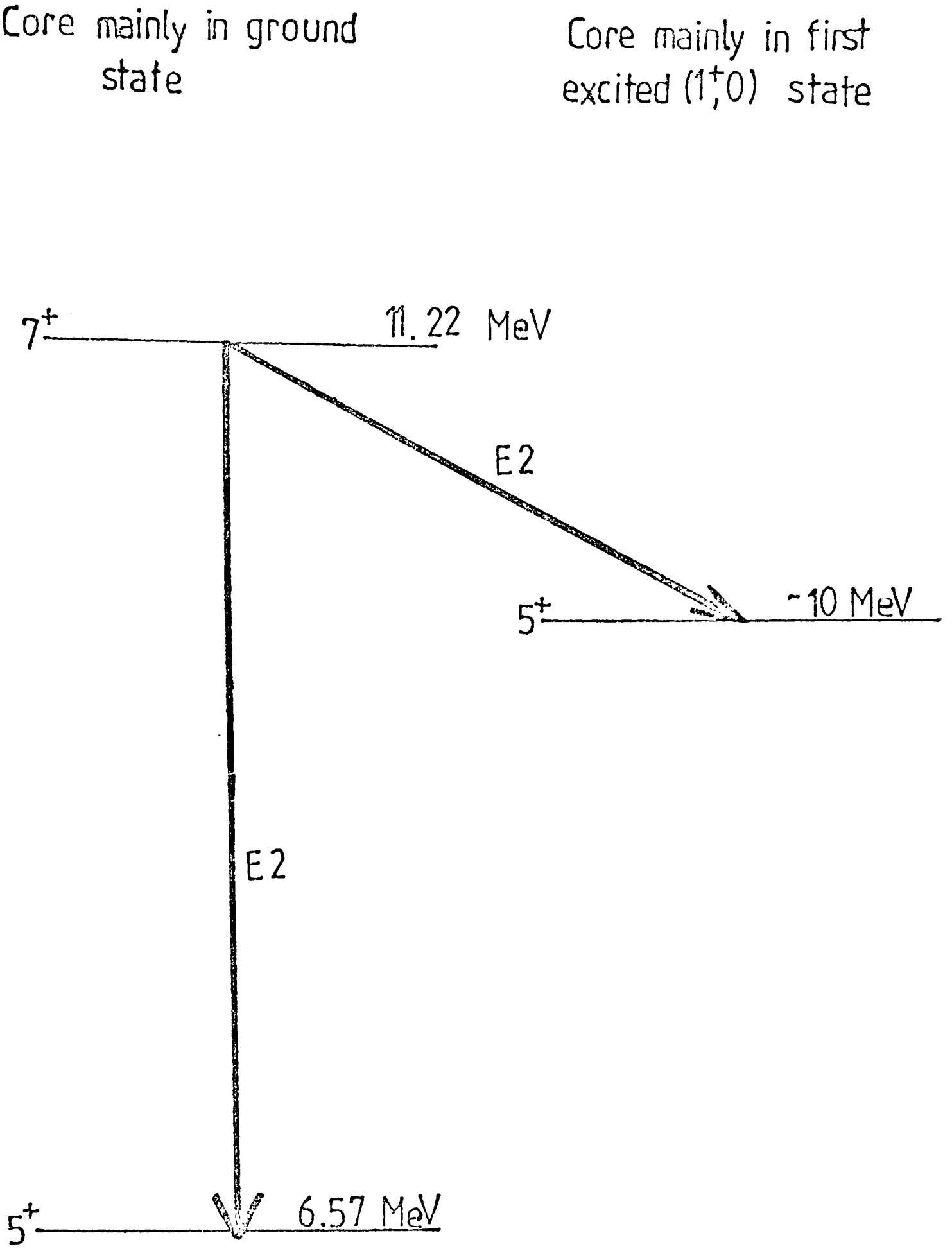


FIG. 11

Fig. 11. The possible electromagnetic decays of a 7^+ alpha cluster state in ^{18}F, for which the core has a large ground state ^{14}N component, to 5^+ states. The lower 5^+ state has a core with a large ground state ^{14}N component, whilst the core of the higher 5^+ has a large overlap with the 1^+ state at 3.9 MeV in ^{14}N.

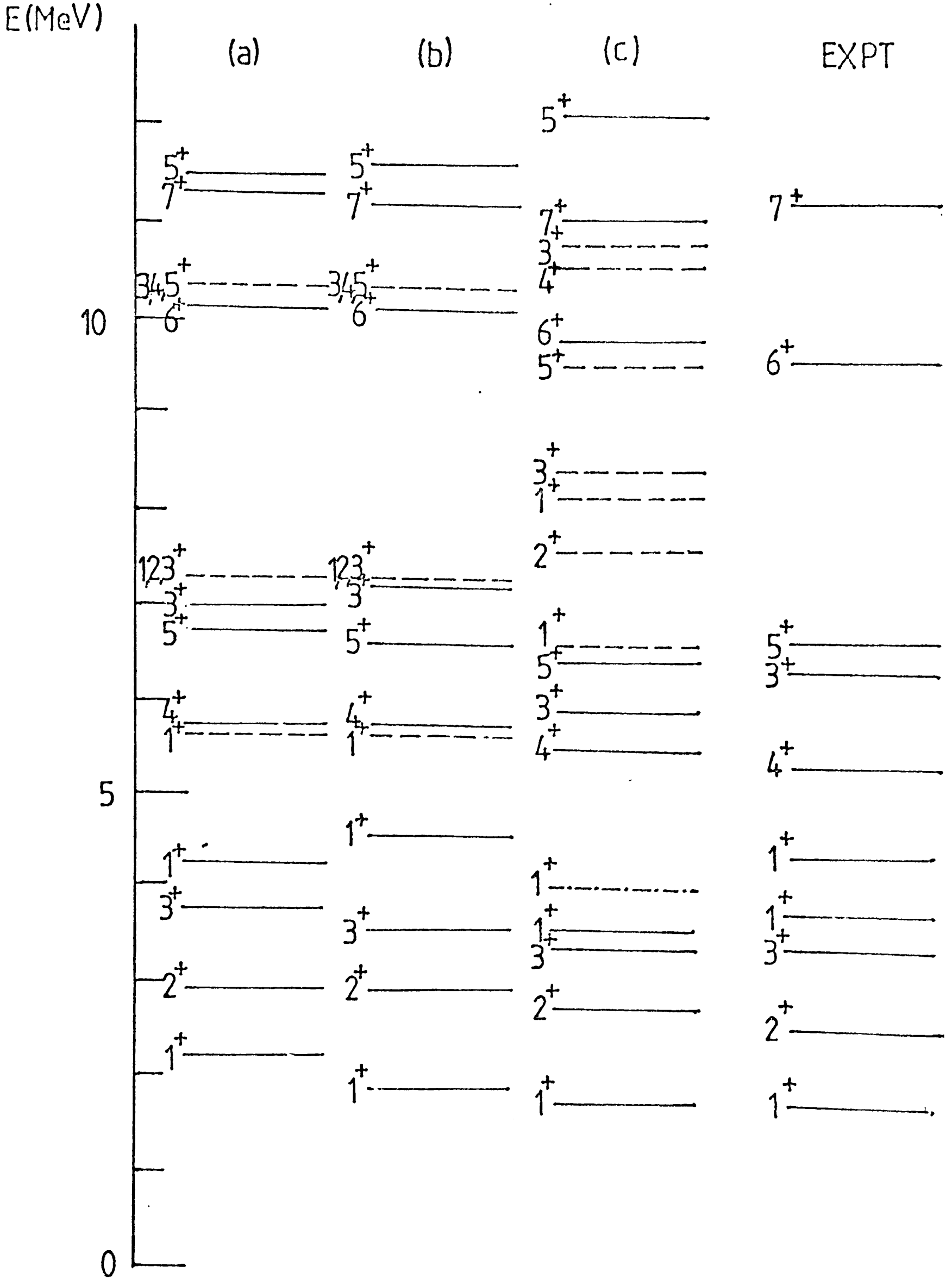


FIG. 12

Fig. 12. Spectrum of alpha cluster states in ^{18}F. In (a) the core is taken to be one of the $(1^+,0)$ states available to a free ^{14}N nucleus, and no L-mixing due to the tensor force between cluster and core is introduced. In (b) the mixing of odd-J states is included, but the core is still in a "pure" state. In (c), the core state may be a mixture of the three $(1^+,0)$ states of ^{14}N which may be formed by coupling two p-shell holes, so full mixing is included. The experimental cluster states are discussed in Section 3.1.

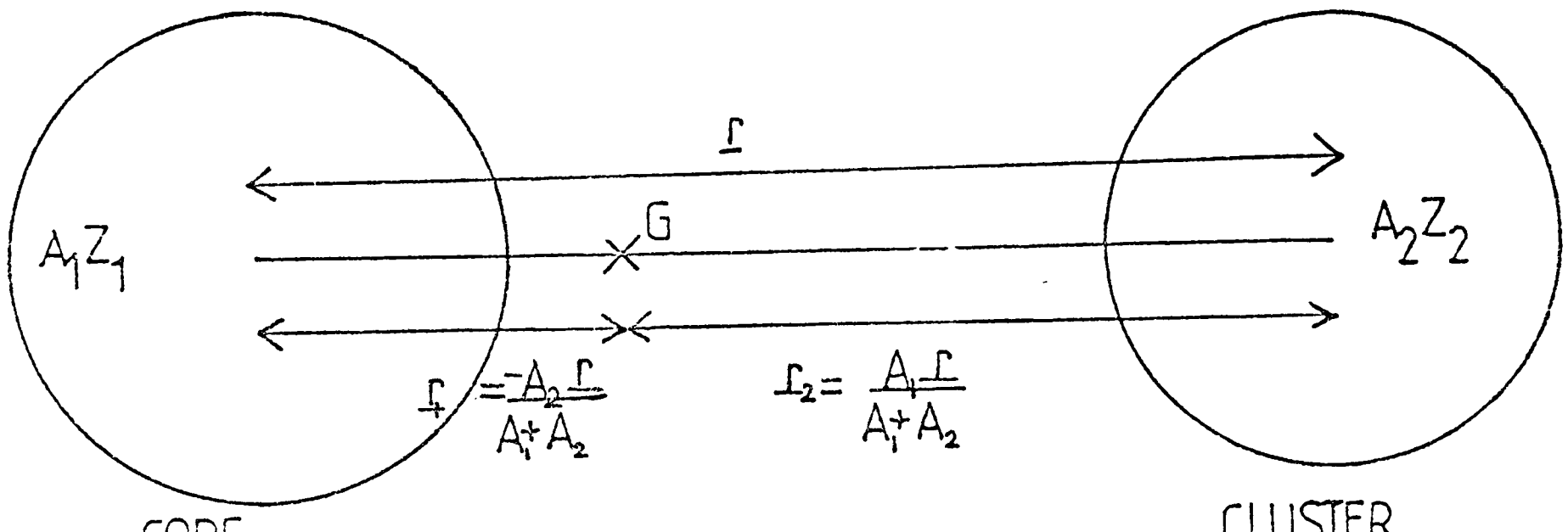


FIG . 13

Fig. 13. The cluster (A_2 nucleons, Z_2 protons)-core (A_1 nucleons, Z_1 protons) system, separated by a distance r. G is the centre of mass of the system.